STIFFENED PLATES SUBJECTED TO IN-PLANE LOAD AND LATERAL PRESSURE

ZHU DONGQI

B. Eng. (Hons.), NUS

A THESIS SUBMITTED

FOR THE DEGREE OF MASTER OF ENGINEERING

DEPARTMENT OF CIVIL ENGINEERING

NATIONAL UNIVERSITY OF SINGAPORE

2004

ACKNOWLEDGEMENTS

The author would like to express his deep appreciations to his supervisors, Professor N E Shanmugam and Associate Professor Choo Yoo Sang, for their invaluable guidance, suggestions and encouragement throughout this research project.

The author would like to express his gratitude to Mr. B.C. Sit, Mr. W.M. Ow, Mr. B.O. Ang, Mr. Y.K. Koh, Mr. Kamsan, Ms Annie and other staffs in NUS Structural Steel & Concrete Laboratory for their immeasurable help and assistance in experimental testing and instrumentations.

Special thanks are given to staffs from CALES for their assistance in solving software application problems whenever encountered.

Finally the author would like to take this opportunity to express his heartfelt thanks to his parents, sister and his wife Ms Zhang Xueyan for their exceptional love and affection over the years, which cannot be expressed in words.

TABLE OF CONTENTS

ACKNOWLEDGEMENTS I

SUMMARY V

LIST OF TABLES VI

LIST OF FIGURES VII

LIST OF SYMBOLS XI

CHAPTER 1 INTRODUCTION 1

1.1 Background 1

1.2 Objective 2

1.3 Scope of Investigation 2

CHAPTER 2 LITERTURE REVIEW 4

2.1 Introduction 4

2.2 Analytical Methods 4

2.2.1 Orthotropic Plate Approach 5

2.2.2 Discretely Stiffened Plate Approach 6

2.2.3 Strut Approach 8

2.2.4 Finite Element and Finite Strip Method 9

2.3 Failure Modes of Stiffened Plates 11

2.4 Stiffened Plates under In-plane Loading 13

2.5 Stiffened Plates under Combined In-plane and Lateral Loading 19

2.6 Design of Stiffened Plates 22

2.7 Optimizations of Stiffened Plates 31

CHAPTER 3 EXPERIMENTAL INVESTIGATION 41

3.1 Introduction 41

3.2 Details of Test Specimens 41

3.3 Imperfection Measurement 43

3.4 Experimental Setup 44

3.5 Instrumentations 45

3.6 Test Procedure 46

3.7 Measurement of Contact Area of Air Bag 47

CHAPTER 4 NUMERICAL INVESTIGATION 58

4.1 Introduction 58

4.2 ABAQUS Pre-processing 59

4.2.1 Boundary and Loading Conditions 59

4.2.2 Mesh Generation 60

4.2.3 Material Non-Linearity 62

4.2.4 Initial Imperfection 62

4.3 ABAQUS Processing 63

4.4 ABAQUS Post-processing 65

4.5 Limitations of Finite Element Analysis 65

4.6 Accuracy of ABAQUS Analysis 66

CHAPTER 5 RESULTS AND DISCUSSION 77

5.1 Experimental Results 77

5.1.1 Initial Imperfection 77

5.1.2 Ultimate Load of Series A and Series B 77

5.2 Comparison of FEM Results with Experimental Results 80

5.3 Comparison of Experimental Results with Design Methods 82

5.4 Parametric Studies 85

5.5 Ultimate Load of Stiffened Plates under Combined Loads 87

5.5.1 Influence of Plate Slenderness Ratio, b/t_p 88

5.5.2 Influence of Intensity of Lateral Pressure 89

5.5.3 Influence of Boundary Conditions 90

5.5.4 Influence of Initial Imperfection 91

5.5.5 Influence of Residual Stress 93

5.6 Design Recommendations 94

CHAPTER 6 CONCLUSIONS 125

6.1 Conclusions 125

6.2 Recommendations 126

REFERENCES 128

APPENDIX A DESCRIPTION OF DATABASE 155

APPENDIX B MATERIAL STRESS-STRAIN CURVES 159

APPENDIX C TYPICAL ABAQUS INPUT FILE 163

APPENDIX D MEASURED INITIAL IMPERFECTION 165

SUMMARY

This research provides a study of the behaviour of stiffened plates subjected to in-plane loading and lateral pressure. Experimental investigation as well as numerical investigation using finite element package ABAQUS were carried out.

The collapse load of stiffened plates under combined action of in-plane load and lateral pressure has been studied on twelve stiffened plates with two different base plate slenderness ratios (b/t_p =76 and 100). An inflatable air bag with maximum load capacity of 70 tonnes was used to apply lateral pressure on the stiffened plates. Initial geometric imperfection was measured by a purpose built device. The strains, axial shortening and lateral deflections of the test specimen were recorded during the experiments. The tested specimens were modelled and analyzed using a non-linear elasto-plastic finite element package ABAQUS. Experimental results were compared to both FEM results and results from limited design methods available in the literature.

Parametric studies were carried out on the ultimate load of stiffened plate by varying various parameters. A series of stiffened plates with plate slenderness ratios ranging from 30 to 100 were studied. Effect of plate slenderness ratio of base plate, intensity of lateral pressure, boundary conditions, initial imperfection as well as residual stress on the ultimate load of stiffened plates was investigated. Based on both experimental and numerical investigations, a few conclusions were drawn and recommendations were made for future works.

LIST OF TABLES

Table No.	Title	Page
Table 2.1	Summary of Experiments on Stiffened Plates	34
Table 3.1	Dimensions of All Specimens	49
Table 3.2	Material Properties for Base Plate and Stiffeners	50
Table 4.1	Yield Stress and Young's Modulus of Material (Kumar's specimens)	69
Table 4.2	Comparison of Experimental and FEM Results for Specimens Tested by Kumar	69
Table 4.3	Comparison of Experimental and FEM Results for Specimens Tested by Smith	70
Table 5.1	Summary of Experimental Results	96
Table 5.2	Comparison of Experimental Results with Existing Design Methods	97
Table 5.3	Dimensions of Stiffened Plates for Parametric Studies	98
Table 5.4	Summary of Parametric Study Results	98
Table 5.5	Summary of Ultimate Loads with Different Boundary Conditions	99
Table 5.6	Effects of Initial Imperfection on the Ultimate Loads of Stiffened Plates	99
Table 5.7	Effects of Residual Stress on the Ultimate Load of Stiffened Plates	100

LIST OF FIGURES

Figure No.	Title	Page
Figure 2.1	Orthotropic Plate Idealization	39
Figure 2.2	Discretely Stiffened Plate Idealization	39
Figure 2.3	Strut Approach Idealization	40
Figure 2.4	Finite Element Idealizations	40
Figure 3.1	Dimensions of Series A Specimen	50
Figure 3.2	Dimensions of Series B Specimen	51
Figure 3.3	Tensile Coupon Specimen	51
Figure 3.4	Typical Stress-Strain Curve for Steel Used	52
Figure 3.5	Imperfection Measurement Device	52
Figure 3.6	Side View of Imperfection Measurement Device	53
Figure 3.7	Typical Example of Measured Initial Imperfections in a Stiffened Plate	53
Figure 3.8	Overall View of the Test Rig	54
Figure 3.9	Sectional View of the Experimental Setup	54
Figure 3.10	Location of Strain Gauges and Displacement Transducers for Series A Specimens	55
Figure 3.11	Location of Strain Gauges and Displacement Transducers for Series B Specimens	55
Figure 3.12	Initial State of Air Bag during the Test	56
Figure 3.13	Illustration of Contact Area Measurement	56
Figure 3.14	Top View of Contact Area Measurement	57
Figure 3.15	Change of Lateral Pressure on Specimen with Change of Lateral Load	57

Figure 4.1	Three Stages of Analysis	71
Figure 4.2	Flow Chart of Numerical Investigation	72
Figure 4.3	Change of Contact Area at Different Loadings	73
Figure 4.4	Typical Mesh of Stiffened Plate	74
Figure 4.5	Typical Buckling Shape of Stiffened Plate	74
Figure 4.6	Typical Load vs Displacement Curve	75
Figure 4.7	Dimension of Kumar's Specimen	75
Figure 4.8	Comparison of Failure Shapes	76
Figure 5.1	Measured Initial Imperfection for Series A Specimens	101
Figure 5.2	Measured Initial Imperfection for Series B Specimens	102
Figure 5.3	View after Failure Shape of the Specimen A1	103
Figure 5.4	View after Failure Shape of the Specimen A2	104
Figure 5.5	View after Failure Shape of the Specimen A3	105
Figure 5.6	View after Failure Shape of the Specimen A4	105
Figure 5.7	View after Failure Shape of the Specimen A5	106
Figure 5.8	View after Failure Shape of the Specimen A6	106
Figure 5.9	View after Failure Shape of the Specimen B1	107
Figure 5.10	View after Failure Shape of the Specimen B2	107
Figure 5.11	View after Failure Shape of the Specimen B3	108
Figure 5.12	View after Failure Shape of the Specimen B4	108
Figure 5.13	View after Failure Shape of the Specimen B5	109
Figure 5.14	View after Failure Shape of the Specimen B6	109
Figure 5.15	Lateral Load vs Displacement Curves for Series A	110
Figure 5.16	Lateral Load vs Displacement Curves for Series B	110

Figure 5.17	Load vs Displacement Curves for Specimens under Axial Load Only	111
Figure 5.18	Maximum Principle Stress at Locations of Strain Gauges for Specimen B3	111
Figure 5.19	Comparison of Load vs Displacement Curves for Specimen A1	112
Figure 5.20	Comparison of Load vs Displacement Curves for Specimen A2	112
Figure 5.21	Comparison of Load vs Displacement Curves for Specimen A3	113
Figure 5.22	Comparison of Load vs Displacement Curves for Specimen A4	113
Figure 5.23	Comparison of Load vs Displacement Curves for Specimen A5	114
Figure 5.24	Comparison of Load vs Displacement Curves for Specimen A6	114
Figure 5.25	Comparison of Load vs Displacement Curves for Specimen B1	115
Figure 5.26	Comparison of Load vs Displacement Curves for Specimen B2	115
Figure 5.27	Comparison of Load vs Displacement Curves for Specimen B3	116
Figure 5.28	Comparison of Load vs Displacement Curves for Specimen B4	116
Figure 5.29	Comparison of Load vs Displacement Curves for Specimen B5	117
Figure 5.30	Comparison of Load vs Displacement Curves for Specimen B6	117
Figure 5.31	Comparison of Failure Shapes for Specimen under Combined Loads	118
Figure 5.32	Comparison of Failure Shapes for Specimen under Axial Load Only	118
Figure 5.33	Interaction Curves for Series A and Series B	119
Figure 5.34	Geometry of Stiffened Plate for Parametric Study	120
Figure 5.35	Initial Imperfection Modes Considered In Parametric Study	120
Figure 5.36	Mode 1 Initial Imperfection in ABAQUS Analysis	121
Figure 5.37	Mode 2 Initial Imperfection in ABAQUS Analysis	121
Figure 5.38	Mode 3 Initial Imperfection in ABAQUS Analysis	122

Figure 5.39	Idealization of Residual Stress	122
Figure 5.40	Interaction Curves for Stiffened Plates Considered in Parametric Studies	123
Figure 5.41	Influences of Lateral Pressure on the Ultimate Load of Stiffened Plates	123
Figure 5.42	Changes of Failure Shapes Due to Boundary Conditions	124

LIST OF SYMBOLS

L, B	Overall length and width of stiffened plate
l, b	Length and width of sub-panel
B_e	Effective width of plate
t_p, t_s	Thickness of plate and stiffener
h	Height of stiffener
P, P_u	Axial load and ultimate axial load
P_{exp}	Experimental ultimate axial load
P_{abq}	ABAQUS ultimate axial load
P_{squ}	Squash load
Q, Q_u	Lateral load and ultimate lateral load
Q_{exp}	Experimental lateral load
Q_{abq}	ABAQUS lateral load
E	Young's modulus
σ_y	Yield strength
σ_{exp}	Experimental ultimate stress
σ_{abq}	ABAQUS ultimate stress
υ	Poisson's ratio
λ	Column slenderness $\left(\frac{L}{r}\sqrt{\frac{\sigma_y}{E}}\right)$
r	Radius of gyration of the sectional area

CHAPTER 1 INTRODUCTION

1.1 Background

In many engineering structures, especially in aircraft and ship construction, it is important to save weight to alleviate structures themselves. One of the commonly used structural components is stiffened steel plates. Stiffened and unstiffened plates form the basic members for deck structures and habitation units in offshore structures. Stiffened plates can be longitudinally stiffened or stiffened both longitudinally and transversely. The stiffeners not only carry a portion of load but also subdivide the plate into smaller panels, thus increasing considerably the critical stress at which the plate will buckle. The advantage of reinforcing a plate by stiffeners lies in tremendous increase of strength and stability while minimum increase of weight to the overall structures.

Stiffened plates in marine and offshore structures are usually subjected to combined in-plane load and lateral pressure. For example, the bottom shell of the ship's hull is subjected to flexural compressive stress due to the hogging bending moments and lateral water pressure. Under such combined loading, stiffened plates become unstable due to the presence of axial compression before the unrestricted plastic flow can take place. Thus to predict the ultimate load-carrying capacity of stiffened plates, interaction between the in-plane load and lateral load must be studied completely. The stability of stiffened plates under various loading has been a topic of interest for many years. Researchers investigated the behaviour of stiffened plates either experimentally or numerically. Due to its complexity and many parameters involved, a complete understanding of all aspects of behaviour is not fully realized. Over the years, several

codes and design recommendations for stiffened plates have been developed. However, it is found that no single code provides the most efficient guidance for the design of all structural components subjected to a whole range of loading. Hence, the experimental and analytical study on the strength of the stiffened plates stiffened in both longitudinal and transverse directions and subjected to combined action of axial load and lateral pressure has gained importance.

1.2 Objective

The objective of this study is to investigate the behaviour of stiffened plates subjected to in-plane load and lateral pressure. Both experimental and numerical investigations have been performed to gather sufficient data and understanding of stiffened plates. Finite element package ABAQUS has been used for generation of data for parametrical study. The effects of initial imperfections and residual stresses are investigated. The behaviour of stiffened plates and effects of various parameters are discussed.

1.3 Scope of Investigation

Research efforts have been made on the buckling and collapse behaviour of unstiffened and stiffened plates since 1940s. In the past few decades, a considerable amount of research has been directed towards to the stability of stiffened plates. In the present study, an effort is made to compile all related research topics in a database. Abstract, summary and available experimental data have been included in the database. Available design codes and recommendations are summarized according to the type of applied loading. A search engine has been provided in the database to

facilitate users to find relevant papers by keywords of title and author. A brief review of papers collected in the database is presented in Chapter 2.

A total of twelve stiffened plate specimens with two different slenderness ratios were tested to failure. The specimens were simply supported on edge stiffeners and subjected to different combinations of in-plane load and lateral pressure. The details of stiffened plates, material properties obtained from tensile coupon tests, instrumentation, experimental setup and loading procedures are given in Chapter 3.

With the advance in computer technology, finite element method has become a popular method to the experimental investigation. A finite element package ABAQUS is used for numerical analysis of stiffened plates. The accuracy of the finite element method is verified by comparing the analytical results with the available experimental results. Chapter 4 presents a brief explanation of the finite element method and models used for parametric study.

In Chapter 5, experimental results are summarized and those from the parametric study are given in the chapter. The behaviour of stiffened plates under both axial load and lateral pressure are discussed. Some key parameters such as plate slenderness ratio, imperfection and residual stress affecting the behaviour of stiffened plates are highlighted. Finally conclusions and recommendation for future works are given in Chapter 6.

CHAPTER 2 LITERATURE REVIEW

2.1 Introduction

Stiffened steel plates are used extensively for ship decks and hulls, components of box girder, bridge decks and offshore and aerospace structures. Stiffened plates in marine and offshore structures are usually subjected to the combined action of lateral and in-plane loads. Stiffeners may be provided in longitudinal or transverse directions or both directions. The advantage of stiffening lies in achieving an economical and lightweight design. The presence of stiffeners increases the ultimate load capacity of the plate significantly but it makes the design more complicated due to involvement of more parameters.

In the past few decades, extensive research works have been carried out either analytically or experimentally. A summary of experimental investigations is shown in Table 2.1. Many design methods have been proposed to determine the buckling load and ultimate load capacity of stiffened plates subjected to various loading cases. In order to facilitate the access of related studies on stiffened plate in future, it is necessary to review and summarize the past works. In the present study, an effort is made to compile the publications available to date into a database. A brief description of database is shown in Appendix A. In this chapter, review of papers collected in database is presented.

2.2 Analytical Methods

Over the years, researchers performed the analysis of stiffened plates and many solutions to the problem were presented. Methods have been developed to analyze the

behaviour of stiffened plates. They are generally based on orthotropic plate approach, discretely stiffened plate approach, strut approach and finite element and finite strip methods.

2.2.1 Orthotropic Plate Approach

The basis of the orthotropic plate approach is to convert the stiffened plate into an equivalent plate with constant thickness by smearing out the stiffeners. As illustrated in Figure 2.1, the converted structural element is composed of original plate and equivalent plate. Non-linear equilibrium and compatibility conditions of the plate are solved numerically by large deflection theory. It is found that the method can approximately predict the ultimate strength of stiffened plates with closely and equally spaced stiffeners. However, this method has limited use in understanding the structural behaviour of stiffened plates since it does not consider the discrete nature of the structure. Local buckling of the adjoining plate and tripping of stiffeners are not taken into account. Moreover, difficulty arises when the stiffeners are not equally spaced since the thickness of the converted plate become non-uniform. A major advantage of the orthotropic plate approach over the strut approach is that it accounts for plate action ignored by the latter.

An example of orthotropic plate approach can be found in Hoppman and Baltimore [1]. In their study, orthotropic plate approach was used to analyze simply supported orthogonally stiffened plates under bending and twisting. The stiffness of stiffened plates under static loading was determined experimentally. Their study was extended to dynamically loaded orthogonally stiffened plates with attached stiffeners.

Huffington and Blacksburg [2] investigated the bending and buckling of orthogonally stiffened plate by conceptually replacing the plate-stiffener combination by an "equivalent" homogeneous orthotropic plate of constant thickness. This method was subjected to the limitation of the theory of thin homogeneous plates of constant thickness and also the ratio of stiffener rigidity to plate rigidity.

Soper [3] presented a study on large deflection of stiffened plate subjected to static lateral load using the concept of equivalent orthotropic plates. Equations were derived from von Karman's equations for isotropic plates. Rectangular plates were considered in detail, and an approximate solution was obtained through trigonometric series. The solution from Soper's method allowed for rotational constraint along the plate boundary.

Okada et al [4] used orthotropic approach to investigate the buckling strength of stiffened plates containing one longitudinal or transverse girder under compression. The stiffened plate was idealized by an equivalent orthotropic plate. Non-dimensional design table giving the critical stress for the symmetric buckling of the system were presented and the effective breadth of the stiffened plate which acts with the girder was also calculated.

2.2.2 Discretely Stiffened Plate Approach

In discretely stiffened plate theory, stiffened plates are treated as a collection of plate elements. The plate and the stiffeners are analyzed separately and the assembly is forced to act in a composite manner. The problem thus simplified as analysis of an unstiffened plate with a line of discontinuity in the loading. An illustration of

discretely stiffened plate approach is shown in Figure 2.2. Local buckling and overall buckling as well as the interaction of adjacent elements can be taken into account in the analysis. Moreover, it makes possible to incorporate residual stress and initial imperfection into the analysis with relative accuracy.

Dean and Omid'varan [5] presented a study for analysis of rectangular plates reinforced by flat section stiffeners using a closed form field approach. Three categories of plate-stiffener interaction behaviour were considered. The first approach was a 'composite membrane analysis', in which full composite action was considered in the plane of the plate while the flexural capacity of the plating was ignored. The second approach was a 'non-composite flexural analysis', in which plate-stiffener interaction was considered while in-plane deformations and in-plane continuity were ignored. The third approach was a 'composite membrane-flexural analysis', in which all interactions were considered. The governing equation for all these categories were solved in closed form to obtain deformations in terms of applied loading.

Webb and Dowling [6] presented a new mathematical formulation for the analysis of eccentrically stiffened plates, subjected to the combined or separate actions of lateral and in-plane loading. The proposed formula covered angle and tee section stiffeners as well as rectangular flats. The governing equations were solved numerically by the application of dynamic relaxation to their finite difference equivalents. The effects of initial deformation, combined lateral and in-plane loading and the use of hybrid plates were investigated. Geometrical non-linearity and material non-linearity were considered in the formulation.

2.2.3 Strut Approach

Strut approach or beam-column approach is commonly used in practical design. The main advantage of this approach is the ease of use and because of that, many existing design codes such as British Standard BS 5400 [7], API [8], AISC [9], BCSB [10], ABS method [11] and Norsek Standard [12] are all based on the strut approach. In the strut approach, the stiffened plate is treated as a series of unconnected struts. A strut is composed of a stiffener with associated effective width of plate as shown in Figure 2.3. If any transverse stiffeners present, they are treated as stiff elements to provide nodal lines acting as simple, rotationally free supports to the longitudinal struts. Moment-thrust-curvature relationships for beam-column are employed to obtain the deflected shape of the plate under any applied loading. However, strut approach is not applicable when only a few longitudinal stiffeners are used.

To determine the moment-thrust-curvature relationships, the stress-strain behaviour of the cross-section must be identified. Applicability of the method is dependent on the assumptions made at this stage in the analysis. Kondo [13] presented an analytical investigation of the ultimate strength of longitudinally stiffened plates under axial load by beam column theory. An elastic-perfectly plastic stress-strain relationship was assumed and was modified if necessary to take account of residual stress. The longitudinally stiffened panels failed by excessive bending and can be treated by beam-column if local buckling of the plate is prevented. Study of Ostapenko and Lee [14] found that a longitudinally stiffened panel subjected to lateral loading and axial compression behaves essentially as a beam column. In both Kondo [13] and Ostapenko [14] studies, the unloaded edges were free out of plane.

2.2.4 Finite Element and Finite Strip Method

With advance in computer technology and development in computer software, finite element method (FEM) has become a popular and effective way to analyze the behaviour of stiffened plates. In this method, the stiffened plate is modeled as a series of interconnected elements. The stiffeners are idealized as beam or discretized plate elements as shown in Figure 2.4 (a) and (b). Accuracy of finite element method is dependent on the shape functions (or type of element), number of elements and boundary conditions simulating compatibility along the element boundaries.

Tvergaad and Needleman [15] used Raylegh Ritz finite element method to analyze the buckling of eccentrically stiffened elastic-plastic panels on two simple supports or multiply supported. In their analysis, initially imperfect panels were computed numerically using an incremental method. It is found that the stiffened plates considered are imperfection sensitive, both for panels that bifurcate in the plastic range and for panels with a yield stress a little above the elastic bifurcation stress.

Soreide and Moan [16] studied the behaviour and design of stiffened plates in the ultimate limit state using finite element method. A comprehensive finite element program considering general loading conditions, material properties, geometry, boundary conditions and initially deflections was used. The problems considered include perfect and initial deflected plate-strips, beam columns and failure of a stiffened plate designed for simultaneous local and overall buckling.

Louca and Hauding [17] used finite element method to investigate the torsional behaviour of flat-bar stiffeners in longitudinally stiffened panels subjected to axial

loading. The outstand was modeled both individually and as part of a stiffened panel. The effects of plate slenderness, stiffener slenderness and boundary conditions were considered.

Bai [18] presented a nonlinear finite element procedure based on the Plastic Node Method by combining elastic large displacement analysis theories with a plastic hinge model, directly accounting for the geometrical and material non-linearity and the influence of initial deformation and residual stress. A set of finite elements, such as beam-column elements, stiffened plate elements, and shear panel elements was developed. Applications to the analysis of ultimate strength of stiffened plate were presented and results were compared with tests.

The analysis of stiffened plates by finite element method were also reported by Belkune and Ramesh [19], Chai and Zheng [20], Komatsu et al [21], O'Leary and Harari [22], Guo and Harik [23], Hrabok and Hrudey [24], Sabir and Djoudi [25], Belkune and Ramesh [26], Bhattacharyya et al [27], Bhimaraddi et al [28], Cichocki et al [29], Gendy and Saleeb [30], Grodin et al [31], Jiang et al [32], Kaeding and Fujikubo [33], McEwan el al [34], Mukhopadhyay and Mukherjee [35], Nordsve and Moan [36], Orisamolu and Ma [37], Rossow and Ibrahimkhail [38], Zhou and Zhu [39], Fujikubo and Kaeding [40],Sheikh et al [41], Turvey and Salehi [42, 43], Yao et al [44] and Hu and Jiang [45].

Besides finite element method, finite strip method is also commonly used. Finite strip is a specialized version of finite element method. In the finite strip method, element shape functions use polynomials in the transverse direction, but trigonometric

function in the longitudinal direction. Judicious choice of the longitudinal shape function allows a single element, "strip" to be used. The finite strip method has been used in stability analysis of stiffened plates. This method was employed by Delcourt and Cheung [46] for analysis of continuous folded plates. Kakol [47] used this method to analyze the stability of stiffened plates. Higher order strip was employed to improve the convergence of the method. Guo and Lindner [48] presented a theoretical study on the elastic-plastic interaction buckling of imperfect longitudinally stiffened panels under axial loads by finite strip method. Wang and Rammerstorfer [49, 50] used finite strip method to determine effective width of stiffened plates. Finite strip methods were also reported by Chen et al [51], Sheikii et al [52], Kater and Murray [53], Lillico et al [54], Eduard [55], Yoshida and Maegawa [56] and Xie and Ibrahim [57-59].

2.3 Failure Modes of Stiffened Plates

Stiffened plates in real structures can be subjected to the combined action of in-plane and out-of-plane loadings. Collapse or failure modes of stiffened plates under such loads can be categorized in three types, namely plate collapse, overall grillage collapse (or Euler buckling) and lateral torsional buckling of stiffeners. A panel may be subjected to all failure modes and it will finish up collapsing in the mode which corresponds to its lowest strength. Therefore, a design method must account for all these possible failure modes.

Plate failure usually occurs in the short stiffened panels with a length approximately equal to the width between stiffeners. In real ship structures, the panels are generally much longer than the stiffener spacing and therefore the possibility of having plate

failure is low. Plate failure only exists in some special cases, for example, a stiffened plate with high strength stiffeners and with relatively low strength nearly perfect plate. Under such conditions the plates show a very steep unloading characteristic and the stiffeners are not able to accommodate the drop in load due to plate failure.

Overall grillage collapse is also known as beam-column failure mode. The failure mode of orthogonally stiffened plate is grillage collapse which involves longitudinal and transverse stiffeners. This failure can be influenced by local buckling of base plate or of stiffeners. However it is generally not found in ship structures but may be relevant for lightly stiffened panels founding superstructure decks. Some researchers found that the optimum design of a compressed stiffened plate would be obtained when the strength of the overall buckling mode equal to the strength of the local buckling mode. However, research also found that the interaction of local buckling and overall buckling makes the panel imperfection sensitive and plate fails with violent collapse. These characteristics are undesirable from a safety point of view and therefore stiffened plates are usually designed to exhibit interframe failure. In the case of interframe failure, overall failure of beam-column is triggered by local buckling of the plate or stiffener (without rotation of stiffeners). Overall grillage failure mode is believed to be most favorable mode of failure since it has a more stable post buckling behaviour.

Lateral torsional buckling of stiffener is also referred to as tripping of the stiffener. Tripping involves a rotation of the stiffener about a junction between the plate and the stiffener. Tripping of the stiffener is dependent on the torsional stiffness of the stiffener, which believed to be a determining factor in deciding whether the failure

mode will be plate buckling or stiffener tripping under axial compression. Failure by tripping of the stiffener is the least desirable failure mode since it is characterized by a sudden drop in load capacity just after the peak load is reached.

2.4 Stiffened Plates under In-plane Loading

In the past, many researchers have presented the analysis of stiffened plates under uniaxial compression. There are two different basic approaches for the design of stiffened plates under uniaxial compression. The first method is based on the Rankine equation of failure stress of a simply supported column. The formulas are based on experimental data and are very simple to use. The second approach is well known effective width concept. It is found that for plates wide and thin enough to buckle under load the ultimate load which could be carried does not increase in proportion to the width. Thus effective width instead of actual width is used to calculate the ultimate strength of stiffened plates. Most of the codes and design recommendations are based on the second approach.

Wittrick [60, 61] presented a very general approach to the determination of initial buckling stresses of long stiffened panels in uniform longitudinal compression using finite strip method. The individual flats are assumed to be subjected to sinusoidally varying systems of both out-of-plane and in-plane edge forces and moments, superimposed on the basic state of uniform compression. The panels are assumed to consist of a series of long flat strips, rigidly connected together at their edges. Some computer programs based on the finite strip method have been written for analysis of both isotropic and orthotropic, multi-plate structures in compression.

Dorman and Dwight [62] carried out a series of tests on stiffened panels subjected to uniaxial compressive load. Residual stress and initial geometrical imperfections were measured. Their study found that the presence of residual stress has only a secondary effect on the strength of a stiffened panel. It is also found that the effective breadth approach contained in BS153 appears to give a satisfactory approach for heavily stiffened panels but is unsafe panels have a high b/t value. Experimental investigation of longitudinally stiffened plates under in-plane loads was also reported by Komatsu et al [63, 64], Hu et al [65], Kitada et al [66], Ellinas et al [229], Zha et al [230, 231] and Yamada et al [235].

Plank and Williams [67] presented a method for computing the critical load of prismatic assemblies of rigidly inter-connected thin flat rectangular plates. The plates considered can be isotropic or anisotropic and can carry uniform in-plane shear stresses and transverse stresses in addition to a longitudinal stress which varies linearly over the cross section but is longitudinally invariant. In the complementary method, interaction curves were given for common types of panel in combined in-plane shear and longitudinal compression and bending. It is found that half of these curves are nearly parabolic while some others differ greatly from the parabola but the errors are on the safe side for all the results presented.

Nishihara [68] investigated theoretically the ultimate longitudinal strength of a mid-ship cross section. A simplified analytical method for evaluating the ultimate compressive strength of deck and bottom panels of ship structure was developed. The method was further extended to the case of stiffened panels subjected to compressive loadings and lateral pressure. A parametric study was carried out based on the

proposed method, and two approximate formulas to calculate the ultimate strength of structural elements in a cross section were developed. Based on the ultimate strength of cross section, ultimate bending strength of a cross section was analyzed.

In a series of investigations, Bedair and Sherbourne [69-75] presented their findings on local buckling of stiffened plates under uniform compression and non-uniform compression. Interaction between the plate and stiffener element was highlighted. The influence of rotational restraint, in-plane bending and translation restraints upon the local buckling and post buckling behaviour were investigated. The research was expanded by Bedair and Sherbourne to determine the local buckling load of stiffened plates under any combination of in-plane loading, i.e. compression, shear and in-plane bending.

Ueda et al [76-78] investigated the behaviour of stiffened plate under in-plane loading in a few papers. Investigation into the effectiveness of a stiffener against the ultimate strength of a stiffened plate was carried out. Buckling, ultimate and fully plastic strength interaction relationships for rectangular perfectly flat plates and uniaxially stiffened plates subjected to in-plane biaxial and shearing forces were reported. The validity of the interaction relationships was verified by comparison with the results reported by the researchers. Ueda [79] also presented a simple prediction method for welding deflection and residual stress of stiffened panels.

Alagusundaramoorthy et al [80, 81] presented experimental studies on longitudinally stiffened plates with and without cutouts under uniaxial compression. Stiffened plates with varying plate slenderness ratio and column slenderness ratio were tested to

failure. Initial geometrical imperfection was measured in the experiment. In their first paper, the influence of square openings on the ultimate load of stiffened plate was investigated. They further extended the research to the effect of circular openings and the effects of reinforcement around openings in their second paper. Studies on the stiffened plate with openings were also reported by Shanmugam et al [82], Kuranisi et al [83, 84], Lee and Klang [85] and Guo and Wang [86].

Paik et al [87, 88] investigated analytically the characteristics of local buckling of the stiffener web in the stiffened panels and the tripping failure of flat-bar stiffened panels subjected to uniaxial compressive. The effects of stiffener tripping and plating collapse as well as the influence of elasto-plastic rotational restraint at the plate-stiffener intersection were included in the analysis. Tripping of stiffened plate under axial compression was also investigated by Danielson [89, 90].

Fujikubo and Yao [91] derived an analytical formula for estimating elastic local buckling strength of a continuous stiffened plat subjected to biaxial thrust. The influence of plate/stiffener interaction and welding residual stresses was considered in the formula. The accuracy of formula was verified by FEM results.

Zhang et al [92] presented a semi-analytical method of assessing the residual longitudinal strength of damaged ship hull. Based on the definition of effective area coefficient of damaged ship structural components, the influences of initial deformation on longitudinal strength were regarded as the reduction of section modulus of ship hull. Both longitudinally and transversely stiffened plates were investigated.

Niwa et al [93] presented a new approach to predict the strength of compressed steel stiffened plate from a knowledge of the catastrophe theory. Strength predictions for both local and global buckling were included. The elastoplastic buckling stress was obtained with consideration of the elastoplastic behavior of the material and the residual stresses of both stiffeners and plate panels. Based on the concept of the bifurcation set in the catastrophe theory, the reduction of the ultimate strength due to the initial out-of-flatness can be explicitly determined by the imperfection sensitivity curve.

Wei and Zhang [94] proposed a method based on CPN (Counterpropagation Neural Networks) to predict the ultimate strength of stiffened panels. Numerical study was carried out to verify the validation of this method. Experimental results were also used for verification. Fok et al [95, 96] presented an analysis of the elastic buckling of infinitely wide stiffened plates. The analysis was based on a simplified model of the panel and aimed to determine the interactive behavior of the overall mode of buckling and the local buckling of the stiffener outstands. It is found that stiffened plate is imperfection sensitive for geometries in which the local and overall critical loads are close.

Fan [97] investigated the nonlinear interaction between overall and local buckling of stiffened panels with symmetric cross-sections. In his study, the nonlinear interaction between local and overall buckling modes was taken into account by including a second local buckling mode having the same wave length as the primary mode analytically. Both perfect and imperfect stiffened plates were considered in the analysis. Koiter [98-100] presented interaction of local and overall buckling of

stiffened panels consisting of a flat plate and stiffeners built up from flat plate strips in a series of papers. The concept of slowly varying functions was employed in the derivation of approximate energy expression governing combined local and overall buckling of the panel. Torsion of stiffeners was considered in the analysis. Interaction of local buckling and overall buckling was also studied by Kolakowski [101] and Li and Bettess [102].

Tvergaad [103] studied the imperfection sensitivity of wide integrally stiffened panel under compression. Overall buckling of the panel as a wide Euler column and local buckling of the plates between the stiffeners were considered. It is found that panel is very sensitive to geometrical imperfections when local buckling and overall buckling occur simultaneously. Imperfection sensitivity analysis was also reported by Deng [104].

Numerical analysis of stiffened plate under in-plane loading were also carried out by Chan et al [105], Chong [106], Dohrmann et al [107], Ellinas [108], Elishakoff et al [109], Frieze and Drymakis [110], William and Thomas [111], Hoon [112], Ierusalimsky and Fomin [113], Lillico et al [114], Josef [115], Mikami et al [116], Nakai et al [117], Okada et al [118], Rahal and Harding [119], Rahman and Chowdhury [120], Roren and Hansen [121], Satsangi and Mukhopadhyay [122], Zahid et al [123], Sridharan and Peng [124], Steen [125], Taczala and Jastrzebski [126], Williams and Diffield [127], Yoshinami and Ohmura [128], Yusuff [129], Little [130], Yin and Qian [131], John and Evangelos [132], Toulios and Caridis [133], Dexter and Pilarski [134], Pu and Faulkner[135] and Wen et al [136, 137].

2.5 Stiffened Plates under Combined In-plane and Lateral Loading

Smith et al [138-142] investigated analytically the behaviour of grillage under lateral pressure alone and under combined axial and lateral loads. A generalized plate-beam analysis applicable to interconnected systems of rectangular plates and parallel beams was presented. Computer program was developed based on an approximate method. Influence of torsion on deflections and bending moments in a wide range of grillage structures was accounted. Besides analytical investigation of stiffened plates, Smith conducted a series of tests on full scale welded steel grillages representing typical warship deck. Simply supported specimens were subjected to compressive load combined in some cases with lateral pressure. Initial imperfections and residual stresses were measured in the experiment. A method for approximate prediction of stiffened plate under both axial load and lateral pressure was proposed.

Parsanejad [143] presented a method for the nonlinear analysis of orthogonally stiffened plates subjected to lateral and axial loads using a simple mathematical model. The stiffened plates were assumed to be only longitudinally stiffened and continuous over the transverse stiffeners. Post-buckling behaviour of the plate and the large deflection elasto-plastic behaviour of longitudinal panels were taken into consideration.

Bonello and Chryssanthopoulos [144] proposed a method for predicting the structural reliability of stiffened plates for situations where buckling response was important. Based on the idealization of the load end-shortening relationship by piece-wise linear segments, a plate panel model was developed for predicting the buckling strength of stiffened plates. The proposed model can trace the complete load end-shortening

response of a stiffened plate under axial and lateral loading as well as examine the reliability of the panels under axial compression and lateral pressure. Special emphasis was devoted to examine the effect of the amplitude and mode of the initial geometrical imperfections and of the level of the welding residual stresses.

Danielson et al [145] studied buckling behaviour of stiffened plates subjected to a combination of axial compression and lateral pressure. Von Karman plate equations were used to model the plate and beam theory was employed for stiffeners. Buckling load corresponding to a torsional tripping mode of stiffeners was obtained from the analysis. The effects of various boundary conditions, imperfections and residual stresses were considered in the analysis. Shanmugam and Arochiasamy [146] carried out experiments on longitudinally and transversely stiffened plates under combined loads. Stiffened plates simply supported on all four edges and subjected to combined action of axial and lateral loads were tested to failure. The test specimens were analyzed by finite element method and a comparison between experimental results and finite element analysis results was made.

Bradford [147] carried out a buckling analysis of longitudinally stiffened plates under bending and compression. Verified nonlinear stiffness equations that predict local and post-local buckling of plates and plate assemblies were given. A set of graphs was presented to predict the optimum position of a stiffener in a web plate.

Caridis et al [148, 149] presented a flexural-torsional elasto-plastic buckling analysis of stiffened plates using dynamic relaxation in a series of papers. The development of a numerical model describing the large-deflection elasto-plasto behaviour of flat

plates and attached flat bar stiffeners including the effects of interaction was described in the first part. Verification of theory by experimental results was presented in part two. Several aspects of the behavior of the stiffener and the base plate have been examined and critical buckling strains and loads, and plastic collapse loads have been compared with the test results.

Wang and Moan [150-152] preformed ultimate strength analysis of stiffened panels subjected to biaxial and lateral loading using nonlinear finite element method. The calculated results were compared with the predictions using a beam-column formulation to assess the validity of the beam column approach. It is found that beam-column model is nonconservative in plate-induced failure mode for the interaction of axial compression and significant lateral pressure. Yuren Hu et al [153] studied the tripping of stiffeners in stiffened panels under combined loads of axial force and lateral pressure. A generalized eigenvalue problem for tripping of stiffeners was derived by using the Galerkin's Method. The effect of the lateral pressure to the critical axial stress upon tripping was investigated by solving the eigenvalue problem. An approximate equation to estimate the critical tripping stress with the effect of the lateral pressure was proposed. The modified proposed equation could be applied in design rules for the purpose of checking the tripping strength of the stiffeners.

Hughes and Ma [154] developed an energy method for analyzing the flexural-torsional and lateral-torsional buckling behavior of flanged stiffeners subjected to axial force, end moment, lateral pressure and any combination of these. Total potential energy function was derived based on a strain assumption which coincided with van der Neut's assumption. The study was extended to inelastic tripping, and

results from proposed method were compared with FEM and experimental results. Mansour [155-160] investigated theoretically the behaviour of stiffened plate under combined load in a series of papers. The existing methods of predicting the behavior and ultimate strength of Marine Structure stiffened panels were evaluated, examined and in some instances, further developed. Based on the orthotropic approach, the post-buckling behavior of a stiffened plate with small initial curvature was presented.

Strength of stiffened plate under combined action of in-plane and lateral loads were also investigated by Cui el al [161, 162], Hart el al [163], Ma and Orisamolu [164], Moghtaderi-Zadeh and Madsen [165], Mori et al [166], Nikolaidis et al [167], Paliwal and Ghosh [168], Tanaka et al [169, 170], Yehezkely and Rehfield [171], Zheng and Das [172], Zhou and Wang [173], Kumar [232] and George et al [233].

2.6 Design of Stiffened Plates

In the past few decades, many design methods for stiffened plates have been proposed. Tan [174] summarized the design formulas for stiffened plates subjected to uniaxial load and combined loads. Schade [175-177] presented the design curves for cross-stiffened plating under uniform bending load. Four boundary conditions were considered in the design curves. Any of the possible combinations can be easily analyzed for maximum deflection and stresses by using the design curves. An expression

$$\lambda / b = \sum \frac{\frac{\overline{\lambda_n}}{b} K_n}{\frac{\overline{\lambda_n}}{b} + \beta} \Bigg/ \sum \frac{K_n}{\frac{\overline{\lambda_n}}{b} + \beta} \qquad [2.1]$$

in which $\bar{\lambda}/b$ is boundary function, K_n is loading function and β is section function was proposed to predict the effective width of stiffened plating.

Klitchief et al [178] studied the stability of plates reinforced by a large number of transverse ribs and subjected to compressive loading. Based on the expression for critical compressive forces previously developed by Timoshenko, an expression that gives directly the required rigidity of the ribs was developed. Use of trigonometric series was made to calculate effective width of plate. Effective width of flanges can be calculated as:

$$2S_1 = \frac{2}{(\sigma_y)_{x-s}} \int_0^s \sigma_y dx = \frac{b}{\pi} \frac{4\sinh^2\theta}{\pi(3+\nu)\sinh\theta\cosh\theta - (1+\nu)\theta} \qquad [2.2]$$

where $\theta = \pi s/b, \sigma_y = \left\{ A\cosh\frac{\pi x}{b} + D\left(2\cosh\frac{\pi x}{b} + \frac{\pi x}{b}\sinh\frac{\pi x}{b} \right) \right\} \cos\frac{\pi y}{b}$, s is the effective width of flange and b is overall width of flange.

Dwight and Moxham [179] reviewed the provisions for effective width in BS 153 and BS 449 for plates in compression. A comparison was made between the design method and recent research results. Interaction between local buckling and overall buckling was taken into account. Effect of residual stresses caused by welding was considered and an approximate method was presented for relating residual stress to size of weld. New design rules were tentatively proposed for welded plates in compression based on a load factor of 1.7. The stresses can be calculated as:

(a) Web: $f = \left(\frac{1.65\sqrt{E\sigma_y}}{b/t} - \sigma_r \right) \div 1.7$ *or* $\sigma_y/1.7$, whichever is less. [2.3]

(b) Flange: $f = \sigma_y/1.7$ with b limited as follows:

As welded $b \le \left(0.56\sqrt{E/\sigma_y}\right)t$ [2.4]

Non-welded or stress relieved $b \le \left(0.63\sqrt{E/\sigma_y}\right)t$ [2.5]

Dwight and Little [180] proposed a method for calculating the strength of stiffened steel compression flanges. Local buckling of plate was allowed for and overall buckling between cross-frame is covered by a column-type treatment. An essential feature was the use of an 'effective yield' approach for dealing with the interaction between local and overall buckling, instead of the 'effective section' method. The predicted average compressive plate stress at failure, σ_{pm}, is the lower root of the quadratic:

$$\left(\sigma_y' - \sigma_{pm}\right)\left(\sigma_{pe} - \sigma_{pm}\right) = \eta\sigma_{pe}\sigma_{pm} \quad [2.6]$$

Where $\sigma_y' = \sigma_y$ when shear stress $\tau \le 0.175\sigma_y$, $\sigma_y' = 1.05\sqrt{\sigma_y^2 - 3\tau_1^2}$ when $\tau > 0.175\sigma_y$, σ_{pe} is a stress depends on b/t ratio.

Murray [181, 182] derived a new expression for collapse load of stiffened plates subjected to axial load based on elastic-rigid-plastic idealization of structures. It was shown that Perry-Robertson formula accurately predicts the collapse load and the direction of collapse provided the initial imperfections of stiffened plate were interpreted in a logical manner. The following interaction formula was proposed:

$$\frac{1}{\sigma_f^{\,n}} = \frac{1}{\sigma_E^{\,n}} + \frac{1}{\sigma_c^{\,n}} + \frac{1}{\sigma_y^{\,n}} \quad [2.7]$$

Where σ_E and σ_c are elastic buckling stresses for overall strength and local strength respectively. σ_f is failure stress and $\sigma_{y\,is}$ yield stress. n is a number dependent on the total imperfections.

Carlsen [183-185] proposed a method for stiffened plate under axial load based on Perry-Robertson formulation together with effective width approach. The effective width of stiffened plate stress is given by:

Plate induced effective width: $\frac{b_e}{b} = \frac{1.8}{\beta} - \frac{0.8}{\beta^2} \; for \; \beta > 1$ [2.8]

Stiffener induced effective width: $\frac{b_e}{b} = 1.1 - 0.1\beta \; for \; \beta > 1$ [2.9]

Where β is reduced plate slenderness ratio.

An empirical formula was derived by Allen [186] based on experimental results. According the Allen, ultimate strength of stiffened plate under axial compression can be expressed as

$$\sigma_{ua} = \frac{\sigma_{fs} A_s + \sigma_{fp} A_p}{A_s + A_p} \quad [2.10]$$

σ_{fs} and σ_{fp} are calculated separately through a modified Rankine formula.

$$\frac{1}{\sigma_{fi}^2} = \frac{1}{\sigma_{Ei}^2} + \frac{1}{\sigma_{cri}^2} + \frac{1}{\sigma_{yi}^2}, i = s, p \quad [2.11]$$

Distance from the center of failure to the center of the plate can be obtained by

$$D = \frac{\sigma_{fs} A_s (d + l)}{2\left(\sigma_{fs} A_s + \sigma_{fp} A_p\right)} \quad [2.12]$$

Allen's method is simple but it significantly overestimates the ultimate stress.

Faulkner [187] proposed a method for predicting the ultimate strength of stiffened plate under axial load based on a beam column approach. A comprehensive review of effective plating for use in the analysis of stiffened plating in bending and

compression was also presented by Faulkner [188]. According to Faulkner, the effective width of the plate can be expressed:

$$\frac{b_e}{b} = \frac{2}{\beta} - \frac{1}{\beta^2} \qquad [2.13]$$

This formula was used by the British Navy and has been recommended in Europe for box-girder bridge design.

In a series of investigations, Horne and Narayanan [189-193] proposed a method of computing the collapse load of an axially loaded plate with open-section stiffeners uniformly spaced on one side. In their method, the stiffeners were assumed to be stocky enough to develop yield at their extreme fibers before collapsing by local buckling. The plate was then treated as series of continuous struts which consist of a stiffener and effective width of plate. Perry Robertson formula was used to analyze the strut. The loss of stiffness of the plate and torsional buckling of slender stiffeners were considered in the analysis. The effects of residual stresses and loss of stiffness of wide plates were accounted for by enhancing the initial plate imperfections.

Narayanan and Shanmugam [194] proposed an approximate method of analyzing axially loaded stiffened plates. Energy method was employed and the loss of stiffness of the flange plate and of the stiffener was account for. The influence of residual stresses was considered in the analysis. Long panels were analyzed as axially loaded individual single span struts which could be treated as beam column. Modified form of the Perry-Robertson formula was used for analysis. Collapse load of stiffened plate can thus be calculated as:

$$\sigma_{cs} = \sigma_a + 0.003\left(\frac{l - l_o}{r}\right)\left(\frac{\sigma_a.\sigma_e}{\sigma_e - \sigma_a}\right) \qquad [2.14]$$

Where $l_o = 0.2\pi r\sqrt{\left(E/\sigma_{ys}\right)}$ when $l \geq l_o$, $l_o = l$ when $l < l_o$, σ_a is mean stress causing failure, σ_e = Euler Stress.

Shanmugam et al [195] proposed a design method for stiffened steel panels using effective width concept. Stiffeners were assumed to be stocky and the local buckling of stiffeners was neglected in the analysis. The effective width can be calculated by

$$b_e = b\sqrt{\frac{\sigma_c}{\sigma_e}}\left(1 - 0.25\sqrt{\frac{\sigma_c}{\sigma_e}}\right) \qquad [2.15]$$

Where σ_c is the longitudinal stress at the junction of stiffener and plating, σ_e can be assumed to be from $\sigma_{cr}/4$, b is overall width of plate and b_e is effective width of plate. The research was further extended to stiffened plates containing circular or square openings subjected to axial load by Shanmugam et al [82]. Experiments were conducted and an approximate method predicting the ultimate strength of stiffened plates with openings was proposed.

Soares and Gordo [196, 197] proposed a simplified method for design of stiffened plates under predominantly compressive loads based on the existing methods. Behaviour of unstiffened plate elements and of stiffened panels was considered. The validity of the proposed method was assessed by comparing the results obtained from the proposed method with experimental results and numerical calculations.

Based on the orthotropic plate approach, Jetteur [198] proposed a new simplified method for the design of stiffened compression flanges of large steel box girder bridges. Non-uniform stress distribution in the flange was taken into account in the

design method and shear lag effects on the plate buckling was allowed. Physical differences between plate buckling under uniform and non-uniform compression were observed.

Taido et al [199] presented a design method to evaluate the ultimate strength of stiffened plates used for the wide compression flange plates of shallow box girders. A design criterion to ensure the buckling stability of wide orthogonally stiffened plates subjected to uniaxial compression was first developed. An alternative design method for orthogonally stiffened plates was proposed. The ultimate strength of stiffened plates subjected to biaxial forces was discussed based on the finite element analysis and experimental study. Boote et al [200] proposed a simplified formulation for calculating plate breadth that acts with stiffener. Finite element method was used to analyze the effective breadth regarding both stiffness and strength. From their proposal, effective width B_σ can be obtained as:

$$B_\sigma / B = \left[1 - e^{(0.005t - 0.649).(L/B)^{(-0.027t + 1.067)}} \right] \qquad [2.16]$$

Where B_σ is an artificial effective breadth on which the distribution of stresses is assumed to be uniform across the breadth and equal to the maximum value.

Bonello et al [201] compared the predictions of ultimate load from several codes with numerical results from an inelastic beam-column formulation and test results. In order to explore the inherent differences in column behavior separately from discrepancies arising due to plate panel behavior, the code predictions were reevaluated adopting a common plate panel effective width formulation.

Design of stiffened plate under lateral pressure only was proposed by Caridis [202]. The analysis was carried out using Dynamic Relaxation, a finite-difference based procedure which had been used to solve the Marguerre equations in the large-deflection elasto-plastic range. According to Caridis, lateral load to cause 3-hinge collapse in fully built in plate can be presented by

$$q_0 = \frac{4\sigma_y}{\left(1-\nu-\nu^2\right)}\left(\frac{t}{b}\right)^2 \qquad [2.17]$$

Based on the orthotropic plate theory, Mikami and Niwa [203] proposed an approximate method to predict the ultimate strength of orthogonally stiffened steel plates subjected to uniaxial compression. All possible collapse modes which occur on the orthogonally stiffened plates were considered in the proposed method. The ultimate strength predicted by the proposed method was compared with test results of longitudinally and orthogonally stiffened steel plates subjected to uniaxial compression.

Based on the strut approach, Usami [204] proposed a method for computing the ultimate strength of stiffened box members in combined compression and bending. The computed results for simply supported stiffened plates in compression and bending were compared with FEM results. Johansson et al [205] presented new design rules for plated structures in Eurocode 3. Design of stiffened plates for direct stress, design of plates for shear and design of plates for patch loading were presented. The statistical calibration of the rules to tests was described.

Gordo et al [206] proposed a method to estimate the ultimate strength of hull girder based on a simplified approach. Degradation of the strength due to corrosion and residual stresses were included in the proposed method. Evaluation of strength of the hull at several heeling conditions was also included. Anderson [207] presented a method to include local post-buckling strength response in the design of stiffened panel. Computer code VICONOPT was used and the post buckling analysis capability developed at the University of Wales was used to provide the post buckling stiffnesses for all plates when the load was greater than the initial buckling load. Design results for column and panel structures were given in the paper. Their results indicated the benefit of reduced mass for panel structures utilizing post-buckling strength.

Kitada et al [208] presented design methods of simply supported, outstands and stiffened plates made of high strength steel and mild steel subjected to compression. Design strength curves were derived as the regression curves of the ultimate strength curves. The stiffened plates concerned were used in the steel bridge. Effect of earthquake was taken into account in the analysis.

In a series of investigations, Paik et al [209-213] presented ultimate strength formulation of stiffened plates under different loading conditions. Failure modes of stiffened plates were categorized into six groups in a benchmark study. The panel ultimate strengths for all potential collapse modes were calculated separately. The results were then compared to find the minimum value which was taken to correspond to the real panel ultimate strength. It was found that the plate-induced failure mode based on Perry-Robertson formula reasonably predicts the panel ultimate strengths in

a specific range of stiffener dimensions which follows the beam-column type collapse mode. It was also found stiffener-induced failure mode based on Perry-Robertson formula generally provides too pessimistic results. Paik's method covered a wide range of loading and failure modes. Verification of Paik's method with experimental results and finite element analysis results showed good agreement.

Chou et al [214] presented a practical method for designing bulb-flat-stiffened plating against local buckling, without limitations on section slenderness. Behavioural insight and validation is provided by 60 finite element solutions. A modified Perry equation was proposed for the design strength of imperfect bulb flat stiffeners, taking into account the restraint provided by the plate. In their method, the strength of the stiffened plate was given by adding the stiffener strength to the plate strength.

Bijlaard [215] presented a method for the design of transverse and longitudinal stiffeners for stiffened plate panels. The structural analysis covered two types of instability. One was the instability of transverse stiffeners subjected to a load which increased with the deformations and was produced by the primary load acting within the plane of the plate. The other was the torsional buckling instability of longitudinal stiffener of open cross-sectional shape which were primarily subjected to compressive load. Rules for the analysis of both forms of instability were derived.

2.7 Optimization of Stiffened Plates

Many researchers contributed to the optimum design of stiffened plates. Lehata and Mansour [216] developed a methodology for structural optimization of stiffened panels based on reliability. The stiffened plates considered were part of ship structure

and assumed to be under still water and wave induced loads. A nonlinear program was developed to calculate the minimum weight with behaviour constraints on reliability and physical constraints on the dimensions. A detailed approach was developed by Mansour et al [217] for assessing structural safety and reliability of ships.

Tvergaad [218] investigated optimum design of an eccentrically stiffened wide panel under compression with simultaneous occurrence of local buckling and overall buckling. Maximum carrying capacities were calculated approximately by application of Galerkin's Method. It was found that the best design is usually one in which the critical stress for Euler-type buckling is smaller than that for local buckling from the point of view of retaining highest stiffness at the highest possible load level. Also, the optimum design from the point of view of post-buckling behaviour often differs significantly from the design with two simultaneous buckling stresses.

Brosowshi and Ghavami [219, 220] presented optimal design of stiffened plates in series of papers. Several experimental investigations were first carried out to establish the most satisfactory approximate method for calculation of the ultimate load of stiffened plates subjected to axial compression load. Perry – Robertson formula modified by Murray [182] was found to be the best approximate method. This formula was used for fast calculation of compromise points for the multi-criteria design of stiffened plates. The design variables considered were the number, the thickness and the height of the stiffeners for a specific plate thickness.

Hatzidakis and Bernitsas [221] proposed optimization design of orthogonally stiffened plates. In the first part, size optimization was discussed. In the second part, shape optimization was performed. Weight optimization designs of stiffened plates were reported by De Oliveira and Christopoulos [222], McGrattan [223], Rothwell [224], Williams [225] and Peng and Sridharan [226]. Farkas and Jarmai [227] presented the optimum design of stiffened plates considering the optimal position of horizontal stiffeners. Toakley and Williams [228] reported optimum design of stiffened plate under compression.

Table 2.1 Summary of Experiments on Stiffened Plates

	Author(s)	Ref. No.	Year	Stiffeners arrangement	Loading(s)	No. of test	Variables studied	Remarks
1	Ostapenko, A. Lee, T. T.	14	1960	Longitudinal	Uniform lateral loading and axial compression	5	Plate slenderness ratio b/t, Aspect ratio of sub-panel l/b, stiffener area to base plate area ratio A_{st}/bt, intensity of lateral load q	T-stiffeners were used
2	Kondo, J.	13	1965	Longitudinal	Axial load and hydrostatic pressure	2	stiffener area to base plate area ratio A_{st}/bt, Stiffener flange area to stiffener area A_f/A_{st}	Beam-column approach was used for analysis
3	Dorman, A. P. Dwight, J. B.	62	1973	Longitudinal	Axial compression	12	Plate slenderness ratio b/t	Imperfection and residual stress were measured
4	Smith, C. S.	141	1975	Longitudinal and transverse	Axial compression and lateral pressure	12	Plate slenderness ratio b/t, stiffener area to base plate area ratio A_{st}/bt, the slenderness ratio a/k* of longitudinal girders	Imperfection and residual stress were measured

Continued on next page

Table 2.1 (continued)

	Author(s)	Ref. No.	Year	Stiffeners arrangement	Loading(s)	No. of test	Variables studied	Remarks
5	Horne, M. R. Narayanan, R.	189	1976	Longitudinal	Axial compression	8		The effects of welding was studied
6	Horne, M. R. Narayanan, R.	190	1976	Longitudinal	Axial compression	34	Plate slenderness ratio b/t, column slenderness ratio l/r, boundary conditions	Residual stress and initial imperfection were measured
7	Komatsu, S. Ushio, M. Kitada, K.	63	1976	Longitudinal	Axial compression	15	Plate slenderness b/t, boundary conditions	Initial deflections were measured
8	Ellinas, C. P. Croll, J. G. A. Kaoulla, P. Kattura, P.	229	1977	Longitudinal	Axial compression	3	Stiffener depth to the lateral spacing between longitudinal stiffeners b/d, stiffener depth to stiffener thickness d/t	
9	Yamada, Y. Watanabe, E. Ito, R.	235	1979	Longitudinal	Axial load	7	Plate slenderness b/t, stiffener area to base plate ratio A_s/bt,	Finite element and simplified element method presented

Continued on next page

Table 2.1 (continued)

	Author(s)	Ref. No.	Year	Stiffeners arrangement	Loading(s)	No. of test	Variables studied	Remarks
10	De George, D Michelutte, M. M. Murray, N. W.	233	1980	Longitudinal	Combined axial and lateral load	18	Loading, failure mode	Bulb flat or trough stiffeners
11	Shanmugam, N. E. Paramasivam, P. Lee, S. L.	82	1986	Longitudinal	Axial compression	15	Plate slenderness b/t, stiffener depth to the lateral spacing between longitudinal stiffeners b/d	Stiffened plates contain circular or square openings
12	Parsanejad, S.	143	1986	Longitudinal and transverse	Axial load and lateral load	15	Plates slenderness ratio b/t, stiffener depth to the lateral spacing between longitudinal stiffeners b/d, Aspect ratio of sub-panel l/b	Analytical method was presented
13	Caridis, P. A. Frieze, P. A	149	1989	Longitudinal	Axial load and lateral load	7	Stiffener slenderness d/t, lateral load	
14	Kitada, T. Nakai, H. Furuta, T.	66	1991	Longitudinal	Longitudinal tension and transverse compression	4	Initial deflections	Open and closed cross section stiffeners were used.

Continued on next page

Table 2.1 (continued)

	Author(s)	Ref. No.	Year	Stiffeners arrangement	Loading(s)	No. of test	Variables studied	Remarks
15	Shanmugam, N. E. Arockiasamy, M.	146	1996	Longitudinal and transverse	Combined axial and lateral loads	10	Plate slenderness ratio b/t, lateral load	
16	Hu, S. Z.; Chen, Q. Pegg, N. Zimmerman, T. J. E	65	1997	Longitudinal	Combined axial and lateral loads	12	Lateral load, boundary condition	T stiffeners were used
17	Alagusundaramoorthy, P. Sundaravadivelu, R. Ganapathy, C.	80	1999	Longitudinal	Axial compression	12	Plate slenderness ratio b/t, column slenderness ratio l/r	Openings were introduced in the stiffened plate
18	Pan, Y. G. Louca, L. A.	234	1999	Longitudinal	Gas explosion	3	Boundary condition, effect of stiffeners	
19	Tan, Y. H.	174	2000	Longitudinal	Combined axial and lateral load	14	Plate slenderness b/t, sub-panel ratio l/b, stiffener area to base plate ratio A_s/bt, intensity of lateral pressure	Lateral load is concentrated point load

Continued on next page

Table 2.1 (continued)

	Author(s)	Ref. No.	Year	Stiffeners arrangement	Loading(s)	No. of test	Variables studied	Remarks
20	Zha, Y. F. Moan, T Hanken, E.	231	2000	Longitudinal	Axial load	25	Stiffener web height, stiffener thickness, plate thickness, heat-affected zone, residual stress	Material is aluminium
21	Lavan Kumar, C.	232	2001	Longitudinal and transverse	Combined axial and lateral load	6	Plate slenderness ratio b/t, column slenderness ratio l/r	Software NISA was used for FEM analysis
22	Zha, Y. F. Moan, T	230	2001	Longitudinal and transverse	Axial load	13	Stiffener web height, stiffener thickness, plate thickness, heat-affected zone	Material for stiffened plates was aluminum

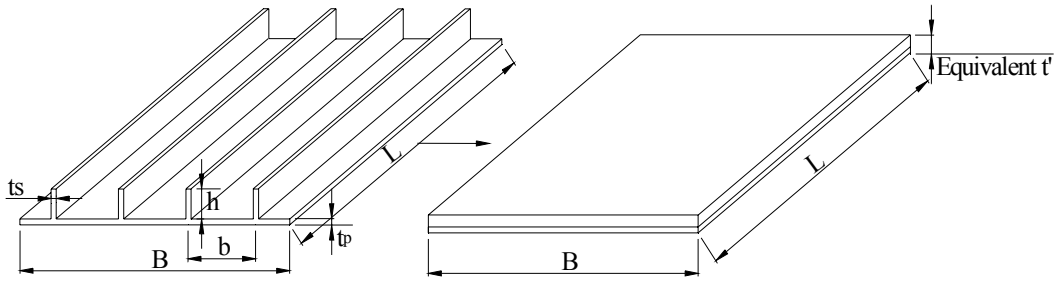

Figure 2.1 Orthotropic Plate Idealization

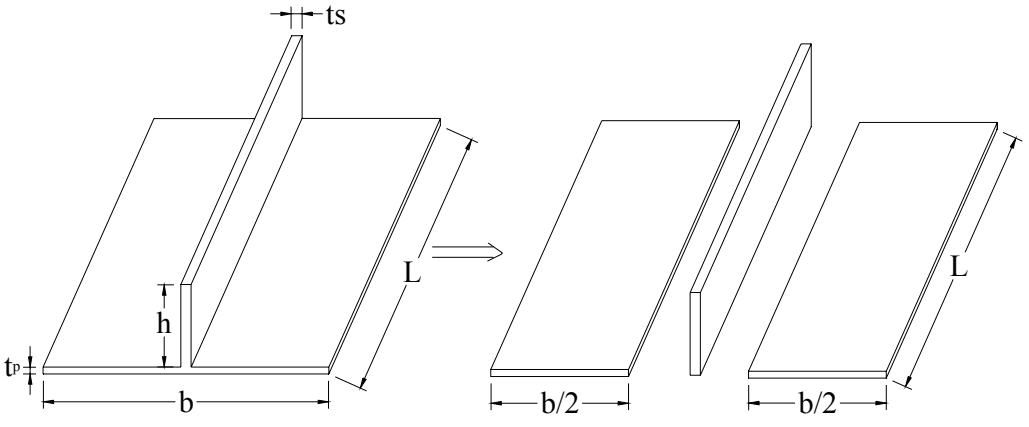

Figure 2.2 Discretely Stiffened Plate Idealization

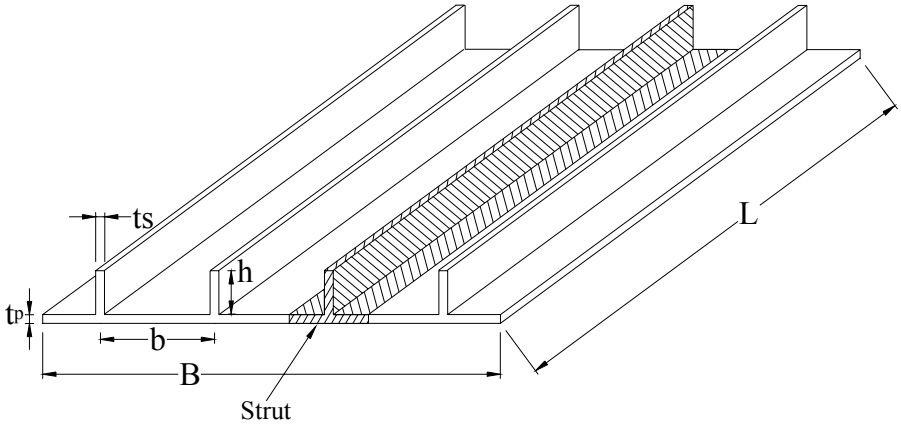

Figure 2.3 Strut Approach Idealization

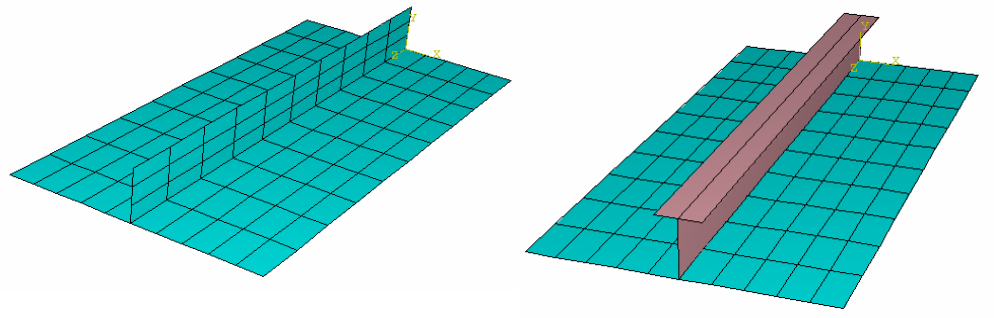

(a) Discretized plate elements (b) Plate and beam elements

Figure 2.4 Finite Element Idealizations

CHAPTER 3 EXPERIMENTAL INVESTIGATION

3.1 Introduction

To investigate the ultimate load capacity of stiffened plates subjected to in-plane load and uniform lateral pressure, 12 specimens were tested to failure. The tested specimens were divided into two groups, namely series A and series B. Plate slenderness ratios (b/t_p) of series A and series B were kept as 100 and 76, respectively. The behaviour of stiffened plates under combined in-plane load and lateral pressure was observed. The interaction of axial load and lateral pressure was investigated. The experimental results were compared to the finite element results to check the validity and accuracy of the finite element modelling. In this chapter, details of the test specimens, imperfection measurement, experimental setup, instrumentation and test procedures are described.

3.2 Details of Test Specimens

The test specimens were fabricated using hot-rolled steel plating of Grade 50 which complied with BS4360. The base plates and stiffeners were first cut to the required size. To avoid any severe distortion and change of material properties, saw cut instead of flame cut were used. The specimens were formed by assembling the base plate and stiffeners in specific locations and tack welded intermittently. Longitudinal stiffeners were first attached to the base plate by means of tack-welding technique. Attachment of shorter sections of transverse stiffeners was achieved by similar technique. Continuous welding was then carried out along the stiffeners. Sufficient time was allowed for cooling to minimize the effect of initial distortion caused by excessive heating at particular location and to keep the residual stress minimum. All welds were

continuous 6 mm fillet welds and E43 electrode was used. Once stiffeners were connected to base plate, two end plates were welded to the stiffened plate. End plates essentially ensure a uniform transmission of axial load from the horizontal thrust girders to the stiffened plate. Completed specimens were free from twist, bends and warps. Care was taken during delivery to ensure no damages to the specimen.

The overall dimensions of the specimens were kept 1200 mm x 900 mm (L x B) and both longitudinal and transverse stiffeners were provided. The thickness of base plate and stiffeners were 2.9 mm and 5.92 mm respectively. The dimensions of specimens were selected based on finite element analysis by considering the limitation on the capacity of hydraulic jacks and size of air bag used to apply lateral pressure. The two series A and B of specimens are identified in the text as A1-A6 and B1-B6, respectively and the detailed dimensions are summarized in Table 3.1. Figures 3.1 and 3.2 illustrate the dimensions of specimens with three sub-panels and four sub-panels, respectively. The plate slenderness ratios (b/t_p) for series A and series B were kept as 100 and 76, respectively. The slenderness ratio of stiffeners for both series was 8.4. The slenderness ratios were selected such that stiffeners remain stocky allowing local buckling in base plate to occur.

Coupons were tested to determine the material properties of the base plates and stiffeners. Four coupon specimens were cut from the same stock of steel section for base plate as well as stiffeners. The coupon test specimen is illustrated in Figure 3.3. Linear strain gauges were mounted on the coupons. Tensile tests were carried out with strain control. Stress-strain curves were drawn and yield strength and Young's modulus were obtained. Typical stress-strain curve is shown in Figure 3.4. The stress-

strain curves for each coupon tested are shown in Appendix B. A summary of material properties is shown in Table 3.2.

3.3 Imperfection Measurement

Due to manufacture and delivery process, geometric imperfections always exist in the stiffened plates. Geometric imperfections refer to deviation of a member from 'perfect' geometry. Imperfections of a member include bowing, warping, and twisting as well as local deviations. Local deviations are characterized as dents and regular undulations in the plate. Thin walled structures like stiffened plates are usually imperfection sensitive. The presence of geometric imperfections may influence buckling and behaviour of structure. It is therefore important to investigate the influence of geometric imperfection on the ultimate load and failure shape of stiffened plates. In this study, geometric imperfections of stiffened plates were measured and included in the finite element analysis.

In order to measure the geometric imperfections, a measurement device simple yet reliable was fabricated. Figure 3.5 shows a view of the device. Figure 3.6 is an illustration of the side view of imperfection measurement device. A 25 mm displacement transducer with an accuracy of 0.002 mm was used for measuring purpose. The displacement transducer can move along the beam and the beam can travel transversely along the supporting frame. The surfaces of beam and supporting frame were machined to smooth and oiled to minimize the friction during measurement. Before the measurement, the specimen was properly placed on the base frame such that there was no disturbance with the movement of displacement transducer. Measurement was started from one corner of the specimen and the first

measurement point was set to zero as reference point. Imperfection was measured by first moving the displacement transducer along the beam in transverse direction followed by movement of the beam along the supporting frame in the longitudinal direction. Readings from the displacement transducer were captured by digital data logger and saved in a floppy disk. After measurement of whole specimen, deflections at some selected locations were measured again to double check reliability of the first time measurement. If readings from the second time measurement for all the selected locations agreed well with the readings from the first set of measurements, the measured initial imperfection was accepted. The number of measurement points along the width and length of specimen are 37 and 49, respectively. Typical imperfection profile obtained from the measured imperfections of a stiffened plate is shown in Figure 3.7.

3.4 Experimental Setup

A test rig in which stiffened plates can be tested under both in-plane load and lateral pressure was used in this project. An overview of test rig is shown in Figure 3.8. The test rig is capable of applying lateral force up to 500 kN and axial force up to 1000 kN. An extremely stiff thrust girder forms part of the axial loading frame to transfer the axial load completely from hydraulic jacks to the specimen. Swivels were introduced at both ends in order to allow rotation at the ends of the specimens. The base support consisted of some smooth harden steel bearing plates oiled to minimize possible friction force when specimen are subjected to axial load. Sufficient stiffeners were provided in the support frame so that the deflections of support frame were negligible under maximum lateral loading. The height of the base support was so adjusted that the centroidal axis of the specimen coincided with the middle plane of the thrust

girder. Axial load was controlled by a loading device capable of applying a total load of 100 tonnes and monitored by two load cells with a capacity of 50 tonnes each. Lateral loading was applied by an actuator with a capacity of 50 tonnes and monitored by a load cell with same capacity. Height of actuator was properly adjusted so that it could compress the air bag to predetermined load within its stroke. All the load cells were connected to a data logger which could capture the loading with the increment of load or with change of time. An air bag with overall dimension of 914 mm x 914 mm was used to apply lateral pressure to specimen. A thick stiff steel plate is attached to the end of the lateral actuator to transfer the lateral load to the air bag. The air bag filled by compressed air was capable of applying load up to 70 tonnes. By compressing the air bag, uniform lateral pressure was applied to the specimen. The details of experimental setup are shown in Figure 3.9.

3.5 Instrumentation

The stiffened plate was instrumented with load cells, displacement transducers and strain gauges to monitor the load, deflections and strains. Two load cells were attached to the axial thrust girder with their centers coinciding with the centers of hydraulic jacks. Vertical load was monitored by a load cell with a capacity of 50 tonnes. Linear Variable Displacement Transducers were used to measure axial shortening of specimen under axial load and lateral deformation under lateral pressure. Two displacement transducers were placed at the extreme ends of the thrust girder to monitor the axial shortening of the specimens. In order to check any possible movement of fixed thrust girder under axial load, a displacement transducer was placed at the center of the fixed thrust girder. Some displacement transducers were located at different stiffener joints to measure the lateral deformations of specimen at

different locations. Rosette electrical resistance strain gauges of gauge length 5 mm were mounted at selected locations on the base plate and stiffeners of stiffened plate. Post yield strain gauges were used so that they were able to function and capture the reading of strain even after yielding of steel. All load cells, displacement transducers and strain gauges were connected to a data logger, which is capable of record readings with increment of load, or with time interval. The load-displacement readings were fed into an X-Y plotter which enabled tracing of the on-set of failure in a specimen. The details of displacement transducer and strain gauge locations for stiffened plates with three sub-panels and four sub-panels are shown in Figures 3.10 and 3.11, respectively.

3.6 Test Procedure

All specimens were tested with four edges simply supported at stiffener side and subjected to different combinations of axial load and lateral pressure. Before testing, strain gauges were mounted at appropriate locations for all the specimens. The specimen was then carefully positioned on the test frame without any disturbance to strain gauges. Care was taken to ensure that the centroidal axis of specimen coincided with the center line of moving thrust girder. The specimen was also adjusted with respect to the actuator applying the vertical load in order to ensure proper application of lateral pressure at pre-determined location. Air bag was placed on top of the specimen and the center was adjusted to coincide with the center line of the vertical actuator and stiffened plate. Compressed air was pumped to air bag until when the depth of air bag reached 240 mm.

After placing the displacement transducers at selected locations, a small trial load was applied, released and re-applied to ensure proper seating of the specimen on the test rig and the functioning of instruments. The axial load and lateral pressure were applied simultaneously with axial load reaching the pre-determined level much faster than lateral pressure. With the axial load maintained constant at that level, the specimen was tested to failure by gradually increasing the lateral pressure. Readings of strain gauges and displacement transducers were recorded for each increment of load as well as each time interval of 20 seconds. Pressure inside the air bag was recorded manually at selected load level. The ultimate lateral load at failure could be determined from the load-deflection curve of computer output.

For both series, all the specimens were tested to failure under different combinations of loadings. A1 and B1 were tested to failure under lateral pressure only. A6 and B6 were tested under axial load only. Rest of the specimens were tested to failure under different combined action of axial load and lateral pressure.

3.7 Measurement of Contact Area of Air Bag

Due to the geometrical shape of the air bag, it became ellipsoid when filled with compressed air. During the test, the contact area of air bag with specimen gradually increased with the increase of lateral load. When the lateral load reached certain value, the air bag became flat and fully in contact with the specimen. Figure 3.12 shows the initial state of air bag. In order to include the change of contact area into numerical analysis, the contact area of air bag with the specimens with change of lateral load was measured.

In the measurement of contact area of air bag with the specimen, a 50 mm thick steel plate instead of specimen was used. The thick plate has little deflection under the maximum lateral loading. Before measurement, the air bag was properly placed on the steel plate with its center coinciding with the center of steel plate and the actuator. The air bag is pumped with compressed air up to a depth of 240 mm which has been used as a standard in all the tests. Figure 3.13 illustrates the measurement. Lines were drawn on the steel plate to help measuring the contact area of air bag with steel plate. Such lines are shown in Figure 3.14. The distances from the boundary to the contact points of air bag with steel plate along all these lines were measured one by one. Readings were taken at the initial state and every 5 kN increment of lateral load. The contact area of air bag with steel plate was calculated. From the measurement, it is found that the contact area of air bag with specimen is approximately a rounded square. It is also found that the air bag is fully in contact with specimen when the lateral load reaches 70 kN. Change of lateral pressure applied on the specimen with change of total lateral load is plotted in Figure 3.15. At the initial stage, pressure does not increase linearly with the increase of lateral load due to change of contact area. When lateral load reaches 70 kN and the air bag becomes flat and comes fully in contact with specimen, pressure on specimen increases linearly with increase of lateral load.

Table 3.1 Dimensions of All Specimens

	Stiffened Plate Components Dimensions												Loadings	
	Base Plate			Longitudinal Stiffener			Transverse Stiffener			End Plate			Axial Load	Lateral Load
	L (mm)	B (mm)	t (mm)	L (mm)	B (mm)	t (mm)	L (mm)	B (mm)	t (mm)	L (mm)	B (mm)	t (mm)	P (kN)	Q (kN)
A1	1200	900	2.9	1200	50	5.92	214	50	5.92	900	75	10	0	246.3
A2													170	201.6
A3													300	147.4
A4													400	112.8
A5													500	75.1
A6													712	0
B1	1200	900	2.9	1200	50	5.92	284	50	5.92	900	75	10	0	250.9
B2													200	203.8
B3													400	145.7
B4													520	95.4
B5													630	93.3
B6													785.4	0

L: Length B: Width t: Thickness

	Series A	Series B

Table 3.2 Material Properties for Base Plate and Stiffeners

	Sample No.	1	2	3	4	Average
Base Plate	Yield Strength (N/mm^2)	343	368	335	341	347
	Young's Modulus E (GPa)	204	190	197	172	191
Stiffeners	Yield Strength (N/mm^2)	333	335	327	337	333
	Young's Modulus E (GPa)	185	191	199	199	194

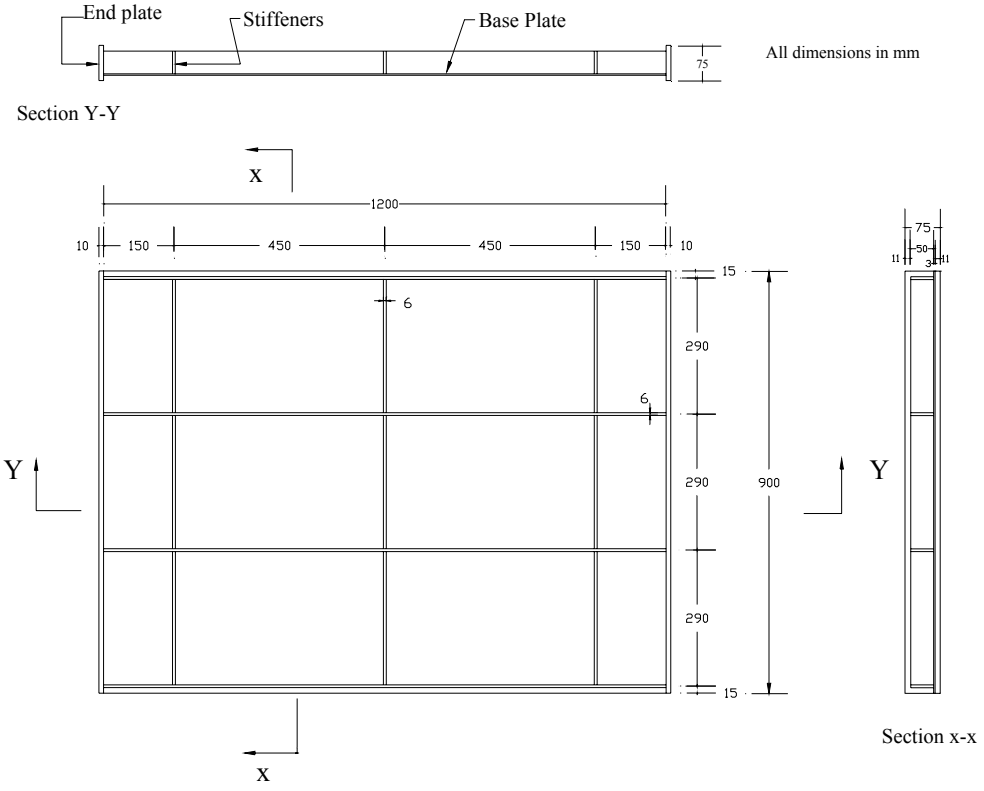

Figure 3.1 Dimensions of Series A Specimen in mm

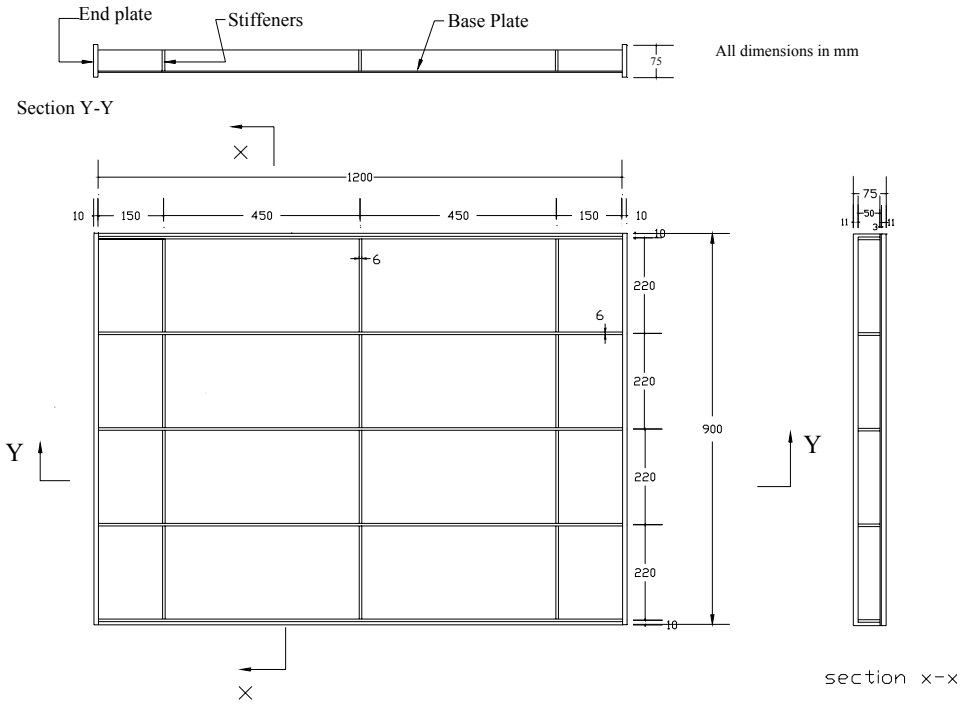

Figure 3.2 Dimensions of Series B Specimen in mm

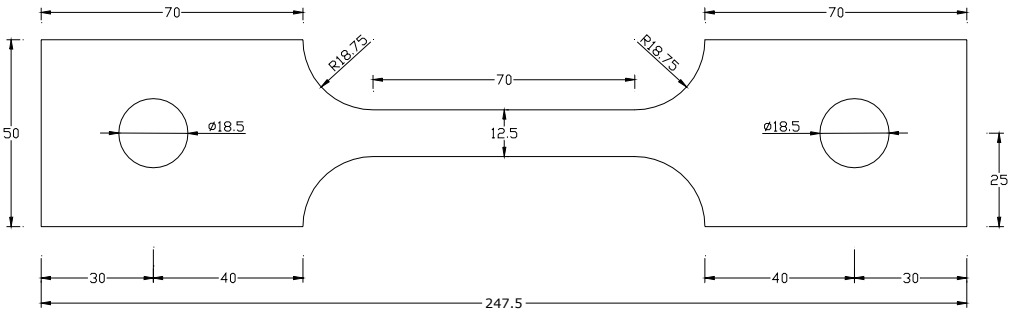

Units: mm

Figure 3.3 Tensile Coupon Specimen

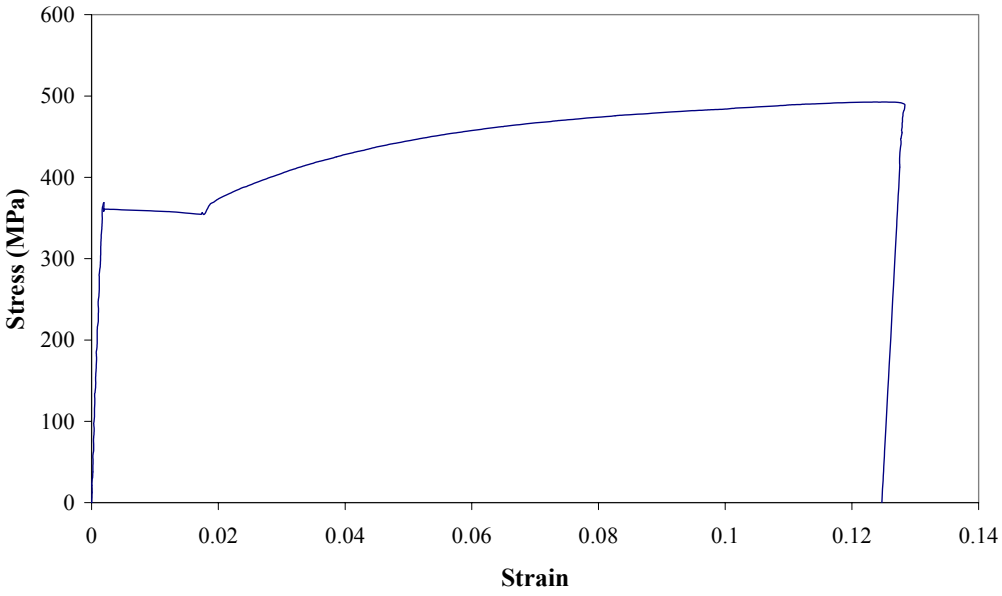

Figure 3.4 Typical Stress-Strain Curve for Steel Used

Figure 3.5 Imperfection Measurement Device

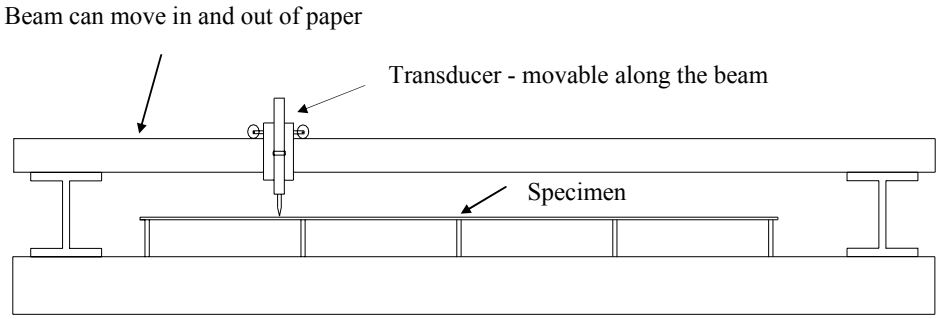

Figure 3.6 Side View of Imperfection Measurement Device

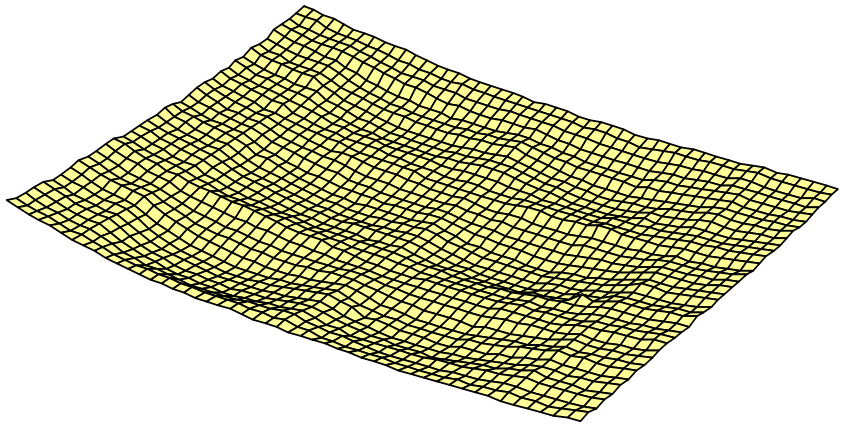

Note: Out-of-plane deflections are magnified

Figure 3.7 Typical Example of Measured Initial Imperfections in a Stiffened Plate

Figure 3.8 Overall View of the Test Rig

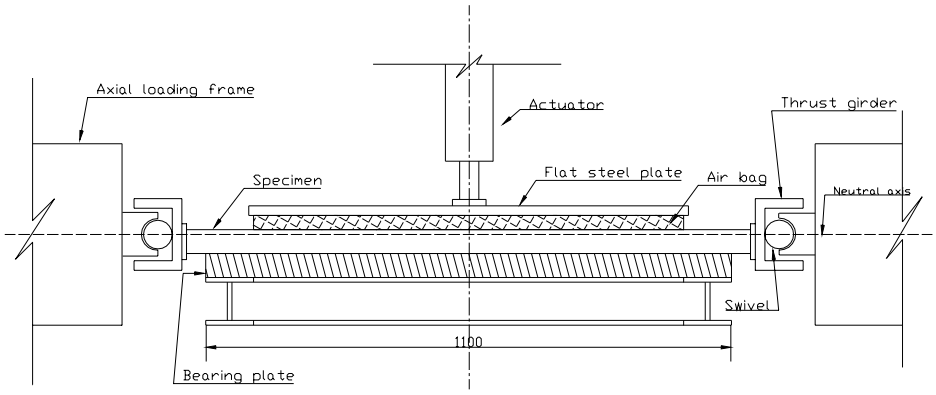

Figure 3.9 Sectional View of the Experimental Setup

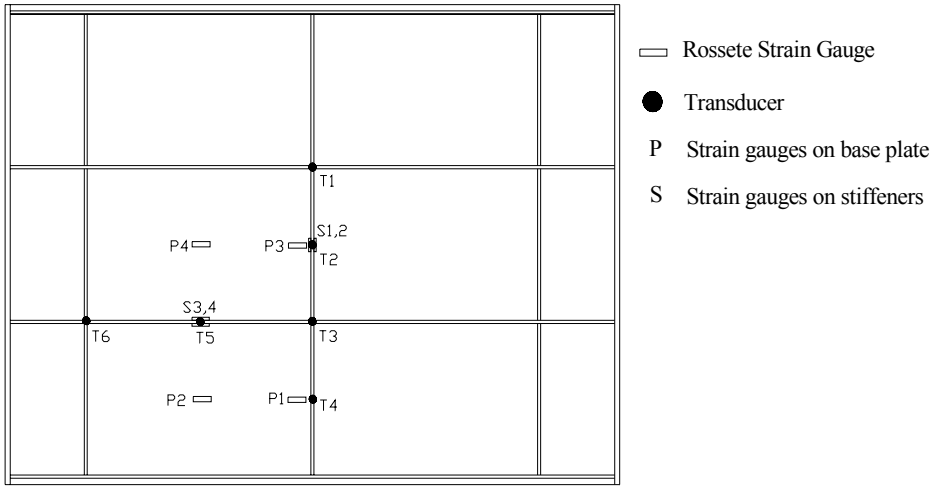

Figure 3.10 Location of Strain Gauges and Displacement Transducers for Series A Specimens

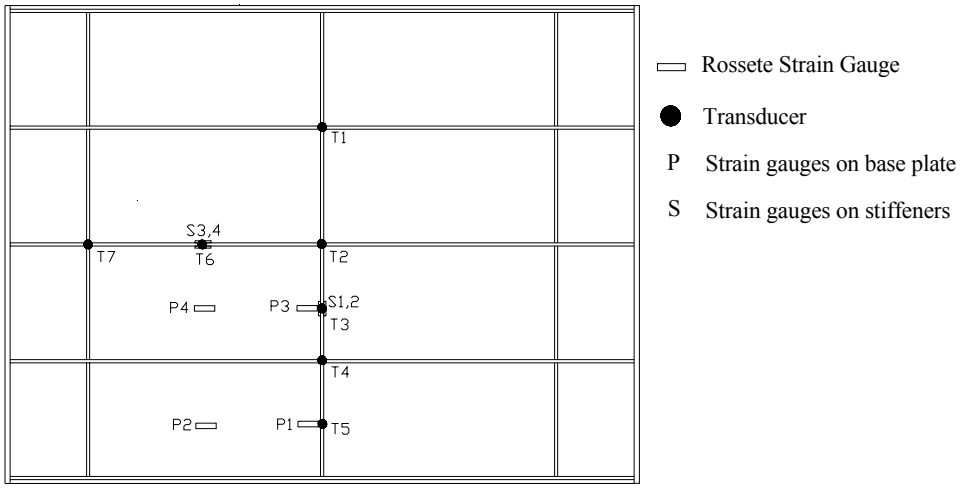

Figure 3.11 Location of Strain Gauges and Displacement Transducers for Series B Specimen

Figure 3.12 Initial State of Air Bag during the Test

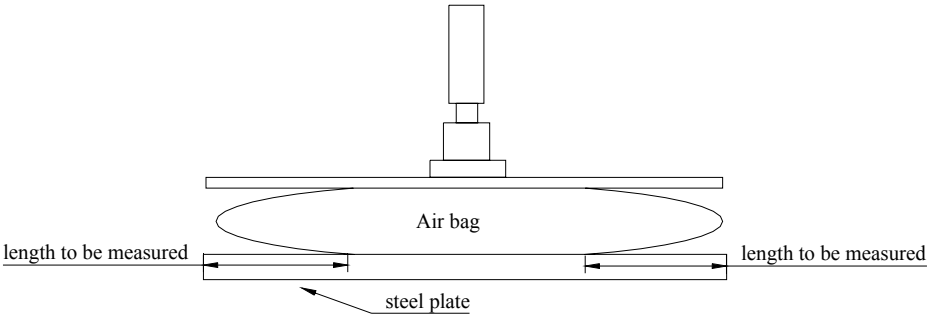

Figure 3.13 Illustration of Contact Area Measurement

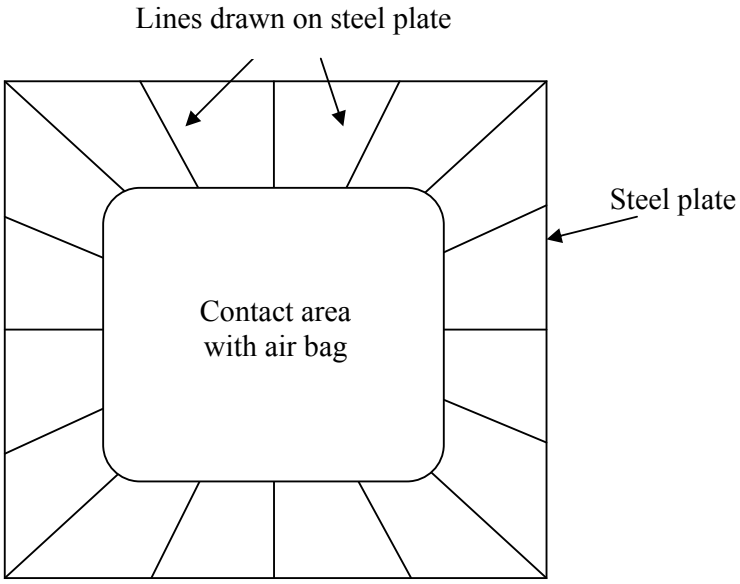

Figure 3.14 Top View of Contact Area Measurement

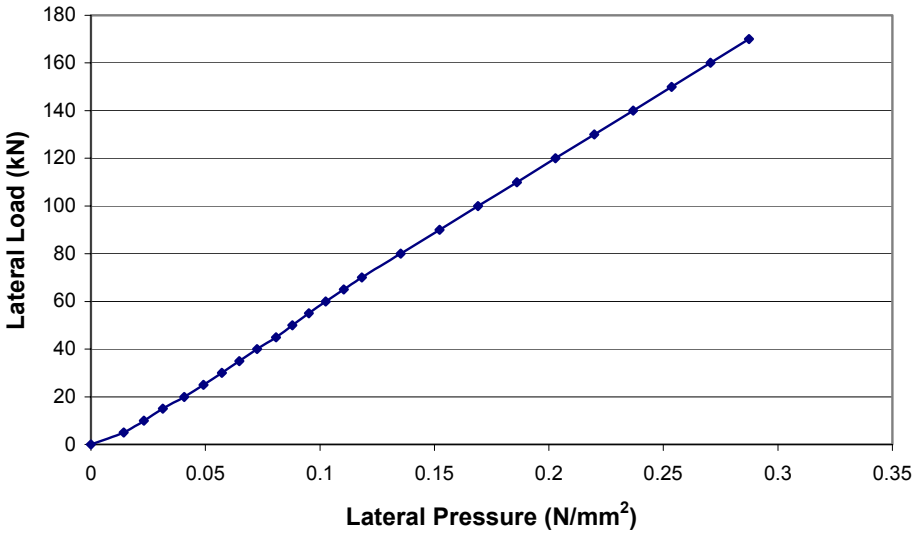

Figure 3.15 Change of Lateral Pressure on Specimen with Change of Lateral Load

CHAPTER 4 NUMERICAL INVESTIGATION

4.1 Introduction

The development of design methodology for a particular structural type normally follows the determination of structural behavior using experimental or numerical studies. The accomplishment of finite element method (FEM) in the analysis of complex structural problems promises outstanding possibilities for solution of the present problem as well. As is well known, the use of finite element techniques results in generality to represent complex geometries and can be versatile enabling the inclusion of large deformation, large rotations and non-linear stress-strain characteristics. In the current study, a comprehensive finite element package ABAQUS is used to simulate the behaviour of stiffened plates subjected to in-plane load and lateral pressure.

Three stages are involved in the finite element analysis, namely pre-processing, processing and post-processing. Preparation of data, such as boundary conditions, loading and mesh generation is carried out using ABAQUS CAE. The processing stage involves stiffness generation, stiffness modification, and solution of equations, resulting in the evaluation of nodal variables. Other derived quantities, such as gradients or stresses, may be evaluated at this stage. The post-processing stage deals with presentation of the processed results, which include deformed configuration, mode shapes, and temperature and stress distribution etc. The three stages involved in the finite element analysis are listed in Figure 4.1.

Nonlinear finite element models of the test specimen were first carried out. Those tested by the author and other researchers were considered for the analyses. Results from the analyses were used to establish the accuracy of the finite element model. Once the accuracy of the finite element analysis is verified, some practical sizes of stiffened plates representing possible ship bottom configurations were modeled to study the effect of some parameters on the behaviour of stiffened plates. Results from the finite element analyses for specimens conducted by the author are plotted and discussions on the results are presented in Chapter 5. An overview of numerical investigation is presented in Figure 4.2.

4.2 ABAQUS Pre-processing

4.2.1 Boundary and Loading Conditions

Boundary and loading conditions are modeled as close to the actual experimental conditions as possible so that the numerical results can be used to validate the reliability of the FEM investigation. Stiffened plates were modeled as simply supported along the edge stiffeners. All nodes along the boundaries were restrained in the vertical direction and the nodes along one of the transverse edges were restrained in the longitudinal direction to simulate the actual boundary conditions in the experiment. Two corner nodes along one of the longitudinal edges were restrained in the model to prevent the free movement of stiffened plates along the transverse direction.

In the modeling by the author, axial load was applied as uniform distributed pressure onto the part of the unrestrained end plate with resultant force of the axial pressure coincided with the centroid axis of the stiffened plate. Uniformly distributed lateral

pressure was applied in three steps with different magnitude and the corresponding contact area. The measured contact area of air bag with the specimen corresponding to lateral pressure was included in the numerical model. The areas of lateral pressure application adopted in each of the steps are shown in the shaded areas in Figure 4.3. According to the experimental measurement, the contact area of air bag with specimen concentrates on the area A in Figure 4.3 when lateral load is less than 10 kN. When lateral load is increased gradually from 10 kN to 70 kN, the contact area increased gradually from area A to area B. Since the change of contact area is not so significant, it is assumed in the numerical analysis that the contact area remained at area B when total lateral load changed from 10 kN to 70 kN. Similarly from 70 kN to the ultimate lateral failure load, the contact area was assumed to remain at area C. All specimens were first applied with axial load followed by stepwise lateral pressure. Sufficient increments were provided in each step and caution was taken to avoid any sudden jump in strain. The size of increment can be determined automatically by program or adjusted manually based on experience. In most cases, the increment determined by program was good enough to provide satisfactory results. However, manual adjustment was always necessary according to the magnitude of loading to ensure convergence of analysis. The ultimate axial load was obtained from the summation of resultant forces in the passive end and the ultimate lateral load was obtained from the summation of vertical resultant forces along the edge stiffeners.

4.2.2 Mesh Generation

A suitable model was developed for the mesh generation process and then the mesh was created to represent the geometry. The success of mesh generation depended on the appropriate selection of element size, shape and type. Type, shape, number and

grading of elements are crucial to the accuracy of the finite element analysis. It is necessary to understand how the structure is likely to behave and how elements are able to behave. In general, the essential of the finite element method is piecewise polynomial interpolation and selection of elements of such a type and size that deformation of the structure over the region spanned by an element is closely approximated by deformation modes that the element can represent. Triangular elements are less accurate than equivalent quadrilateral elements and should not be used in areas where high stress gradients are expected unless a very fine grid is used with due consideration [174].

Hence, in the present study, a surface model consisting of 8-noded doubly curved thin shell, reduced integration, using five degrees of freedom per node was used to avoid any ill-conditioning in the analysis. Many shell element types in ABAQUS use reduced integration to form the element stiffness. The mass matrix and distributed loadings are still integrated exactly. Reduced integration elements usually provide more accurate results, and significantly reduce computer-running time, the elements are of type S8R5 in ABAQUS terminology. The S8R5 element is chosen because it is a powerful eight-node standard ABAQUS plate-bending element that allows for changes in the thickness as well as finite membrane strain. Typical mesh is shown in Figure 4.4. Convergence study was performed in order to establish a suitable mesh size for the analyses of stiffened plates, which give economical computing time and consistent result. For the modelling of specimens conducted by the author, same mesh was used for specimens in each series so that consistent results were ensured. The aspect ratio of element in the current study was kept within the range 1:1 to 1:5.

4.2.3 Material Non-linearity

Material non-linearity can be accounted by appropriate selection of material model in ABAQUS. Classical metal plasticity model is appropriate for general collapse analysis. The classical metal plasticity models in ABAQUS use standard von Mises yield surface models with associated plastic flow. This yield surface assumes that the yield of the metal is independent of the equivalent pressure stress. Associated plastic flow means, as the material is yielding, the inelastic deformation rate is in the direction of normal to the yield surface. In the present study, non-linear elasto-plastic model was selected and perfect plasticity was used. At the analysis stage, non-linear analysis was performed to account for material non-linearity.

4.2.4 Initial Imperfection

Initial imperfection was included in the model. In the present study, finite element analyses were performed both for models with measured imperfection from experiment and for models with nominal imperfection suggested in the ABAQUS manual. The results from models with measured imperfection are compared with those from the models with nominal imperfection and the differences in results are discussed.

For the nominal imperfection, in the ABAQUS model, there are generally two methods to introduce the initial imperfection. The first method makes use of the model anti-symmetry and defines the imperfection by means of a FORTRAN routine that used to generate the perturbed mesh, using the data stored on the results file written during the eigenvalue buckling analysis. The second method uses the *IMPERFECTION option to define the imperfection. This option requires that the

model definitions for the buckling prediction analysis and the post-buckling analysis be identical. The *IMPERFECTION command tells the solver to retrieve the buckling mode shape profile to be included. The solver will then retrieve certain percentage of the contour of specified mode shape profile as the initial geometry of the model and solve the problem from there. In the present study, second method was employed to include nominal geometrical imperfection in the finite element analysis. Full sine curve buckling mode in each sub-panel was assumed for initial imperfection. The initial imperfection imposed is one time of the first elastic buckling mode displacement. A sample input file with simple explanation is shown in Appendix C.

To include the measured imperfection into the analysis, another compatible software PATRAN was used as ABAQUS preprocessor. PATRAN was used mainly to create the mesh and geometry properties of the model. The advantage of PATRAN as preprocessor is that the measured deflections corresponding to the locations can be input in the model. Smooth surfaces were created with measured deflections. Due to the welding process, some corners of stiffened plate were distorted. The distortions of corners were neglected in model to avoid severe distortion of elements. After imperfect geometry creation and mesh generation in PATRAN, the file generated was converted to ABAQUS version 6.3 input file by adding additional information such as boundary conditions and output commands.

4.3 ABAQUS Processing

After the mesh generation, all the meshing data are converted into standard ABAQUS input for analysis. After the conversion, data lines should be included in order to account for all the material and geometric non-linearity, the incremental-iterative load

steps and required output commands in accordance with ABAQUS/Standard program language.

The processing stage involved stiffness generation, stiffness modification, and solution of equation, resulting in the evaluation of nodal variables. To include nominal imperfection into the analysis, two types of analyses were involved. First, bifurcation buckling (eigenvalue) analysis was used to obtain estimates of the buckling loads and modes. Such studies also provided guidance in mesh design because mesh convergence studies were required to ensure that the eigenvalue estimates of the buckling load have converged: this requires that the mesh be adequate to model the buckling modes, which are usually more complex than the pre-buckling deformation mode. First elastic buckling mode displacement was used as nominal imperfection profile in the present study. The second phase of the study was performance of non-linear analysis (load-displacement analysis), usually using the RIKS Method to handle possible instabilities. These analyses would typically study imperfection sensitivity by perturbing the perfect geometry with different magnitudes of imperfection in the most important buckling modes and investigating the effect on the response. For analysis of model with measured imperfection, the bifurcation buckling analysis was not performed since the model created contained the measured imperfection. Only non-linear analysis was performed for models with measured imperfections

In the current modelling, axial force was modelled as uniform axial pressure. Large displacement analysis is used in ABAQUS whenever the large deflection behaviour is

anticipated for stiffened plates under combined action of axial load and lateral pressure. Either the exact or modified Newton's method is used as solver criteria in ABAQUS to establish convergence of solving balance equations. The solution procedure is based on an updated stiffness matrix and changing load vector in this case. Therefore, application of load should prevail in the case of plasticity problem. All these can be done automatically by ABAQUS.

4.4 ABAQUS Post-processing

ABAQUS post analysis provides graphical displays of ABAQUS models and results. Load vs displacement curve can be plotted at any selected load step and deflected shapes at any load step are also made possible by this package. Stress distribution can be presented as graphs or contour plots. The change of deflected shapes and stress distribution can also be visualized by animation. Other major capabilities include model plotting which include deformed and undeformed shapes, contour plotting which displays values of analysis variables as colour regions or lines on the surface of the model, vector plotting, X-Y plotting which display analysis or user-defined data as curves on an X-Y graph, and animation. Numerical results on nodal stresses, reaction forces and displacement are also available. Typical first mode buckling shape of stiffened plate and load vs displacement curve are shown in Figures 4.5 and 4.6, respectively.

4.5 Limitations of Finite Element Analysis

The use of finite element method to predict the behaviour of stiffened plate has some limitations such as modelling and loading limitations. In the current study, difficulties

arose when creating exact measured imperfection from experiment. The corners of stiffened plate used in experiments were mostly distorted due to the heavy welding in the corners of stiffened plate. Modelling of such distorted corners in finite element introduces some distorted elements and causes convergence problem in analysis. Therefore, the imperfections of corners were not modelled to avoid any analysis problem.

Due to limitations in finite element analyses, the loading sequence modelled in finite element method was slightly different from experiment. In the experiment, axial load and lateral pressure were applied simultaneously with axial load reaching predetermined level much faster than lateral pressure. However, in the finite element method, axial load was applied first to predetermined level followed by application of lateral pressure. In the experiment, contact area of air bag with specimen was keep changing with change of lateral pressure. Whereas in the finite element modelling, only three contact areas were used at different level of lateral pressure. The difference of contact area at certain lateral pressure affects the overall deflection of stiffened plate. The method used in finite element only gives an approximate simulation of real experiment.

4.6 Accuracy of the ABAQUS Analysis

Accuracy of ABAQUS analysis needs to be established before the results are used for carrying out any parametric study. The accuracy of finite element analysis depends on a few factors such as material properties, boundary condition and mesh generation etc. The reliability of ABAQUS results has been proven by many researchers despite of

various limitations. In the present study, both experimental data from published literature and the current study were used to verify the accuracy of the ABAQUS analysis. Two sets of experimental studies from the literature were considered in the present investigation. In one set, two series of test on stiffened plate with longitudinal and transverse stiffeners tested by Lavan Kumar [232] under combined in-plane and lateral loads were examined. Two base plate slenderness ratio (b/t=80 and 64) were considered in the experiments. Table 4.1 lists the material properties and, the detailed dimensions of specimens are shown in Figure 4.7. In the second set full scale welded steel grillages tested by Smith [141] were examined in detail. Four specimens tested under combined axial and lateral load were selected for finite element analysis. Details of specimens may be found in Reference [141]. The stiffened plates were loaded with axial load and lateral pressure with lateral pressure reaching required level much faster than axial load. The specimens were tested to failure with gradually increased axial load.

Although ABAQUS is able to produce complete set of results including the stress distribution as well as strain distribution, only ultimate load carrying capacity and failure shapes are compared with existing experimental results. Table 4.2 shows the comparisons of experimental results and ABAQUS results for specimens tested by Lavan Kumar [232]. FEM results from Lavan Kumar which using software NISA are also included in the table. It can be observed from the comparison that ABAQUS can produce quite accurate results. Comparison between the experimental failure loads and finite element loads show reasonable agreement. The ABAQUS failure load to experimental failure load ratio ranges from 1.01 to 1.13. The discrepancy between the results lies within 10% except in the case of sp5b for which it is 13%. Comparing

with two finite element software used, NISA generally gives lower values than experimental results whereas ABAQUS tends to give slightly higher values.

A comparison of experimental results and ABAQUS results for specimens tested by Smith [141] is shown in Table 4.3. Experimental results from Smith were used as verification examples by a few researchers. In Table 4.3, analytical results and FEM results from Paik [213] were included. It can be seen that experimental results are generally lower than ABAQUS results. However the difference between experimental results and ABAQUS results are within acceptable range. Smith [141] reported large residual stresses for the stiffened plate tested. In ABAQUS analysis, residual stresses were not included. The discrepancy between experimental results and ABAQUS results may be due to the effect of large residual stresses. The view after failure of a typical specimen tested and the corresponding finite element prediction are shown in Figure 4.8. It is observed from the figure that ABAQUS analysis can accurately predict the failure pattern of stiffened plate. From the comparisons of two sets of results, it can be seen that ABAQUS can predict not only the ultimate load of stiffened plate but also the failure pattern of stiffened plate. It can, therefore, be concluded that the use of finite element package to predict the ultimate loads of stiffened plates subjected to combined action of axial and lateral loads is reliable. A more detailed comparison of ABAQUS results and experimental results from the current study is presented in Chapter 5.

Table 4.1 Yield Stress and Young's Modulus of Material
(Lavan Kumar's specimens) [232]

No.	Specimen	Thickness (mm)	σ_y (N/mm^2)	E (N/mm^2)
1	Plate	4	218	1.8 x 10^5
2	Plate	5	292	1.8 x 10^5
3	Stiffener	5	300	1.8 x 10^5

Table 4.2 Comparison of Experimental and Finite Element Results for Specimens tested by Lavan Kumar [232]

No.	b/t	Lateral pressure (kN/m^2)	Ultimate load (kN)			P_{abq}/P_{exp}	P_{NISA}/P_{exp}
			P_{exp}	P_{abq}	P_{NISA}*		
sp4a	80	0	983	998	900	1.02	0.92
sp4b	80	60	839	853	750	1.02	0.89
sp5a	64	0	1220	1340	1200	1.10	0.98
sp5b	64	60	1011	1140	1020	1.13	1.01
sp5c	64	120	963	968	950	1.01	0.99

* FEM results from Lavan Kumar [232]

Table 4.3 Comparison of Experimental and Finite Element Results for Specimens Tested by Smith [141]

Grillage No.	Lateral pressure (psi)	Compressive Stress		$\frac{\sigma_{abq}}{\sigma_{exp}}$	$\frac{\sigma_{FEA-1}}{\sigma_{exp}}$ *	$\frac{\sigma_{FEA-2}}{\sigma_{exp}}$ *	$\frac{\sigma_{ULSAP}}{\sigma_{exp}}$ *
		σ_{exp} (tsi)	σ_{abq} (tsi)				
1b	15	12.1	13.1	1.08	0.781	0.781	0.849
2a	7	15.9	16.9	1.06	0.890	0.890	0.868
3a	3	11.1	12.3	1.11	1.000	0.913	1.000
4b	8	13.5	14.1	1.04	0.880	0.916	0.976

1. Exp = Experimental results, abq = ABAQUS results
2. *Analysis results are from reference [213]
3. FEA-1 =with average imperfections, FEA-2 = with actual imperfections
4. ULSAP stands for the software developed for Paik's proposed method

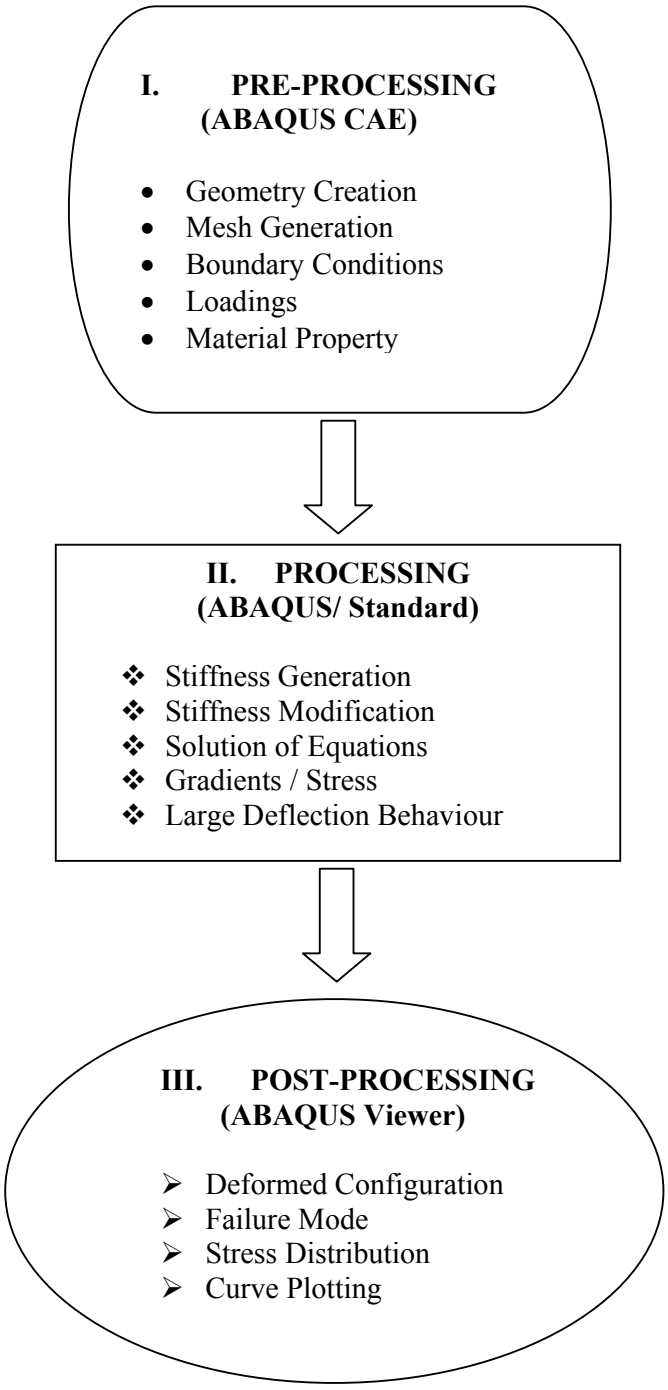

Figure 4.1 Three Stages of Analysis

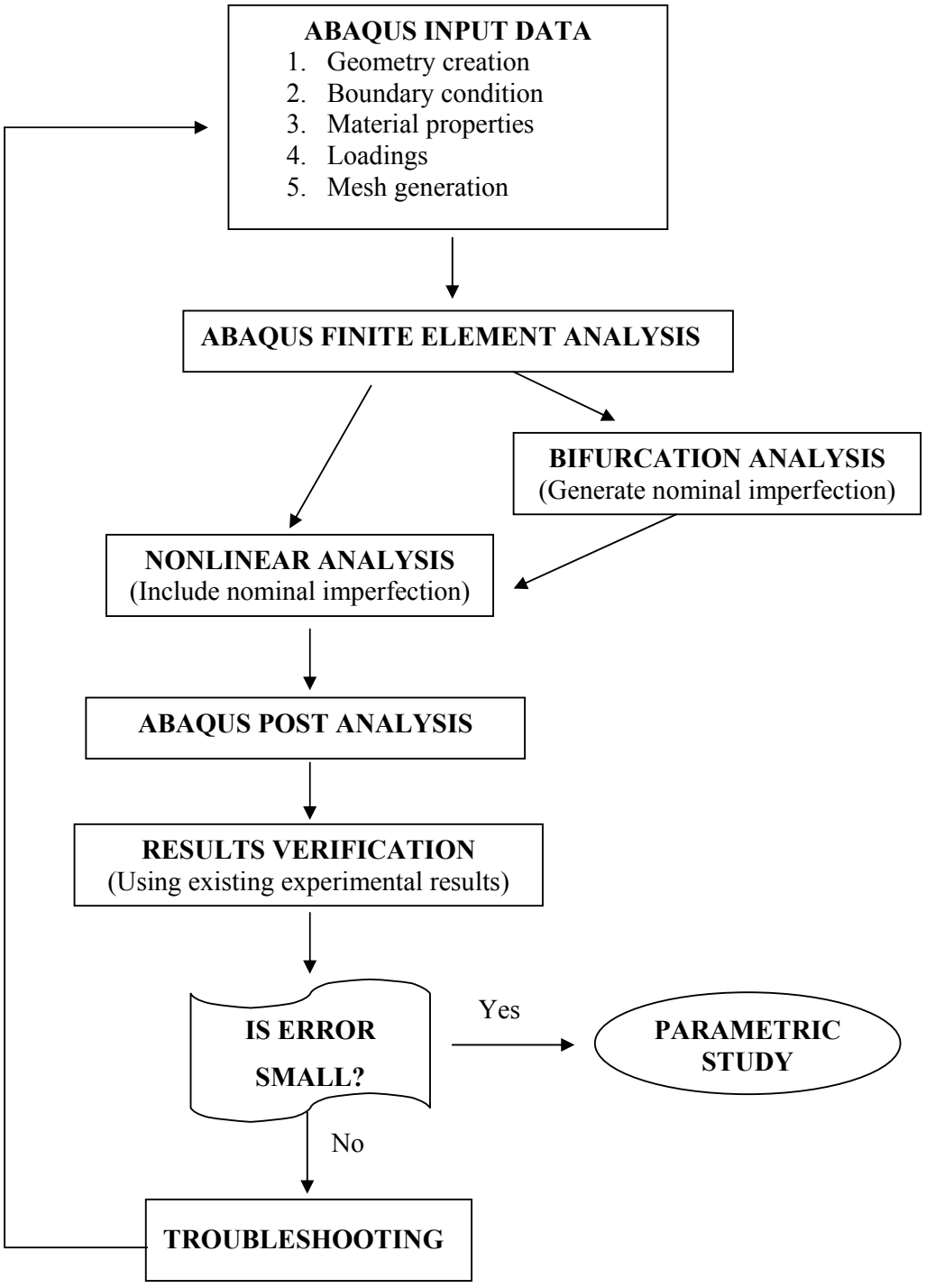

Figure 4.2 Flow Chart of Numerical Investigation

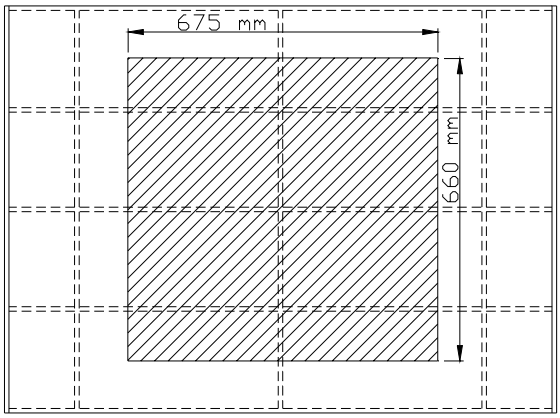

(a) Area A for lateral load from 0 to 10 kN

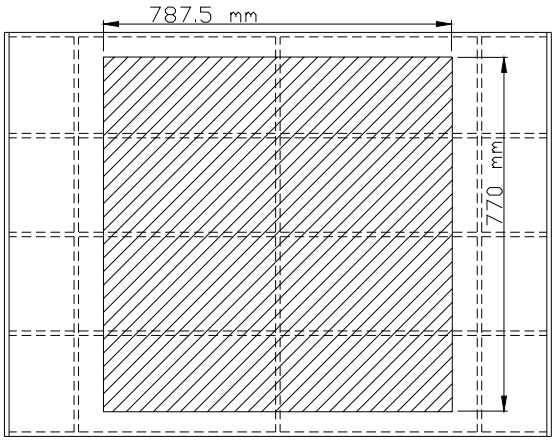

(b) Area B for lateral load from 10 to 70 kN

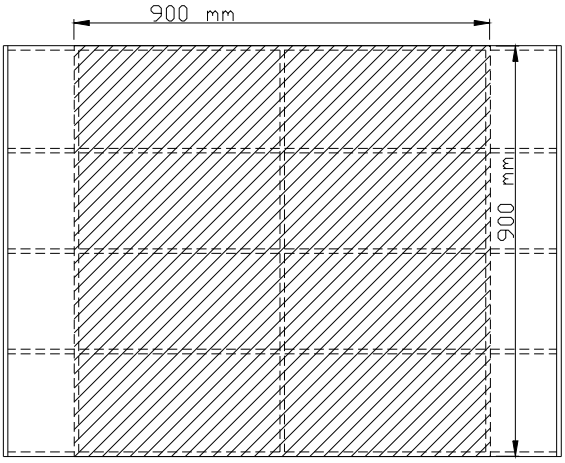

(c) Area C for lateral load from 70 kN onwards

Figure 4.3 Change of Contact Area at Different Loadings

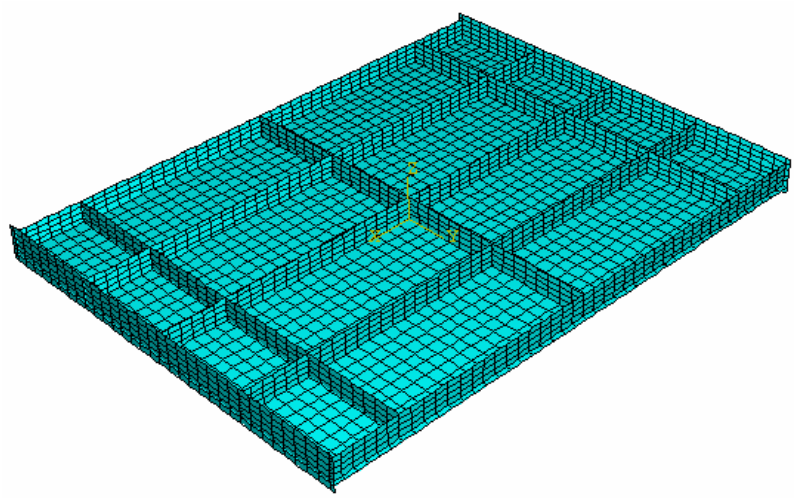

Figure 4.4 Typical Mesh of Stiffened Plate

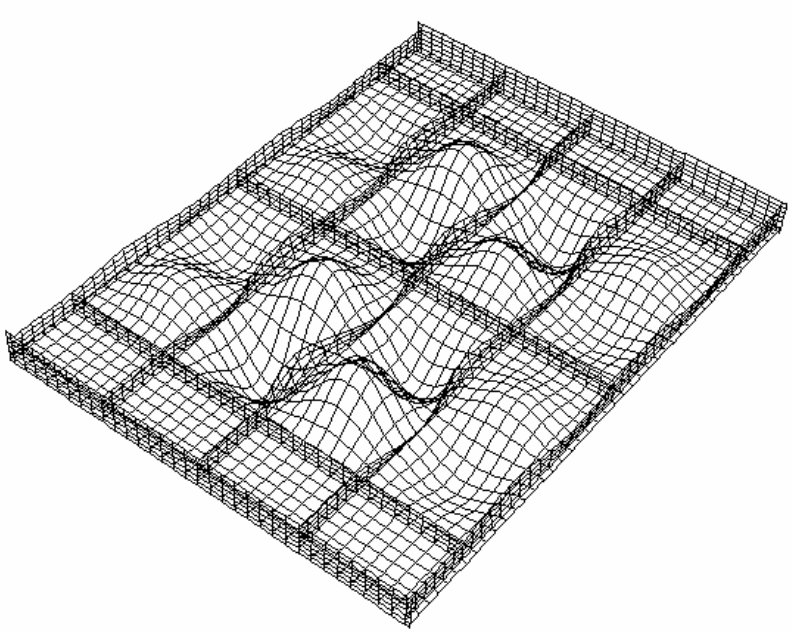

Figure 4.5 Typical Buckling Shape of Stiffened Plate

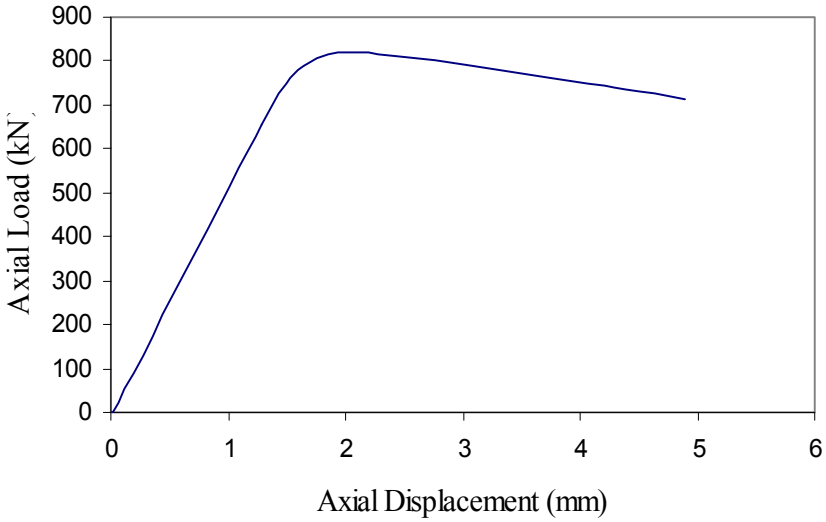

Figure 4.6 Typical Load vs Displacement Curve

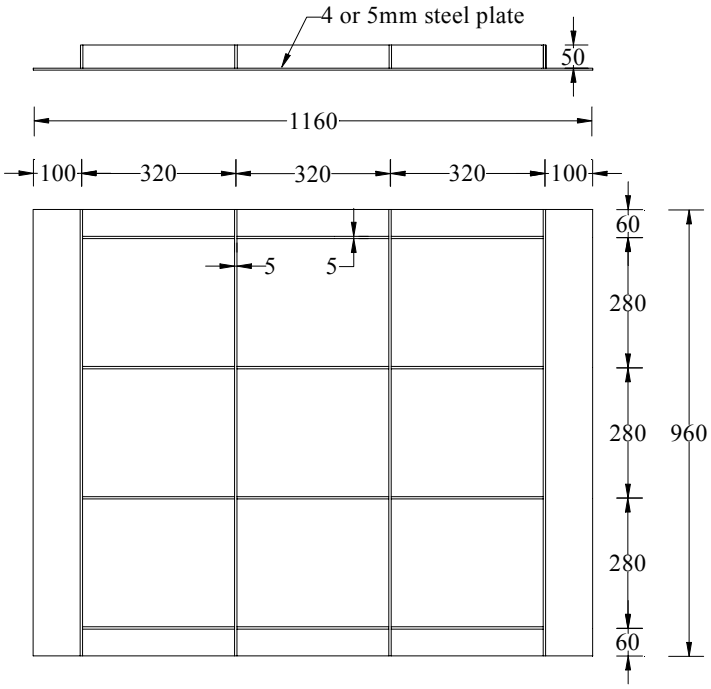

Figure 4.7 Dimension of Lavan Kumar's Specimen [232]

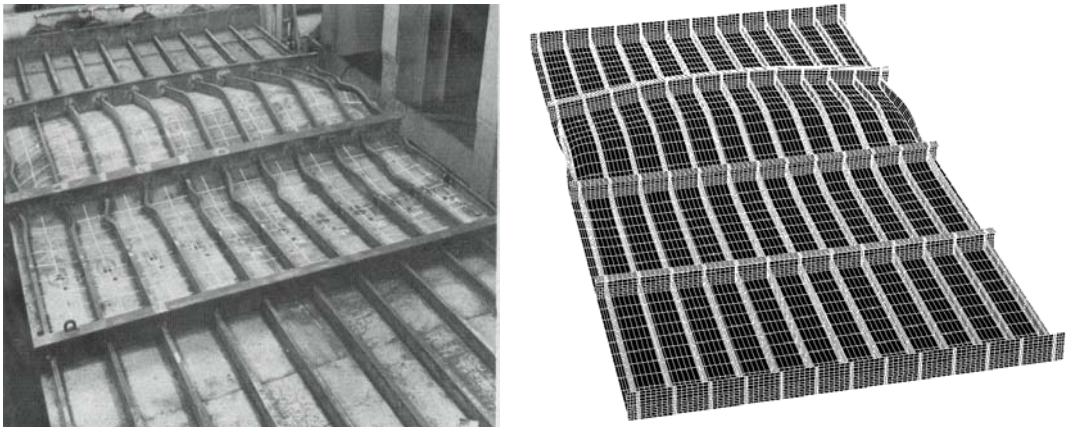

a) A view after failure of the specimen 3a

b) Deformed shape after failure of the specimen 3a predicted by ABAQUS

Figure 4.8 Comparison of Failure Shapes

CHAPTER 5 RESULTS AND DISCUSSION

5.1 Experimental Results

5.1.1 Initial Imperfection

Initial imperfection of the specimen was measured by taking readings for vertical deformations of 1813 points in the stiffened plate relative to one of the corner points. The number of measurement points along the width of specimen and along the length of specimen are 37 and 49 respectively. Possible distortion of stiffeners was not measured since stiffeners were designed to remain stocky before any local buckling occurred in the base plate. It is found from the imperfection measurement that sub-panels of stiffened plate deformed towards stiffener side and the deformation generally followed half sine curve. The deflections of specimen at section CC and section DD for series A and series B are shown in Figures 5.1 and 5.2. Large deflection is observed in some specimens. This is mainly due to the fact that the reference point happened to be located at the severely distorted corner. Generally, stiffened plates in same series have similar initial geometrical imperfection. The plotted initial imperfection for series A and series B are shown in Appendix D. Two sets of typical imperfection measurement data with one each from series A and series B are also shown in Appendix D for references.

5.1.2 Ultimate Loads of Series A and Series B

The observed ultimate failure loads for all the 12 specimens tested and the comparison with ABAQUS analysis results are summarized in Table 5.1. The specimens tested are divided into two series, namely series A and Series B. The plate slenderness ratio is 100 for series A and 76 for series B. Among the 12 specimens,

specimen A6 and B6 were tested to failure under axial load only and specimens A1 and B1 were tested to failure under lateral load only. The rest of the specimens were tested to failure under combined action of axial load and lateral pressure. Axial load was maintained constant at pre-determined level with lateral pressure increased gradually until the collapse of specimen. It is found from Table 5.1 that the presence of axial load reduces the ultimate lateral load capacity of stiffened plates. For example in series A, lateral load capacity is reduced from 246 kN to 75 kN when axial load is increased from 0 to 500 kN. This means that the lateral load carrying capacity is affected quite significantly by the presence of axial load and vice-versa. Specimens A6 and B6 were tested to failure under axial load only. The ratio of ultimate axial load to the squash load is 0.54 for A6 and 0.56 for B6. These ratios show clearly the effect of plate slenderness on the ultimate axial load of stiffened plate. The drop in axial load capacity compared to the respective squash load accounts for both local buckling of base plate and overall buckling of stiffened plate. Comparison between specimen A6 and B6 shows that increase of plate slenderness causes a drop in ultimate axial load capacity of stiffened plate.

Plate initiated failure was observed for specimens under axial load only, while overall column buckling failure was observed for panels under combined action of axial load and lateral pressure. The failure shapes for all the specimens are shown in Figures 5.3 to 5.14. Due to excessive vertical deformation of stiffened plate, disconnections of stiffeners at the joints were found in some specimens after failure. The disconnection of stiffeners from the base plate usually occurred after specimens had reached ultimate load capacity except in the case of B4. It was observed during the test of specimen B4 that disconnection of stiffeners occurred before reaching the ultimate

load followed by a sudden drop of lateral load. In the case of specimen B4, it is believed that the disconnection of stiffeners is caused by improper welding. This can be verified from comparison of ultimate load between specimen B4 and B5. From Table 5.1, an increase of 110 kN axial load between B4 and B5 only results in a decrease of 2.1 kN lateral load. This is not logical from a scientific point of view. Obvious local buckling of sub-panels was noticed for specimens under axial load only. For stiffened plates under lateral load only or under both axial load and lateral pressure, yield line instead of local buckling was observed in the sub-panels. This may be due to the sequence of loading application. In those cases with large lateral pressure and small axial load, lateral pressure dominated the behaviour of stiffened plates. Presence of lateral pressure suppressed the formation of buckling of stiffened plate.

The load vs displacement curves for specimens tested are shown in Figure 5.15 to 5.17. The lateral displacement of most of the specimens was found to be insignificant when only axial load was applied. But when lateral load was applied on the specimens which were already under axial compression, lateral deflection increased significantly in the direction of lateral load. All specimens under both axial load and lateral pressure show linear and stiff behaviour at the initial stage of lateral loading and deflection increases considerably at later stage. The slopes of all curves at the initial stage are almost same. For the two tests with axial load only, slight movement of "fixed end" was recorded by the displacement transducer. The displacement at moving end is not the absolute shortening of specimen along the longitudinal direction. Thus the displacement used in the plotted load vs displacement curves for

specimens under axial load only is the amount of displacement recorded at moving end deducted by movement of "fixed end".

Electrical resistance strain gauges of gauge length 5 mm were used in the test to measure strain. The maximum principal stresses at location of strain gauges were calculated based on the Rosette strain gauge readings. Typical maximum principal stress for specimen B3 is shown in Figure 5.18.

5.2 Comparison of FEM Results with Experimental Results

The specimens tested in the current study were analyzed by ABAQUS finite element package and analytical results were compared to experimental results. In the ABAQUS analyses, models with both nominal imperfection and actual measured imperfection were studied. Table 5.1 shows the comparison of experimental results with the finite element results with nominal imperfection. It is found that ABAQUS results agree well with the experimental results. In most cases the difference between experimental results and the finite element results are within 10% except in the case of B4. It should, however, be noted that in the case of B4, the ultimate lateral load carrying capacity was affected by the disconnection of stiffeners due to improper welding. Thus it can be concluded that the use of finite element package to predict the ultimate load of stiffened plate subjected to both axial load and lateral pressure is reliable to a reasonable accuracy.

Figures 5.19 to 5.30 show the load vs displacement curves for experimental results and the finite element results with nominal imperfection and actual measured imperfection. It is found that load vs displacement curve for experimental results does

not agree well with finite element results for B6. This is mainly caused by the disturbance of moving "fixed end". Comparison of the finite element results with nominal imperfection and actual measured imperfection shows that the difference between ultimate loads is very small. However, it is observed that there is some difference between the deflections at peak load for these two types of analysis. This is due to the fact that both overall deformation of stiffened plate and local deformation of sub-panel were taken into account in the analysis with measured imperfection whereas only local sub-panel deflection was considered in the analysis with nominal imperfection. The maximum deformation in models with actual imperfection is larger than those with nominal imperfection. It is interesting to notice that difference in magnitude of imperfection does not result in much change of ultimate load. It is believed that buckling model component of the deflected shape has the most significant weakening effect. The nominal imperfection used in the current study was first mode of buckling shape. Because the buckling in a rectangular plate always occurs in a higher mode (two half waves in the mid-panels for current model), the overall initial deflection in fact has a stiffening effect. Overall deformation of stiffened plate was included in the models with actual imperfection. This may explain why models with actual imperfection and larger magnitude of deformation do not have lower ultimate load since overall deformation has a beneficial effect. The effect of imperfection is further discussed in section 5.4 of this chapter. From the comparison of experimental results from other researchers and the author with finite element results, it is found that finite element model with nominal imperfection can generally produce sufficient good results. Therefore, it is valid to use nominal imperfection in the parametric study to account for the possible imperfections of stiffened plate.

Failure shape of finite element analysis can be displayed in the ABAQUS Viewer. The failure shapes from finite element analysis were compared to the respective experimental failure shapes. View after failure of a typical specimen tested under combined loads and the corresponding finite element prediction is shown in Figure 5.31. It is found that the finite element prediction agrees well with experimental failure shape. Figure 5.32 shows a comparison of failure shapes for specimens under axial load only. The failure pattern from finite element analysis is similar as that observed in the test. It can be seen from Figure 5.31 and 5.32 that finite element modeling is capable of predicting the failure shape of specimen with sufficient accuracy.

5.3 Comparison of Experimental Results with Design Methods

The experimental results and FEM results were compared to existing design methods. In the past few decades, several design codes and recommendations have been developed for design of stiffened plates. Some examples are BS 5400 [7], API RP2V [8], AISC [9] and DnV [12]. Many design methods for stiffened plates were proposed by researchers such as Allen [186], Winter [236], Faulkner [187] and Narayanan and Shanmugam [194]. Most of design methods only deal with stiffened plates subjected to in-plane loads only. Only a few design methods consider stiffened plates subjected to both in-plane load and lateral pressure. It is noticed that DnV code [12] is the only one accounting for interaction of in-plane compression and lateral pressure among those well-established codes. Design methods for stiffened plates subjected to combined action of in-plane load and lateral pressure were also proposed by Smith [142] and Tan [174]. However, their methods do not cover whole range of loading and are only applicable for small lateral pressure. In this study, design methods from

DnV code [12] and Paik [212, 213] were used to compare with experimental results and finite element analysis results. The comparison of experimental results and existing design methods is shown in Table 5.2.

Paik [212, 213] proposed a design method for stiffened plate under combined axial load, in-plane bending and lateral pressure. The collapse patterns of a stiffened plate are classified into six groups. Ultimate load of stiffened plate for each collapse pattern is calculated separately and lowest value is taken to correspond to the real panel ultimate strength. The stiffened plates in this experimental study fail in the overall collapse mode as lateral pressure is dominant. This failure pattern is categorized as mode 1 in Paik's Method. Orthotropic plate approach is used in Paik's method when stiffened plate fails with collapse mode 1. Stiffened plates in this comparison are assumed to have transverse stiffeners with equal spacing. It is found that both experimental results and FEM results agree quite well with Paik's method in most cases. It is also noticed that Paik's method tends to give lower ultimate lateral load when axial compression force is large. For example in case B5, large discrepancy between experimental results, FEM results and Paik's method is found. However Paik's Method generally gives conservative values.

DnV code was also used to compare the experimental results. It is noticed that DnV code generally gives higher ultimate lateral load compared with experimental results and FEM results. It is also found that presence of in-plane load does not significantly reduce ultimate lateral load using DnV design method. In DnV code, the formula for the design of a plate subjected to lateral pressure is based on yield-line theory. The reduction of the moment resistance along the yield-line due to applied in-plane

stresses is accounted in the formula. The reduced resistance is calculated based on von-Mises' equivalent stress. The formulation is based on a yield pattern assuming yield lines along all four edges, and will give uncertain results for cases where yield-lines cannot be developed along all edges. Furthermore, the formula does not consider second-order effects, buckling due to axial load is not accounted. For the specimens tested, yield lines were not observed along all four edges of sub-panel. Also axial load were presented in most cases and buckling due to axial load should not be neglected. The use of DnV formulation in this case may not be valid.

The Interaction curves of lateral load and axial load for both series are shown in Figure 5.33. Results from experimental tests are compared with those from FEM and design codes. Interaction curves for series A and series B follow a similar trend. They can generally be approximated as parabolic curves. It is found that interaction curves for results from experimental tests, FEM and Paik's method are quite close to straight lines. Comparing the two sets of interaction curves for series A and series B, it is observed that series A with higher plate slenderness ratio gives lower ultimate load. More stiffeners are provided for specimens with lower plate slenderness ratio. The presence of more stiffeners not only directly contributes to the ultimate load but also increases the base plate resistance by minimizing the effect of local buckling. It is noticed that interaction curves for results from FEM and Paik's method agree well with experimental results. Paik's method generally gives lower value than experimental results and FEM results. Significant difference is found between interaction curves from DnV code and those from other methods. This may be due to the fact that formula in DnV code does not consider buckling under axial load in this

case. Also the assumption made in DnV code that yield line developed along all four edges is not applicable to specimens tested.

5.4 Parametric Studies

A series of stiffened plates representing possible ship-bottom configurations was selected to carry out parametric studies. Figure 5.34 shows the stiffened plate used for parametric study. The overall dimensions were kept as 3080 mm x 6000 mm. The width of sub-panel was kept as 600 mm and the thickness of base plate varied according to b/t_p ratio. The dimensions of stiffened plates are summarized in Table 5.3. The stiffeners and base plate were selected such that the stiffened plates fail as plate induced failure. Stiffener induced failure was not considered in the current study. The parameters studied include plate slenderness ratio, intensity of lateral pressure, boundary conditions, initial imperfection and residual stress. The yield strength of steel used in the studies is 275 N/mm^2 and Young's modulus is 205000 N/mm^2.

The model was simply supported along the four edges of the base plate and rotation along the edges of base plate was allowed. For simply supported cases, one of the end plate was restrained to move longitudinally and transversely at centroidal axis. The in-plane loading applied at the other end plate was modelled as uniform nodal displacement at centroidal axis. The application of uniform nodal displacement to model the in-plane compression with resultant force at neutral axis was valid. For fixed ended cases, the passive end was restrained to any displacements and rotations. Only longitudinal displacement was allowed for active end. The two longitudinal edges remained simply supported and rotations were allowed.

In the numerical investigations, the main aim of applying lateral pressure to stiffened plates was to study the effect of preloaded lateral pressure on the ultimate axial load of stiffened plates. Therefore, the sequence of the loading employed in the numerical investigation was different from the experiments. Two steps of loading sequences were involved for stiffened plates subjected to combined action of axial load and lateral pressure. In the first step, pre-determined lateral pressure was applied to the whole base plate and kept constant at the required level. Subsequently in the second step, axial load represented as uniform nodal displacement was applied at the neutral axis of stiffened plate till failure. Ultimate load of stiffened plate could be obtained from the resultant forces at the passive end.

The effects of initial imperfection on the ultimate load of stiffened plates were studied by varying the initial imperfection patterns and the maximum magnitude of initial imperfection. Stiffened plates with three different plate slenderness ratios were modelled with different imperfection modes and magnitude of imperfection. In the present study, three initial imperfection modes were considered. In the first mode of initial imperfection, half since curve pattern was assumed for all the sub-panels. In the ABAQUS analysis, the magnitudes of initial deflection for all the sub-panels were slightly different for mode 1 imperfection. The second mode of initial imperfection was assumed to be a full since curve pattern for whole stiffened plate. The third mode of initial imperfection was taken as half since curve pattern for whole stiffened plate. The initial imperfection modes are shown in Figure 5.35 and the real imperfection modes used in ABAQUS in Figures 5.36 to 5.38.

The welding process involved large temperature change in the stiffened plates and hence considerable residual stresses resulted from the welding operation. Due to the difficulties in measuring residual stresses and the complexity of residual stress distribution, the effects of residual stresses on the behaviour of stiffened plates are still not well known. The influence of welding procedure on residual stress is also not fully understood. In this parametric study, residual stress was included in the ABAQUS analysis by command *INITIAL CONDITIONS, TYPE=STRESS. Residual stress was applied longitudinally to the cross section of shell elements. The idealization of residual stress distribution reported by Dwight and Moxham [179] was adopted in this study. Figure 5.39 illustrates the idealization of residual stress distribution. Residual stress is self-equilibrating and the area of tension blocks must be equal to the area of compression blocks. Tensile stress was assumed to be yield strength and compressive residual stress calculated from tension stress blocks. Researchers found that for a plate of given thickness, with a given thermal history at its edges, the width of tension block ηt was largely independent of the overall width b. Researchers also found the resulting values of η varied from 2 to about 8. In the present study, ηt was assumed to be 40 mm for all the stiffened plates considered regardless of the thickness of plate. Only residual stress in base plate was considered and residual stress in stiffener neglected.

5.5 Behaviour of Stiffened Plates under Combined Loads

Ultimate loads of stiffened plates considered for parametric study are obtained from finite element analysis. The ultimate loads of specimens under axial load only are summarized in Table 5.4. Stiffened plates with different geometrical configurations exhibit different values of strength depending on whether they fail in a plate induced

or stiffener induced mode. The present parametric study only considers stiffened plates with plate induced failure. The strength of stiffened plate depends on a few primary variables such as plate slenderness ratio b/t_p, the column slenderness of the stiffener-plate combination λ. Some secondary variables such as the ratio of stiffener area to plate area A_s/A_p will also affect the behaviour of stiffened plate. The primary variables have a greater effect on strength and normally an increase in these parameter results in a decrease of strength of stiffened plate. The secondary variables have a less marked effect on the behaviour of stiffened plate. The stiffener to plate area ratio A_s/A_p reflects the extent to which a compact stiffener can improve the plate induced column strength. Tan [174] presented the effects of A_s/A_p to the strength and behaviour of stiffened plates under combined action of axial and lateral loads. A few variables that affect the behaviour of stiffened plate are discussed based on the parametric study.

5.5.1 Influence of Plate Slenderness Ratio, b/t_p

Increasing b/t_p generally results in decrease of the plate strength and a reduction in column strength of the stiffener-plate assembly. Figure 5.40 shows the ultimate loads of stiffened plates under different combinations of axial load and lateral pressure for plate slenderness ranging from 30 to 100. The curves show that the increase in b/t_p ratio results in a decrease of ultimate load P_u for all cases, regardless of the intensity of the lateral pressure. The reduction of ultimate load is more significant for b/t_p = 30 to 50. For b/t_p ratio greater than 60, the reduction of strength due to change of b/t_p is not so prominent. Thus for a particular stiffener area and *l*/b ratio, b/t_p ratio is a critical parameter, which affects the loss of ultimate strength of the stiffened plate. From table 5.4, it is found that the ultimate load to squash load ratio is higher with

lower ratio of b/t_p. Stiffened plate is more effective to resist compressive force with low plate slenderness ratio since section is stocky. For stiffened plates with high b/t_p ratio, the effect of local buckling of base plate is more significant. Local buckling reduces the effective width of stiffened panel thus reduces the ultimate axial load capacity. In practice, b/t_p ratio between 40 to 70 is normally adopted in the design of stiffened plates.

5.5.2 Influence of Intensity of Lateral Pressure

Figure 5.41 shows the change of ultimate axial load to squash load ratio (P_u/P_s) with b/t_p under different intensity of lateral pressure. From Figures 5.40 and 5.41, it is observed that ultimate axial load generally reduces with increase of lateral pressure. The influence of lateral pressure on the ultimate axial load is significant in the cases with high b/t_p ratio. It is found that small lateral pressure has little effect on the ultimate axial load for stiffened plates with b/t_p = 30 to 50. The ultimate axial load almost remains same when lateral pressure is smaller than 0.1 MPa in the cases with low b/t_p ratios. It is observed that the reduction of ultimate axial strength is different for same value of increase in lateral pressure. With same amount of increase of lateral pressure, the reduction of ultimate axial load with lower lateral pressure is much smaller than reduction of ultimate axial load with higher lateral pressure. It is also noticed from Figure 5.40 that ultimate axial load and lateral pressure have a near linear relationship in the cases of stiffened plates with b/t_p = 30 to 60 when lateral pressure is greater than 0.1 MPa. The interaction curves can generally be composed of two straight lines for the stiffened plates with b/t_p =30 to 60. Whereas in the cases of stiffened plates with b/t_p ratio smaller than 60, the interaction curves are more close to parabolic curves. Given the magnitude of lateral pressure, the ultimate axial load can

be approximately obtained from the interaction curves in Figure 5.40. In the finite element analysis, it is noticed that overall deformation of stiffened plate is much significant than local deformation of sub-panels under lateral pressure in the cases of stiffened plates with low b/t_p ratio. For stiffened plates with high b/t_p ratio, evident deformation of sub-panels as well as overall deformation of stiffened plate is observed with the presence of lateral pressure. In ship structures, the lateral load does not usually reach high levels compared with the compressive loads. In some practices such as the proposed method by Smith [141], the effect of small lateral load is neglected.

5.5.3 Influence of Boundary Conditions

The effect of boundary conditions on the ultimate axial load of stiffened plates was investigated in the parametric study. The degree of restraint applied to stiffened plates affects the shape of deformation and hence the response of a structure to a given type of loading. Ultimate axial loads for stiffened plates under axial load only with different boundary conditions are summarized in Table 5.5. Given same loading for same stiffened plates, the ultimate axial load is generally lower for the case of simply supported boundary conditions. The fixed ended conditions always demonstrate higher load carrying capacity. This conclusion is rather obvious since more loads can be spread to the fully restrained edges before failure. The increase of ultimate axial load from simply supported condition to fixed ended condition ranged from 1% to 15%. The change of boundary condition also changed the failure shape of stiffened plates. For the cases with simply supported conditions, ultimate failure always occurred at the sub-panels close to end. With additional restrains to the rotation of end plate, the sub-panels close to end appear to have higher stiffness to resist the

compressive force and failure can occur at mid sub-panels. A typical comparison of failure shapes for stiffened plates with simply supported condition and fixed ended condition is shown in Figure 5.42. It is noticed from Figure 5.42 that the location of failure changed from end sub-panels to mid sub-panels with change of boundary condition from simply supported to fixed supported.

5.5.4 Influence of Initial Imperfection

Influence of initial imperfection on the ultimate load of stiffened plate was investigated by performing analysis on three stiffened plates with different modes of imperfection. The results from finite element analysis are summarized in Table 5.6. Initial imperfection of stiffened plates generally tends to decrease the rigidity and causes reduction of compressive strength. In some cases the effect of initial deformation of stiffeners can be beneficial by causing tensile bending stresses which delay compressive yield in stiffener outer fibres. In the current study, only imperfections in base plate are considered and influence of initial stiffener deformations is neglected.

The effect of mode of imperfection was studied by comparing three different modes of imperfection. It is generally agreed that the buckling mode component of the deflected shape has the most significant weakening effect. The other components may have a stiffening effect in the absence of the buckling mode component. It is observed from Table 5.6 that initial imperfection modes do not affect the ultimate load much when maximum magnitude of initial imperfection is small. The stiffened plates studied seem to be more sensitive to mode 2 imperfection compared to mode 1 and 3 imperfections. Given same magnitude of imperfection, the stiffened plates with mode

2 have lower ultimate loads. It is found that mode 3 imperfection does not significantly affect the ultimate axial load. This result agrees well with the previous observation in which small lateral pressure was found to have little effect on the ultimate axial load of stiffened plates. In this study, mode 2 imperfection is believed to have more buckling components to the stiffened plate compared to mode 1 and mode 3 imperfections.

The magnitude of imperfection on the ultimate load of stiffened plates was also included in the study. The strength decreased due to the magnitude of imperfection depends on the amplitude of the buckling mode component. It is noticed that increase of maximum initial imperfection from 1 mm to 10 mm does not significantly reduce the ultimate axial load of stiffened plates for mode 1 and mode 3 imperfections. The effect of magnitude of initial imperfection on the ultimate axial load is significant for mode 2 initial imperfection compared to mode 1 and mode 3 imperfections. It is believed that initial imperfection helps to trigger the failure of stiffened plate thus reducing the ultimate load of stiffened plate. Increase of magnitude of initial imperfection generally reduces the ultimate axial load of stiffened plate. The reduction in ultimate axial load may depend on the magnitude of initial imperfection and on the location of failure of stiffened plate. For the stiffened plates considered, initial imperfection in the end sub-panels is believed to be more important since all failures occur at end sub-panels. Mode 2 imperfection seems to have the most significant weakening effect to trigger the failure at end sub-panels.

The imperfection sensitivity of stiffened plate may depend on the plate slenderness ratio b/t_p. Stocky section with low plate slenderness ratio seem to be more

imperfection sensitive. Take for example mode 2 imperfection, ultimate load changes from 20724 kN to 20332 kN with change of imperfection magnitude from 1 mm to 10mm at b/t_p ratio equal to 30. The reduction of ultimate load is 392 kN in this case. However, the reduction of ultimate load is 165 kN at b/t_p equal to 70 and 128 kN at b/t_p equal to 100.

5.5.5 Influence of Residual Stress

The effect of residual stress on the ultimate load was investigated numerically by comparing the ultimate axial loads of stiffened plates with and without residual stress. The stiffened plates considered were subjected to axial load only and have same initial imperfection. Table 5.7 summarizes the ultimate load of stiffened plates with and without residual stress. Only small difference is observed for the ultimate load of stiffened plates with and without residual stress. In the present study, the compressive residual stress is 50.77 N/mm^2, which is 18.5% of yield strength. A self-equilibrating stress field was included in the analysis for stiffened plate with residual stress. Under the compressive force, stress redistribution was observed in the ABAQUS simulation for stiffened plate with residua stress. However similar failure shapes were noticed at ultimate failure load. It may be concluded that residual stress only has a secondary effect on the strength of stiffened plate.

The validity of current method used to include residual stress need to be verified by experimental results. Due to complexity and limitation of experiment measurement, the effects of residual stress on the behaviour of stiffened plate are still not well known. Experimental tests by other researchers do not lead to a consistent conclusion. Smith [141] concluded residual stresses in stiffened plate result in a significant

reduction in ultimate strength. In his case, the measured residual stress was up to 70% of the yield strength. However Dorman and Dwight [62] reported much smaller residual stress in their experimental measurement. Their study showed that residual stresses only had a secondary effect on the ultimate strength of stiffened plate. Horne and Narayanan [189, 190] conducted an experimental study to investigate the effect of welding to strength of stiffened plate. They observed different welding techniques resulted in different amount of residual stress. However, the effect of residual stresses on the failure load was not consistent. In real structure, the residual stress may be smaller than what measured in experiment since occasional tension loads induce a shake-out of the residual stresses. The effects of residual stress on the ultimate strength of stiffened plate in real structure may not be significant.

5.6 Design Recommendations

Behaviour of stiffened plates subjected to combined action of in-plane load and lateral pressure is complex and design of stiffened plates is not straightforward due to the involvement of many parameters. Although some design methods have been developed, researchers found that no single code provided conservative guidance for design of stiffened plates subjected to a whole range of loading. The purpose of this study is not to propose specific design rules for stiffened plates but to investigate how related parameters affect the behaviour of stiffened plates under combined actions of axial load and lateral pressure. However, experimental and numerical investigations on various parameters suggest certain design guidelines. Stiffened plate with large b/t_p is not recommended for practical use. Due to local buckling in stiffened plate with large b/t_p ratio, ultimate load of stiffened plate is much lower than squash load.

Therefore stiffened plate with large b/t_p is not economical for practical use. In practice, the b/t_p ratio of stiffened plate usually ranges from 40 to 70.

Design methods for strength of stiffened plates under compression force only or lateral pressure only have been proposed by many researchers. The present study found that interaction of axial load and lateral load is approximately a parabolic curve for high b/t_p value and two linear curves for low b/t_p values. With known strength for stiffened plate under axial load only and lateral load only, compressive strength under certain lateral pressure can be roughly estimated by plotting similar interaction curves.

The present study found that Paik's method gives good prediction of stiffened plates under in-plane load and lateral pressure. In Paik's method, the collapse patterns of a stiffened plate are classified into six groups. The collapse of stiffened plate occurs at the lowest value among the various ultimate loads calculated for each of the collapse pattern. The ultimate strength for all potential collapse modes need to be calculated separately and minimum value is taken to correspond to the real stiffened plate ultimate strength. The advantage of Paik's method is all possible failure modes are considered in the calculations for ultimate load rather than only one assumed failure mode in most design methods. However Paik's method is based on orthotropic plate approach and may give uncertain results for stiffened plate with uneven stiffener spacing. Also it is found that Paik's method is quite sensitive to plate initial deflection. A good estimation of the buckling mode initial deflection is critical when Paik's method is used to predict the ultimate strength of stiffened plate.

Table 5.1 Summary of Experimental Results

Series	Specimen No.	Axial load P (kN)	Lateral load Q_u (kN)		$\frac{Q_{exp}}{Q_{abq}}$
			Experimental	ABAQUS	
A	A1	0	246.3	252.1	0.98
	A2	170	201.6	183.0	1.10
	A3	300	147.4	135.2	1.09
	A4	400	112.8	105.8	1.07
	A5	500	75.1	74.7	1.01
	A6 (Axial load only)	P_{exp}= 712.0 kN, P_{abq}=769.2 kN			P_{exp}/P_{abq} =0.93
B	B1	0	250.9	262.6	0.96
	B2	200	203.8	204.8	1.00
	B3	400	145.7	141.2	1.03
	B4	520	95.4	107.7	0.89
	B5	630	93.3	96.4	0.97
	B6 (Axial load only)	P_{exp}= 785.4 kN, P_{abq}=819.5 kN			P_{exp}/P_{abq} =0.96

Table 5.2 Comparison of Experimental Results with Existing Design Methods

Specimen No.	Axial Load P (kN)	Lateral Load Q_u (kN)				$\frac{Q_{abq}}{Q_{exp}}$	$\frac{Q_{DnV}}{Q_{exp}}$	$\frac{Q_{Paik}}{Q_{exp}}$
		Exp.	ABAQUS	DnV	Paik			
A1	0	246.3	252.1	184.5	246.0	1.02	0.75	1.00
A2	170	201.6	183.0	182.2	187.0	0.91	0.90	0.93
A3	300	147.4	135.2	177.4	142.0	0.92	1.20	0.96
A4	400	112.8	105.8	171.8	107.0	0.94	1.52	0.95
A5	500	75.1	74.7	164.4	71.0	0.99	2.19	0.95
B1	0	250.9	262.6	280.6	261.0	1.05	1.12	1.04
B2	200	203.8	204.8	276.7	195.0	1.00	1.36	0.96
B3	400	145.7	141.2	264.8	130.0	0.97	1.82	0.89
B4	520	95.4	107.7	253.6	86.0	1.13	2.66	0.90
B5	630	93.3	96.4	240.5	49.0	1.03	2.58	0.53
Specimens under axial load only								
Specimen No.	Lateral Load P (kN)	Axial Load P_u (kN)				$\frac{P_{abq}}{P_{exp}}$	$\frac{P_{DnV}}{P_{exp}}$	$\frac{P_{Paik}}{P_{exp}}$
		Exp.	ABAQUS	DnV	Paik			
A6	0	712.0	769.0	770.9	699.0	1.08	1.08	0.98
B6	0	785.4	819.5	971.3	769.0	1.04	1.24	0.98

Table 5.3 Dimensions of Stiffened Plates for Parametric Studies

Specimen No.	b/t_p	t_p (mm)	Longitudinal stiffeners		Transverse stiffeners	
			Spacing (mm)	Size (mm x mm x mm x mm)	Spacing (mm)	Size (mm x mm x mm x mm)
SP30	30	20	600	150 x 10 x 80 x 15	1500	250 x 10 x 120 x 18
SP40	40	15				
SP50	50	12				
SP60	60	10				
SP70	70	8.57				
SP80	80	7.5				
SP90	90	6.67				
SP100	100	6				

Table 5.4 Summary of Parametric Study Results

Specimen No.	b/t_p	P_1 (kN) ABAQUS	t_p (mm)	P_2 (kN) Squash load	P_1/P_2
SP30	30	20775	20	21395	0.97
SP40	40	15289	15	17160	0.89
SP50	50	12595	12	14619	0.86
SP60	60	11056	10	12925	0.86
SP70	70	9478	8.57	11714	0.81
SP80	80	8067	7.5	10808	0.75
SP90	90	7283	6.67	10104	0.72
SP100	100	6669	6	9537	0.70

Table 5.5 Summary of Ultimate Loads with Different Boundary Conditions

Specimen No.	Ultimate load (kN)		P_{u2}/P_{u1}
	Simply supported P_{u1}	Fixed ended P_{u2}	
SP30	20775	21175	1.02
SP40	15289	17053	1.12
SP50	12595	14513	1.15
SP60	11056	12201	1.10
SP70	9478	9560	1.01
SP80	8067	8564	1.06
SP90	7283	7669	1.05
SP100	6669	7092	1.06

Table 5.6 Effects of Initial Imperfection on the Ultimate Loads of Stiffened Plates

	Δ_{max} (mm)	b/t_p=30			b/t_p=70			b/t_p=100		
		Mode 1	Mode 2	Mode 3	Mode 1	Mode 2	Mode 3	Mode 1	Mode 2	Mode 3
P_u	1	20775	20724	20796	9478	9449	9460	6669	6650	6649
	5	20761	20595	20770	9449	9348	9419	6665	6567	6643
	10	20754	20332	20738	9428	9284	9410	6606	6522	6620

Table 5.7 Effects of Residual Stress on the Ultimate Load of Stiffened Plates

Specimen No.	Ultimate load P_u (kN)		$\frac{P_{u1}}{P_{u2}}$
	Without residual stress P_{u1}	With residual stress P_{u2}	
SP30	20775	20756	1.001
SP40	15289	15212	1.005
SP50	12595	12503	1.007
SP60	11056	11041	1.001
SP70	9478	9437	1.004
SP80	8067	8053	1.002
SP90	7283	7241	1.006
SP100	6669	6563	1.016

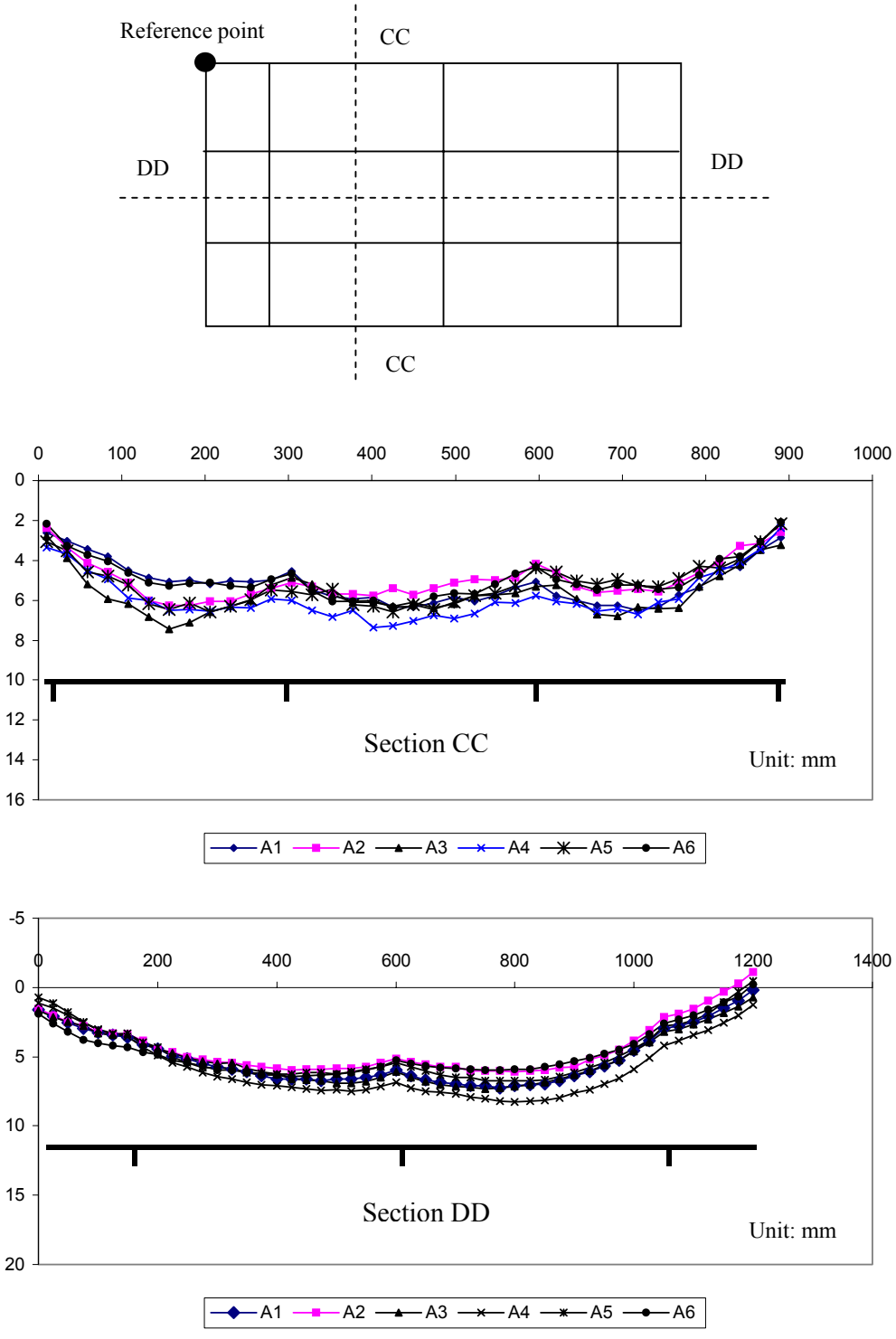

Figure 5.1 Measured Initial Imperfection for Series A Specimens

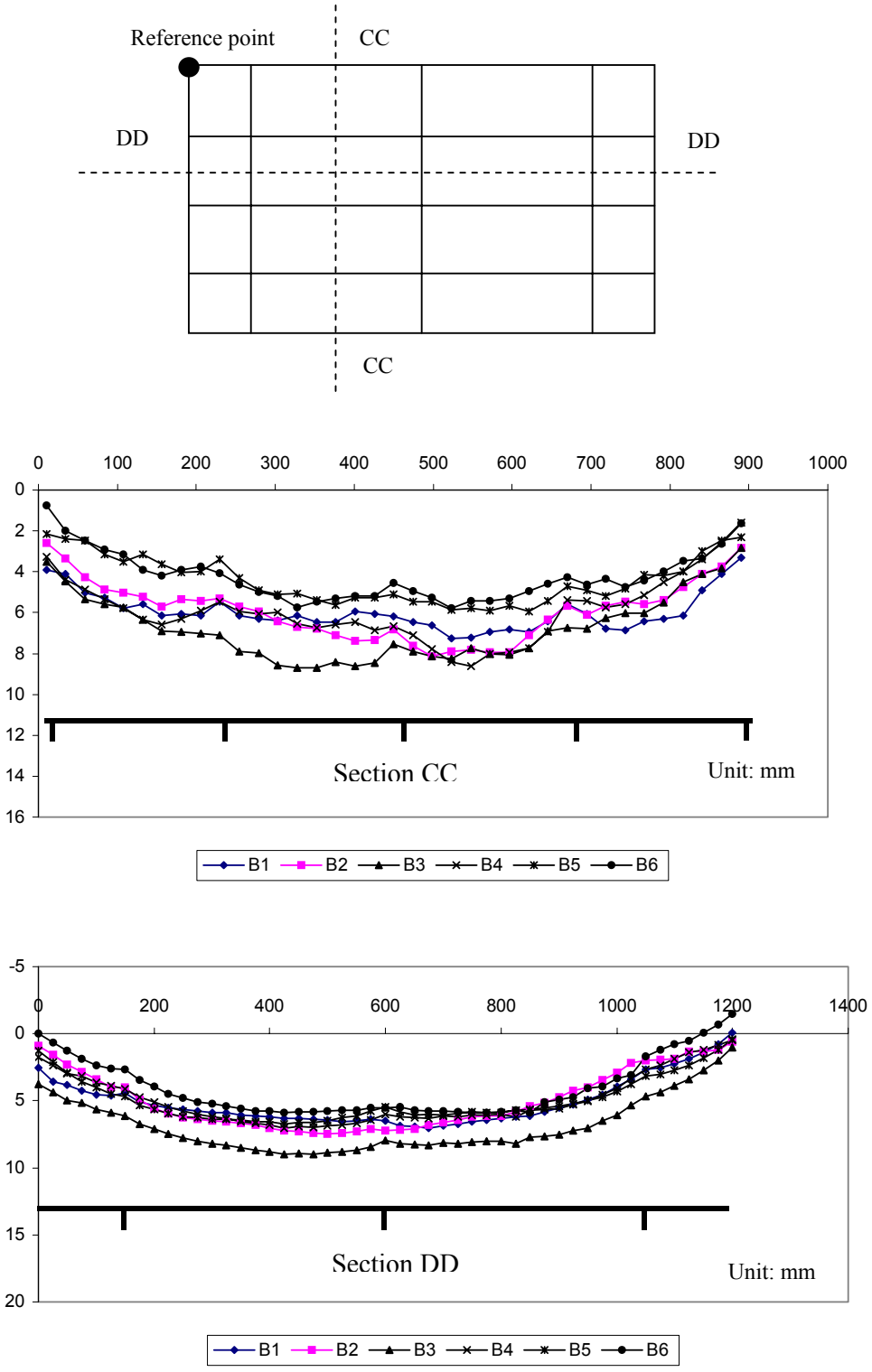

Figure 5.2 Measured Initial Imperfection for Series B Specimens

Figure 5.3 View after Failure Shape of the Specimen A1

Figure 5.4 View after Failure Shape of the Specimen A2

Figure 5.5 View after Failure Shape of the Specimen A3

Figure 5.6 View after Failure Shape of the Specimen A4

Figure 5.7 View after Failure Shape of the Specimen A5

Figure 5.8 View after Failure Shape of the Specimen A6

Figure 5.9 View after Failure Shape of the Specimen B1

Figure 5.10 View after Failure Shape of the Specimen B2

Figure 5.11 View after Failure Shape of the Specimen B3

Figure 5.12 View after Failure Shape of the Specimen B4

Figure 5.13 View after Failure Shape of the Specimen B5

Figure 5.14 View after Failure Shape of the Specimen B6

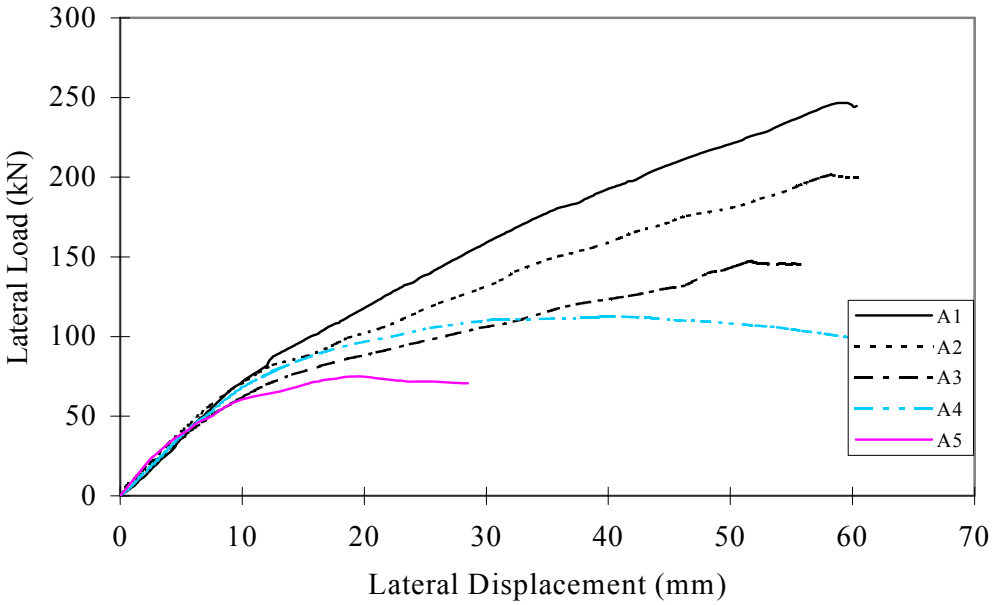

Figure 5.15 Lateral Load vs Displacement Curves for Series A

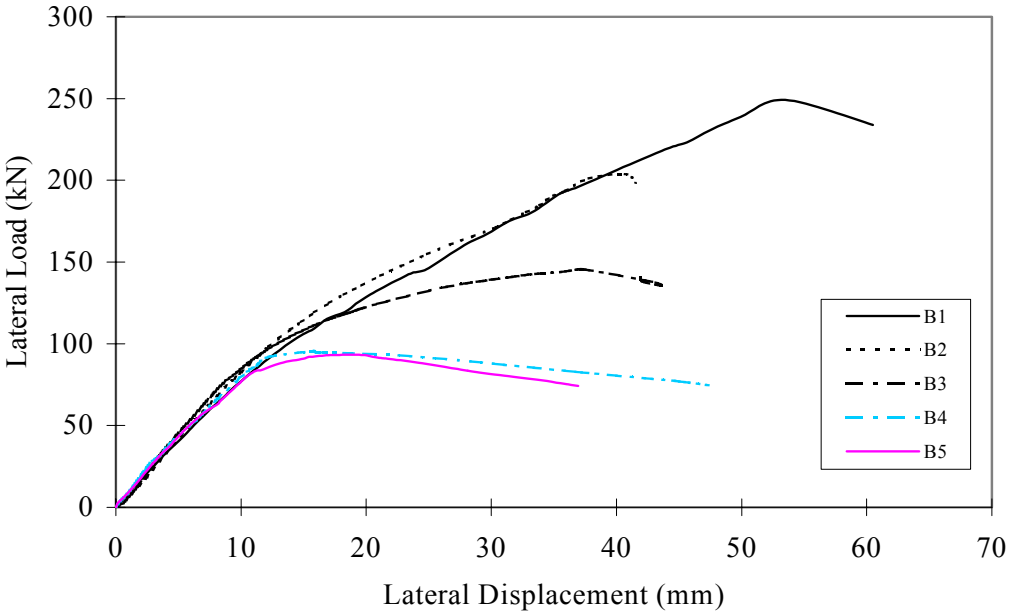

Figure 5.16 Lateral Load vs Displacement Curves for Series B

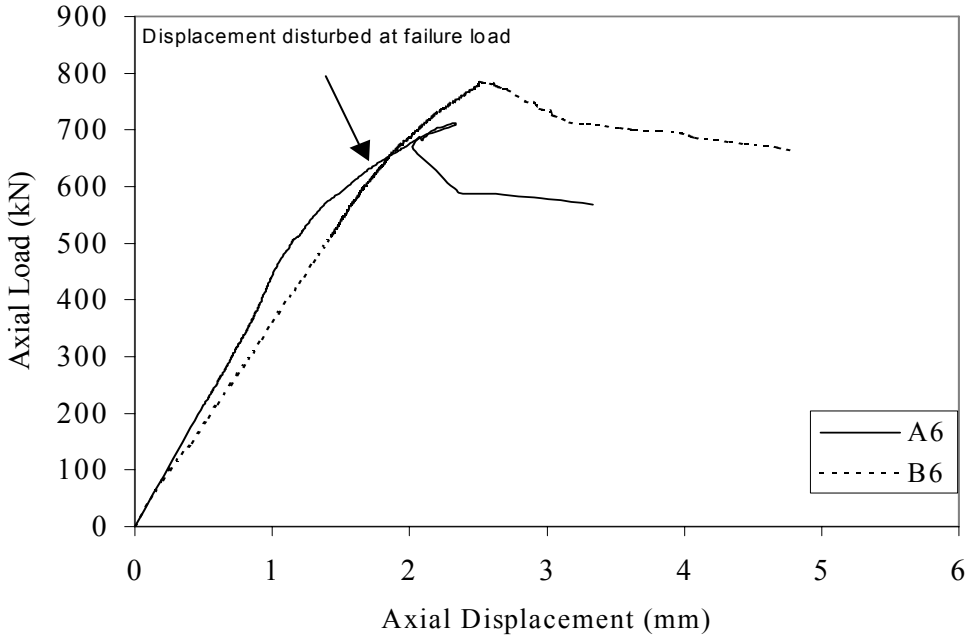

Figure 5.17 Load vs Displacement Curves for Specimens under Axial Load Only

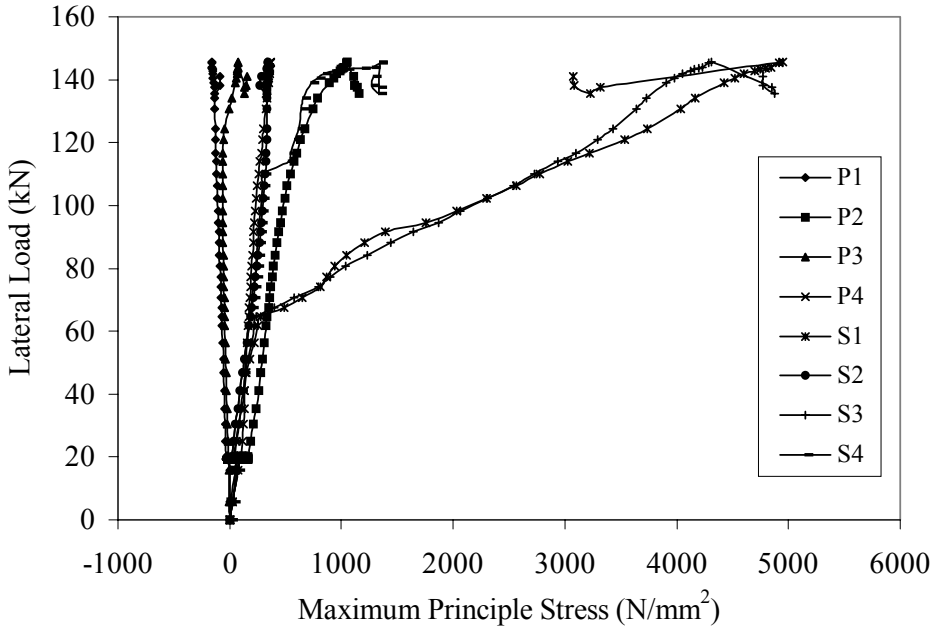

Figure 5.18 Maximum Principle Stress at Locations of Strain Gauges for B3

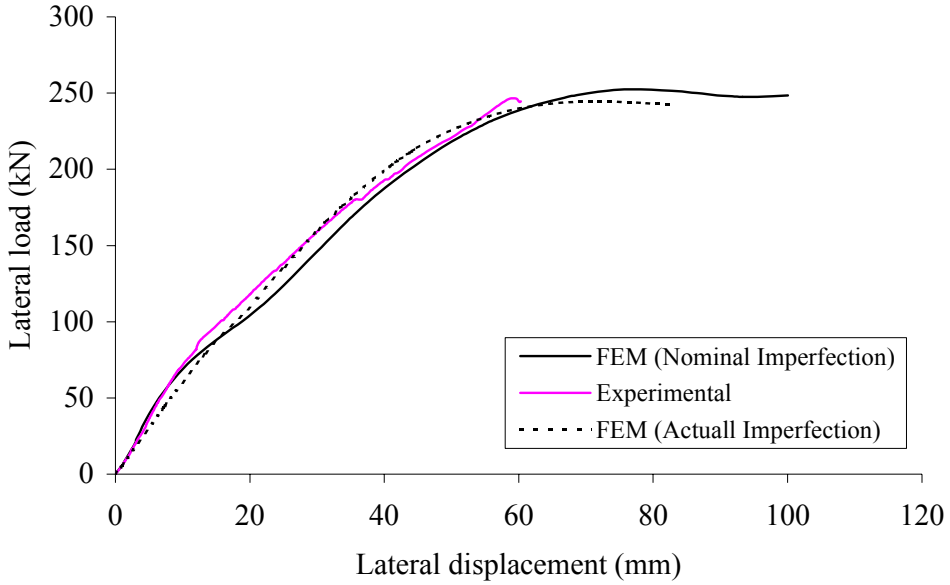

Figure 5.19 Comparison of Load vs Displacement Curves for Specimen A1

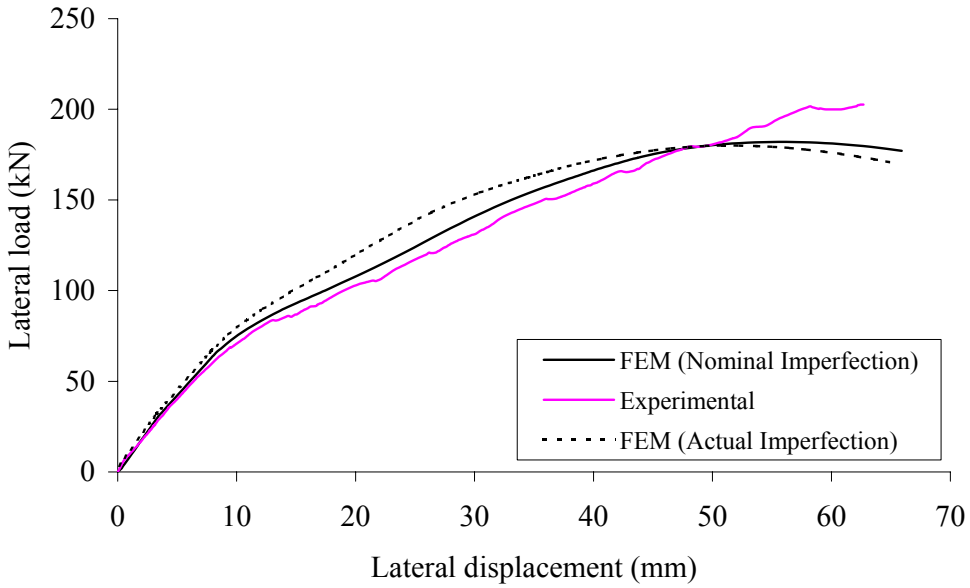

Figure 5.20 Comparison of Load vs Displacement Curves for Specimen A2

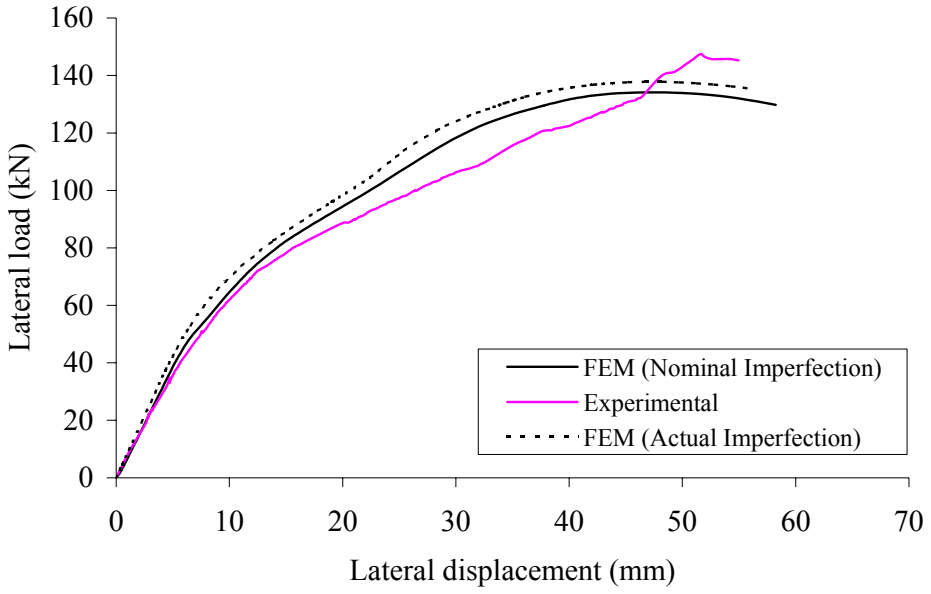

Figure 5.21 Comparison of Load vs Displacement Curves for Specimen A3

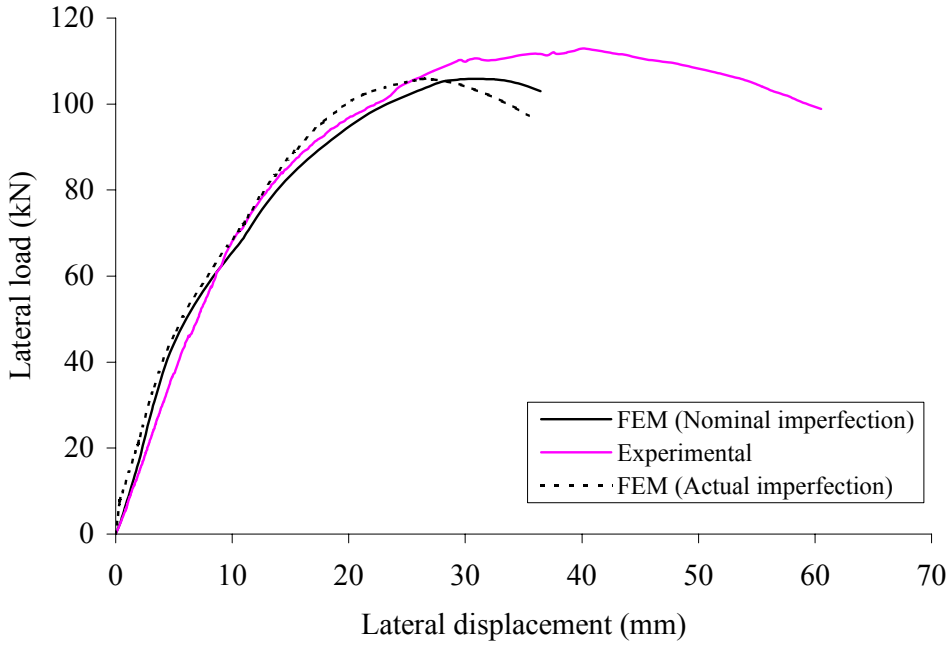

Figure 5.22 Comparison of Load vs Displacement Curves for Specimen A4

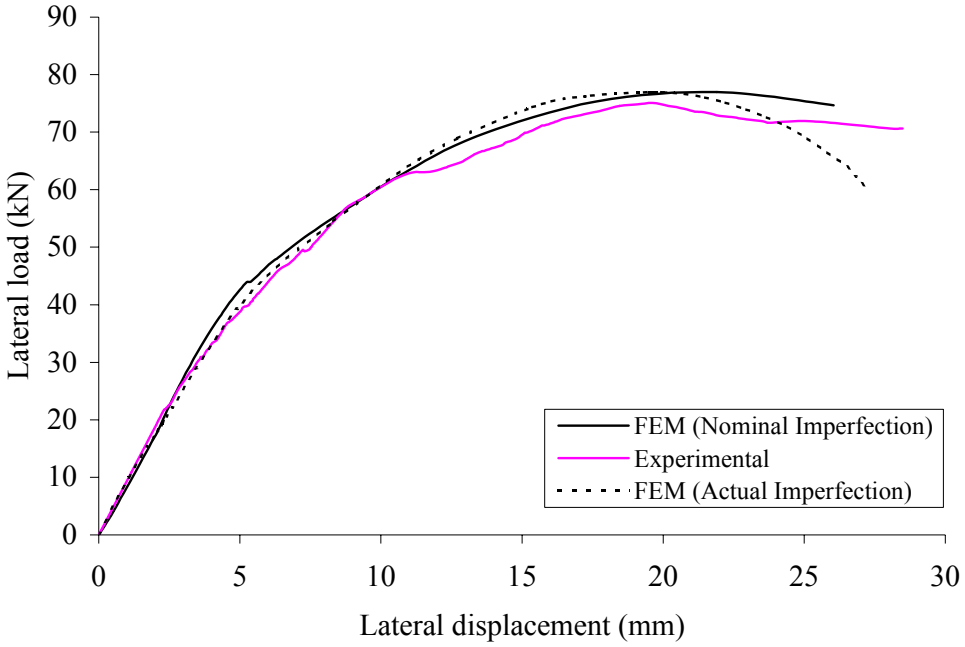

Figure 5.23 Comparison of Load vs Displacement Curves for Specimen A5

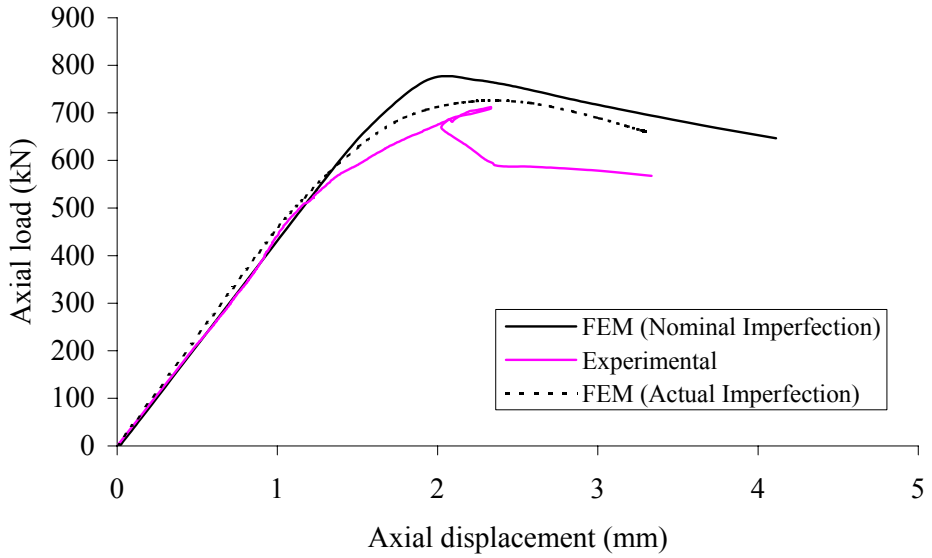

Figure 5.24 Comparison of Load vs Displacement Curves for Specimen A6

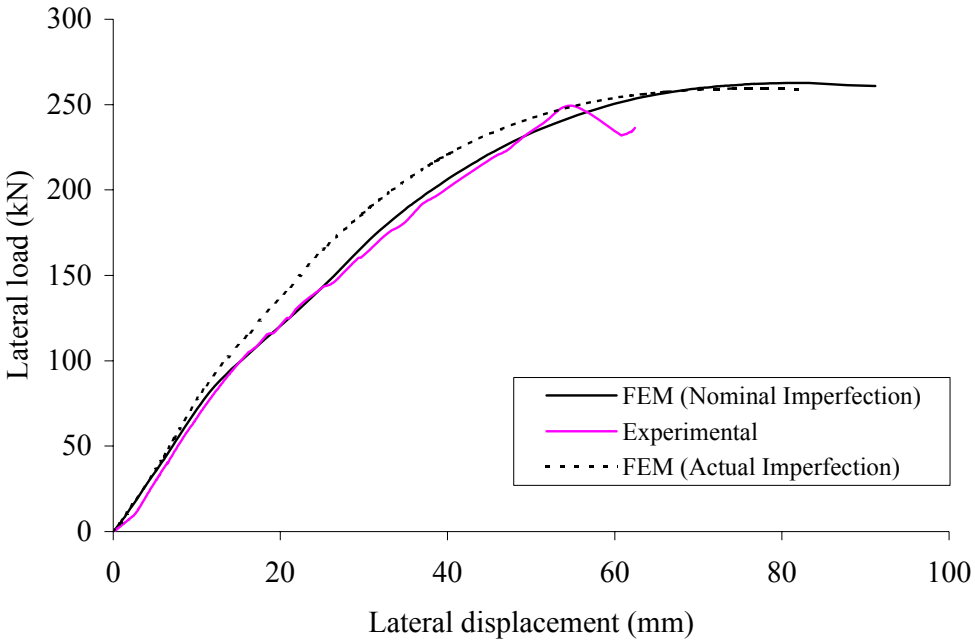

Figure 5.25 Comparison of Load vs Displacement Curves for Specimen B1

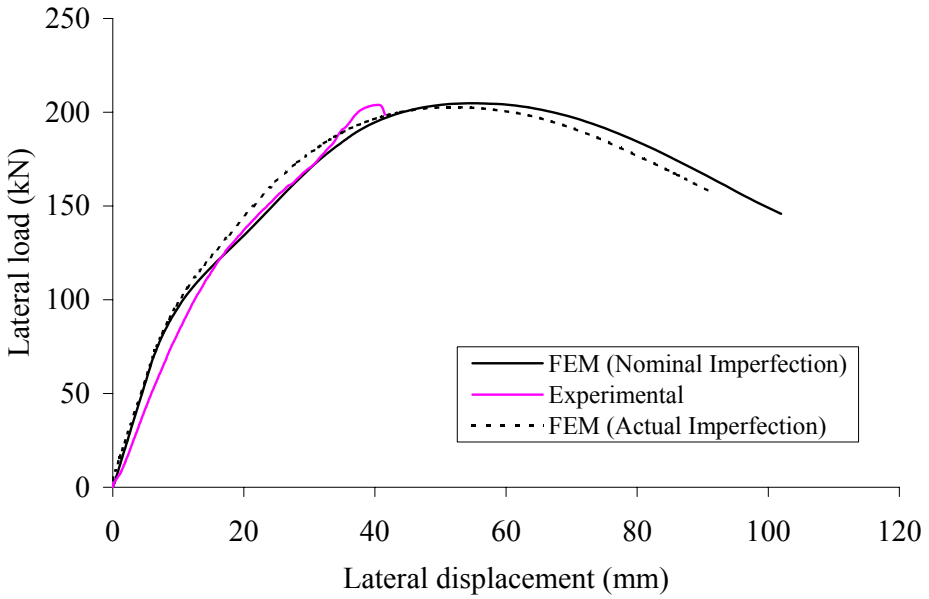

Figure 5.26 Comparison of Load vs Displacement Curves for Specimen B2

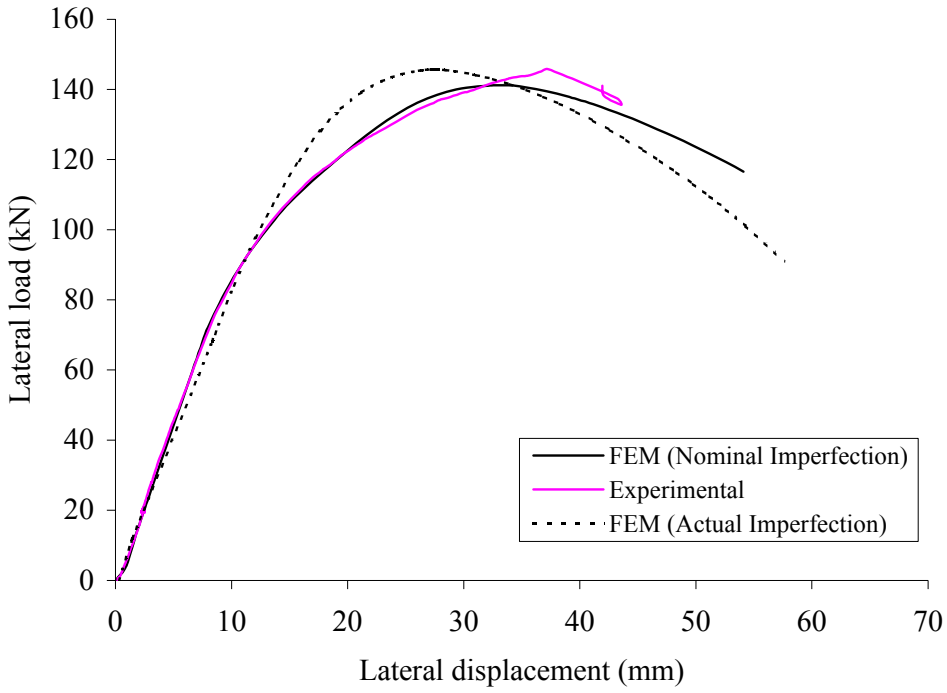

Figure 5.27 Comparison of Load vs Displacement Curves for Specimen B3

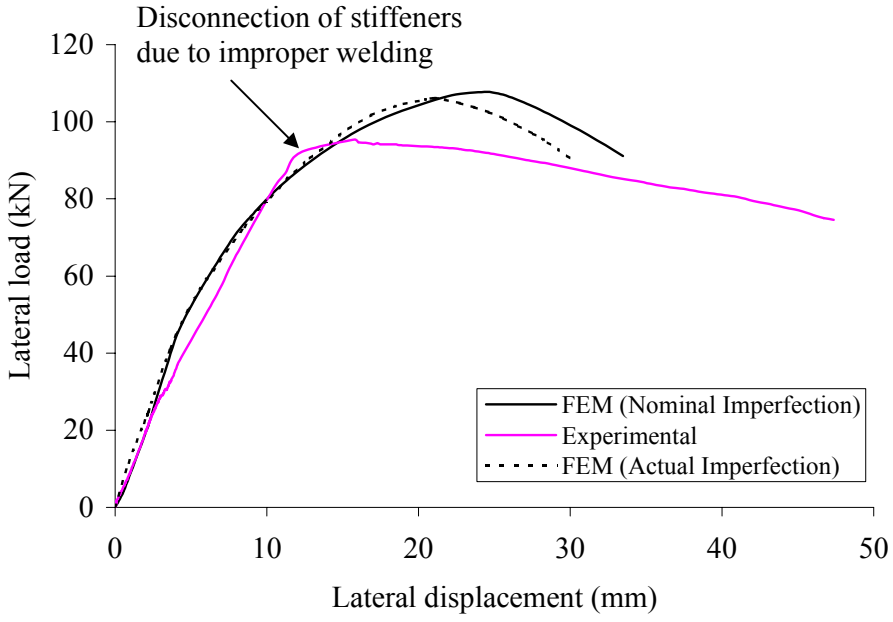

Figure 5.28 Comparison of Load vs Displacement Curves for Specimen B4

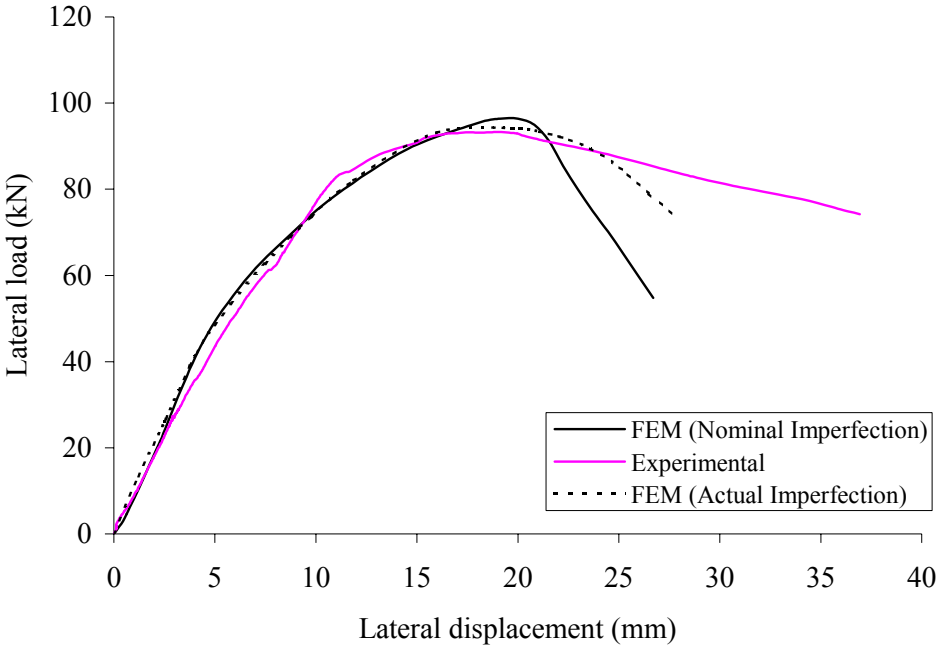

Figure 5.29 Comparison of Load vs Displacement Curves for Specimen B5

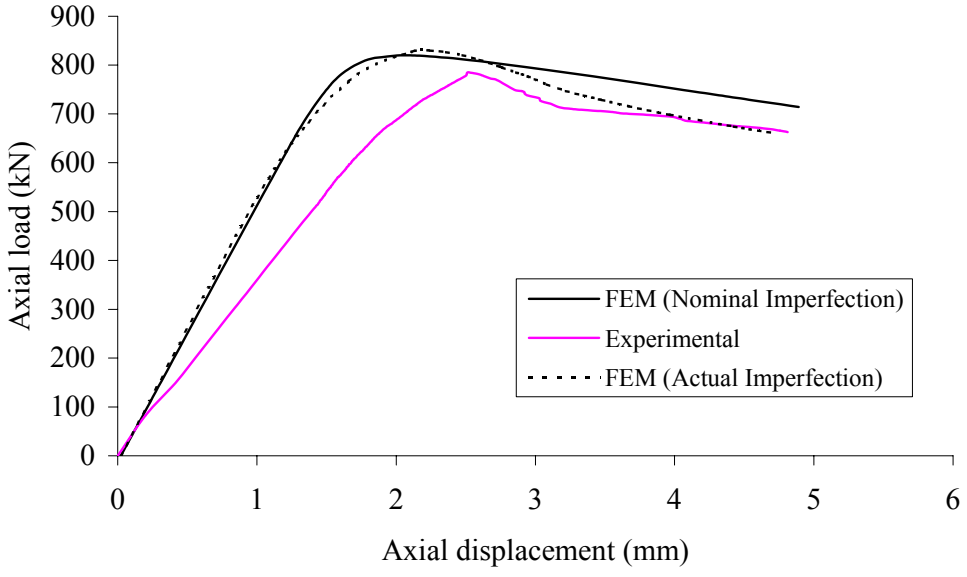

Figure 5.30 Comparison of Load vs Displacement Curves for Specimen B6

Figure 5.31 Comparison of Failure Shapes for Specimen under Combined Loads

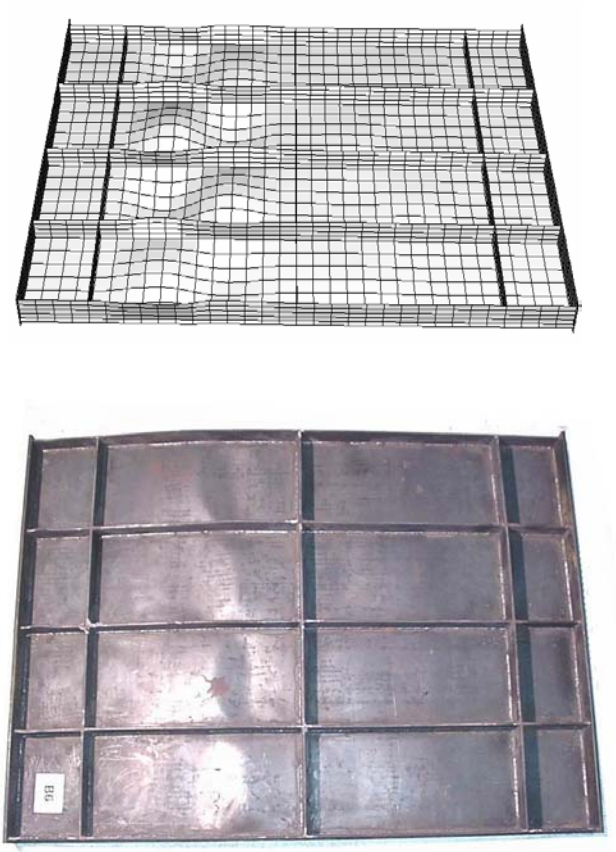

Figure 5.32 Comparison of Failure Shapes for Specimen under Axial Load Only

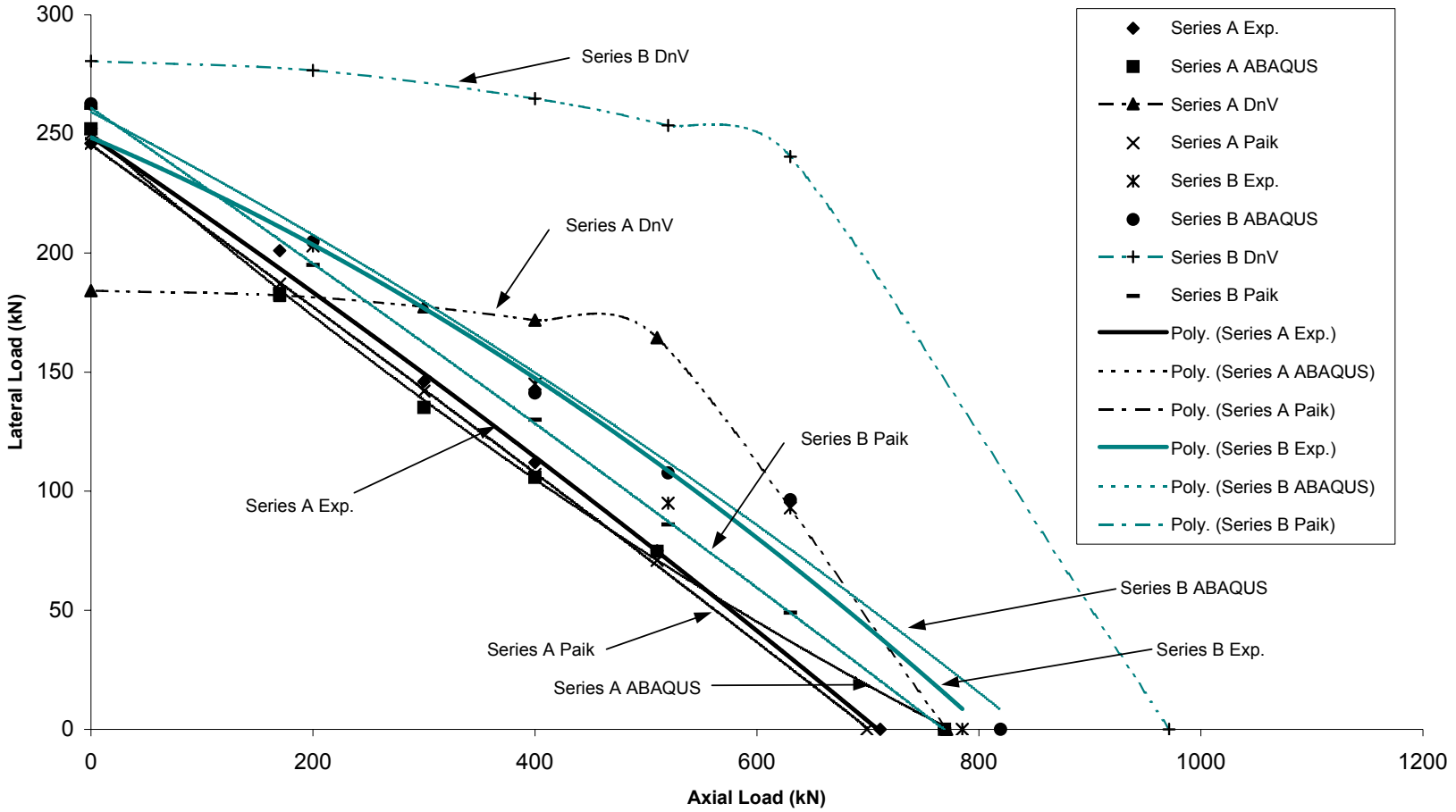

Figure 5.33 Interaction Curves for Series A and Series B

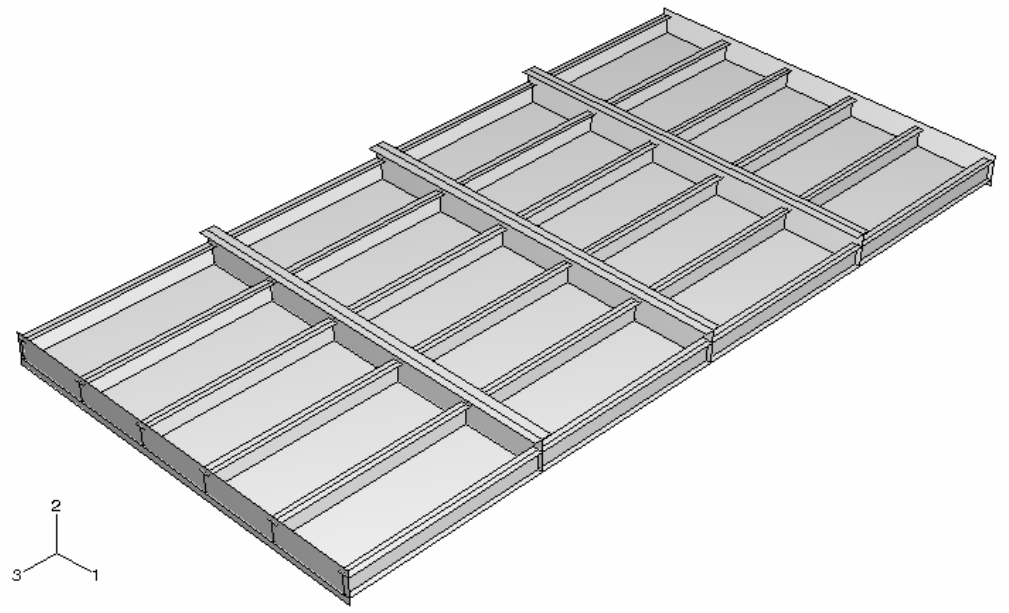

Figure 5.34 Geometry of Stiffened Plate for Parametric Study

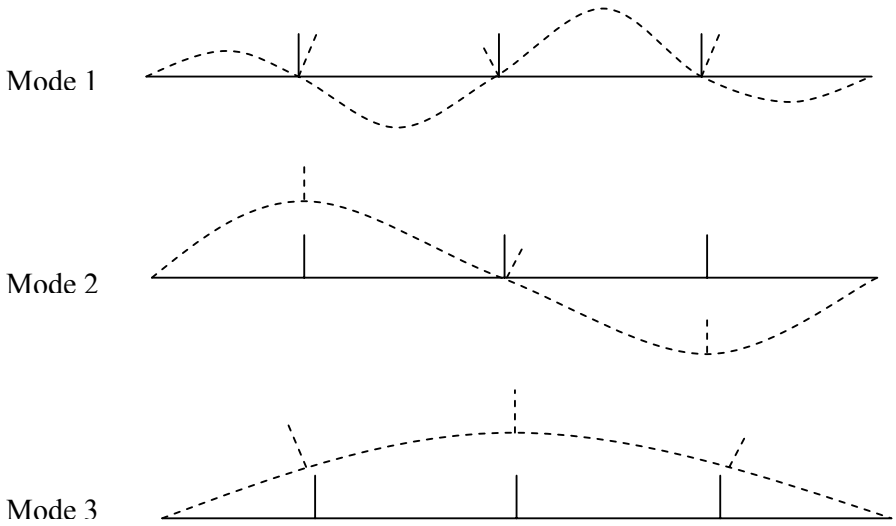

Figure 5.35 Initial Imperfection Modes Considered In Parametric Study

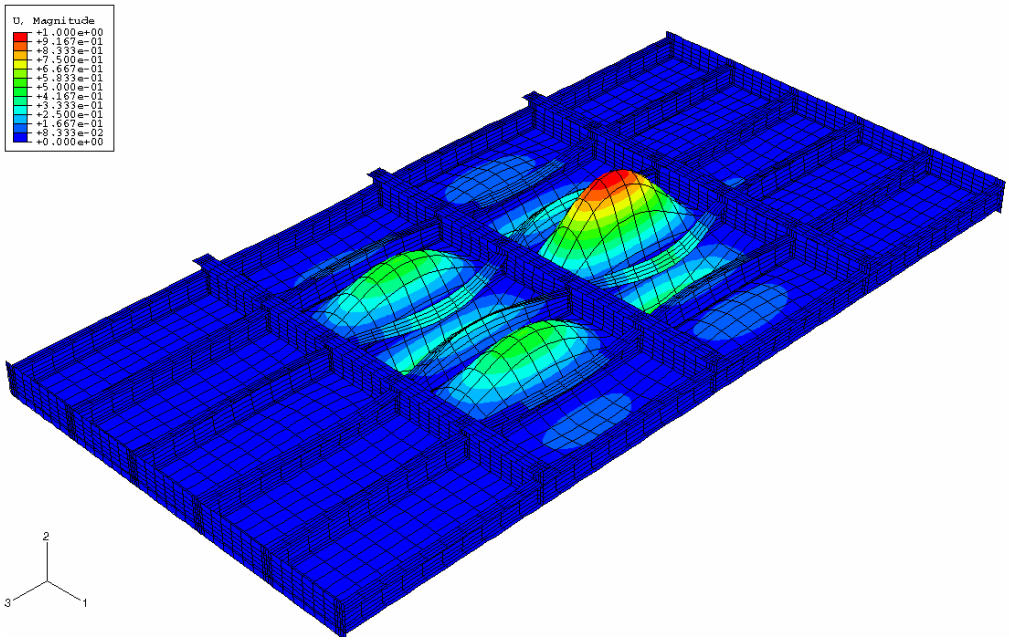

Figure 5.36 Mode 1 Initial Imperfection in ABAQUS Analysis

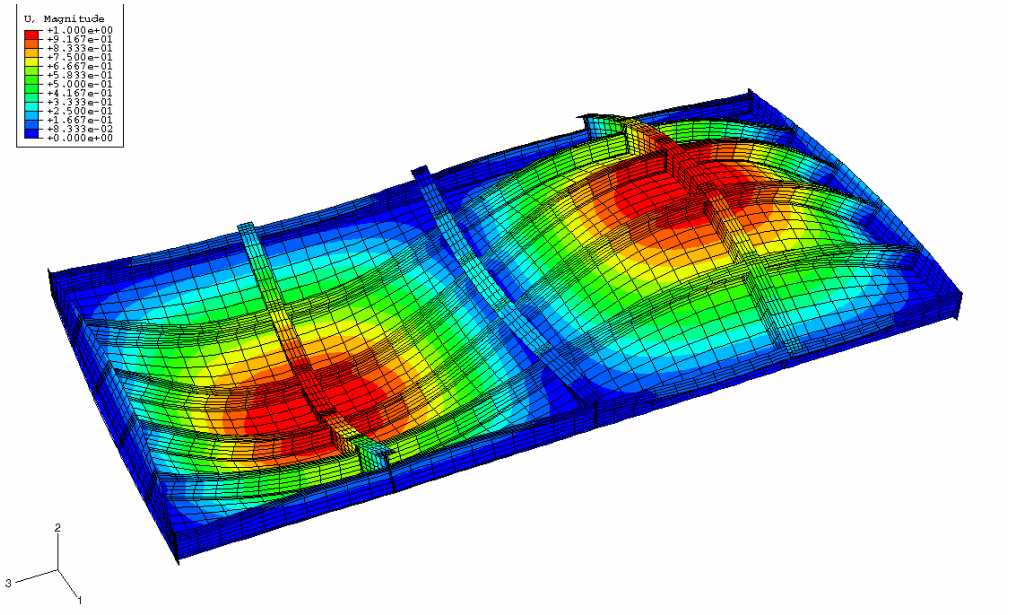

Figure 5.37 Mode 2 Initial Imperfection in ABAQUS Analysis

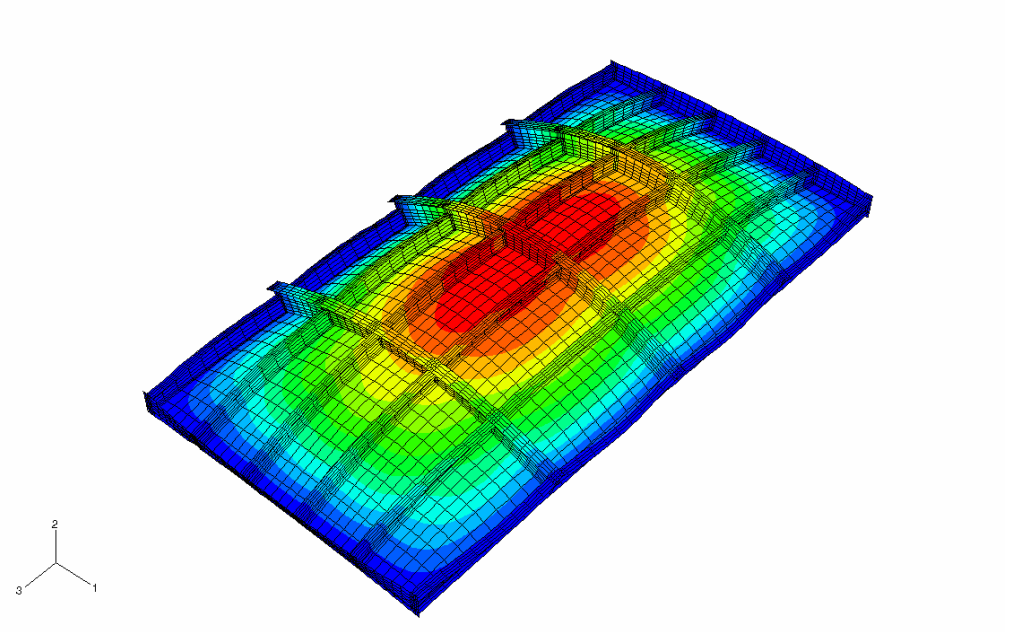

Figure 5.38 Mode 3 Initial Imperfection in ABAQUS Analysis

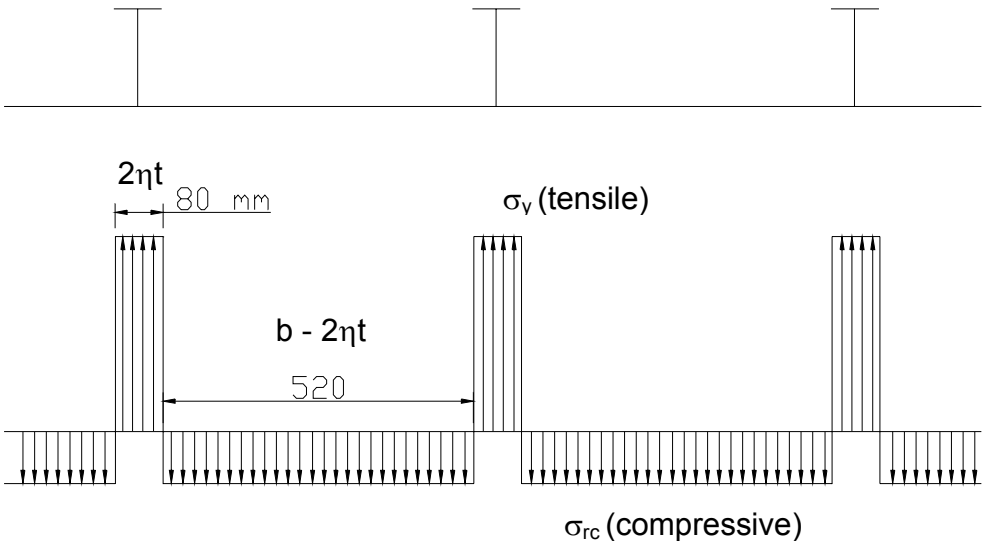

Figure 5.39 Idealization of Residual Stress

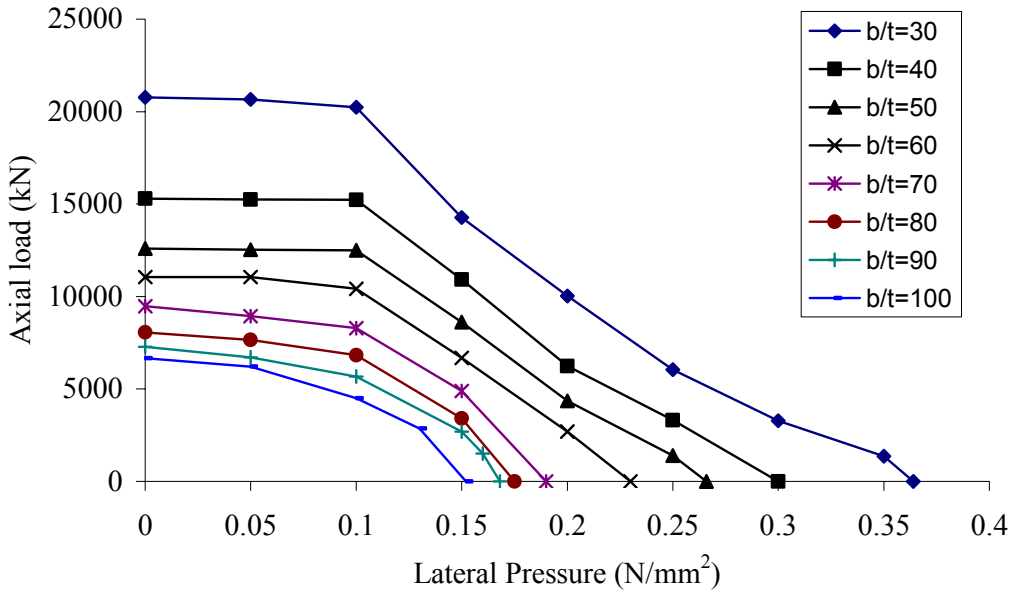

Figure 5.40 Interaction Curves for Stiffened Plates Considered in Parametric Studies

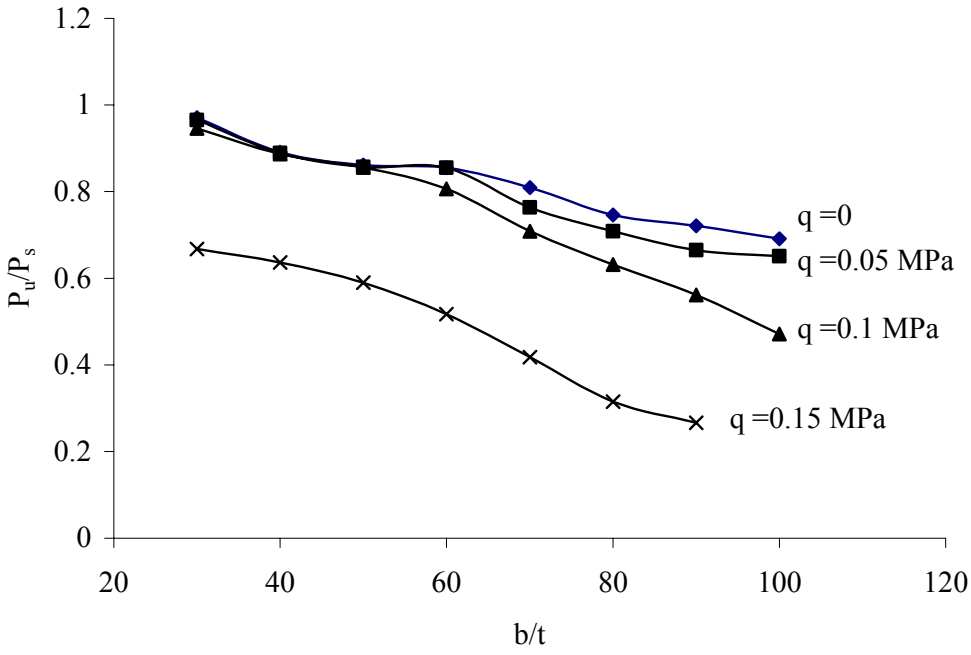

Figure 5.41 Influences of Lateral Pressure on the Ultimate Load of Stiffened Plates

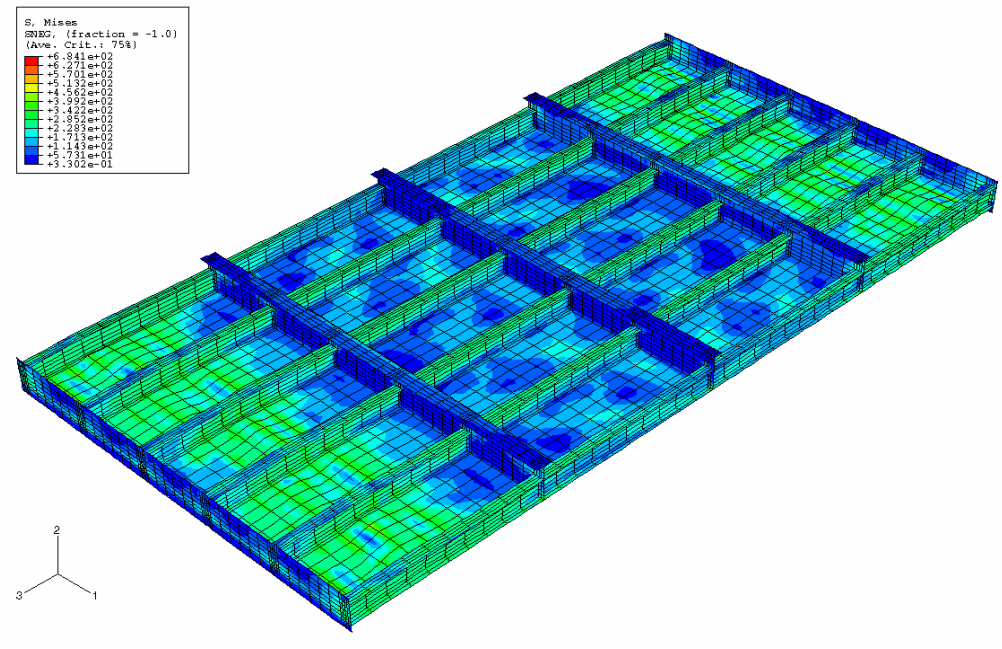

(a) Failure Shape with Simply Supported Condition

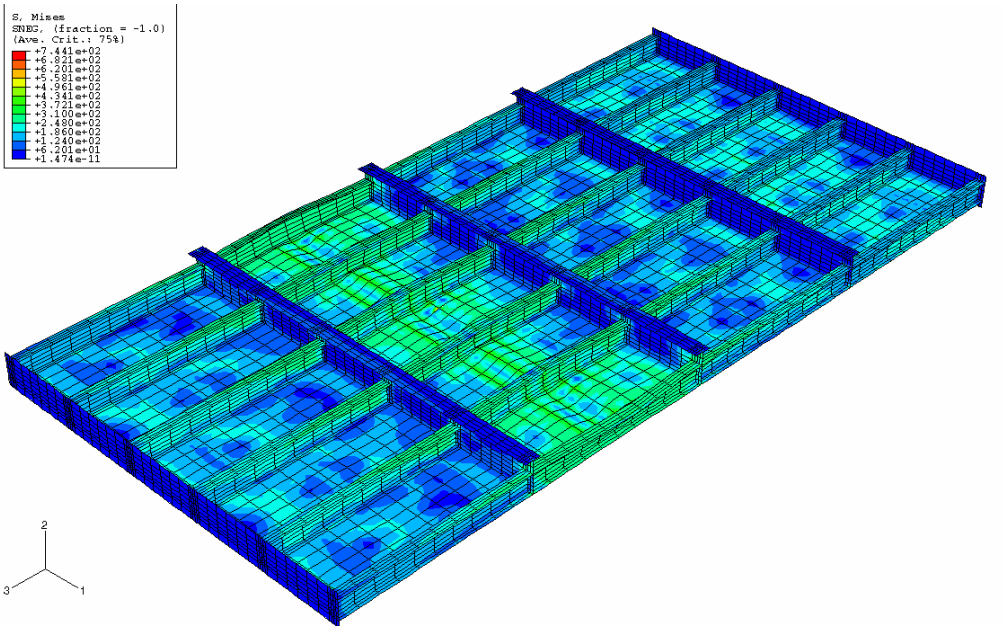

(b) Failure Shape with Fixed Supported Condition

Figure 5.42 Changes of Failure Shapes Due to Boundary Conditions

CHAPTER 6 CONCLUSIONS

6.1 Conclusions

Based on the experimental investigation, finite element analysis and parametric studies, following conclusions can be drawn:

- Finite element analysis package ABAQUS is capable of predicting the elastic and inelastic behaviours, ultimate load and failure modes of stiffened plates subjected to both in-plane load and lateral pressure with sufficient accuracy. The discrepancy between ABAQUS results and experimental results lies within 10%.
- Plate slenderness ratios (b/t_p) have significant influence on the ultimate load of stiffened plates subjected to both in-plane load and lateral pressure. Increase of plate slenderness ratio results in a decrease of ultimate load capacity of stiffened plate.
- When stiffened plates are predominantly under the action of axial compression failure occurs by local buckling and yielding of base plates. The stiffened plate behaves as an orthotropic plate and fails by forming diagonal yield lines when lateral pressure is the major component of the loading.
- Both experimental results and numerical results show that lateral load carrying capacity of stiffened plate drops with increase of axial load and vice-versa. Small lateral pressure does not significantly reduce the axial strength of stocky stiffened plates. The effects of lateral pressure on strength appear to be similar to those of initial imperfection with a pattern of small overall deformation of stiffened plate.

- Stiffened plates with fixed ended boundary condition generally have higher ultimate load than those with simply supported boundary condition. Parametric study shows change of simply supported boundary condition to fixed ended boundary condition results in increase of ultimate load up to 15%. The change of boundary condition not only affects the ultimate load but also influences the location of failure.
- Presence of initial imperfection generally reduces the ultimate load of stiffened plates. Increase in the magnitude of initial imperfection reduces the ultimate load of stiffened plates. Increase of magnitude of imperfection at location of failure has more significant effects on ultimate load than increase of magnitude of imperfection at other locations of stiffened plate.
- Parametric studies indicate that residual stress only has a secondary effect on the ultimate load of stiffened plates for the amount of residual stress considered. Reduction of ultimate load due to residual stress varies from 0.1% to 1.6%.

6.2 Recommendations

It should be noted that different geometry of stiffened plates subjected to combined action of in-plane load and lateral pressure can have different failure modes. In the present study, only plate induced failure was considered both in experimental and numerical investigations. The stiffeners were selected such that they remain stocky before local buckling of base plate. Experimental and numerical investigations can be carried out on the stiffened plates with stiffener induced failure.

It is believed that the types of stiffeners have influence on the behaviour of stiffened plates. Although flat stiffeners were used in experimental investigation and T stiffeners were used in parametric studies in the present study, the effects of types of stiffeners were not studied. Research can be carried out to investigate the effects of types of stiffeners on the behaviour of stiffened plates.

In the current study, only initial imperfection and residual stress in base plate were considered. High tensile residual stresses in the T stiffeners induced by cutting and welding process seem likely to have a beneficial effect on the ultimate load of stiffened plates. Investigations on the stiffened plates can be carried out by including the initial imperfection and residual stress of stiffeners.

The scope of investigations can be extended to develop or incorporate formulae for stiffened plates with various parameters. Experiments can be conducted using the unit panel specimen and full scale specimen to verify the beam-column design approach.

REFERENCES

1. Hoppman, W. H. and Baltimore, MD., Bending of Orthogonally Stiffened Plates, *Journal of Applied Mechanics*, pp. 267-271, 1955.

2. Huffington, N. J. JR. and Blacksburg, VA., Theorectical Determination of Rigidity Properties of Orthogonally Stiffened Plates, *Journal of Applied Mechanics*, pp. 15-20, 1956.

3. Soper, W. G., Large Deflection of Stiffened Plate. *Transactions of the ASME*, pp. 444-448, 1958.

4. Okada, H.; Kitaura, K. and Fukumoto, Y., Buckling Strength of Stiffened Plates Containing One Longitudinal or Transverse Girder Under Compression, *Bulletin of University of Osaka Prefecture, Series A*, Volume 20, Issue 2, pp. 287-306, 1971.

5. Dean, J. A. and Omid'varan, C., Analysis of Ribbed Plates, Journal of Struct. Div., Proc. ASCE, Vol. 95, No. ST3, pp.441-440, 1969.

6. Webb, S. E. and Dowling, P. J., Large Deflection Elasto-Plastic Behaviour of Discretely Stiffened Plates, *Proceedings of the Institution of Civil Engineers (London). Part 1 - Design & Construction*, Volume 69, Part 2, pp.375-401, 1980.

7. BS 5400, Bristish Standard Institute, Steel, Concrete and Composite Bridges, Part 3. Code of Practice for Design of Steel Bridges (2000).

8. American Petroleum Institute, Recommended Practice for Planning, Designing and Constructing Fixed Offshore Platforms-Working Stress Design, 20th edition, 1993.

9. American Institute of Steel Construction, AISC (1980), AISC Specification for the Design, Fabrication and Erection of Structural Steel for Buildings, 8th edition.

10. Brazilian Code for Steel Bridges, Chapmen & Dowling, London, 1982.

11. American Bureau of Shipping, Rules Restatement Report, 1991.

12. Norsek Standard, Design of Steel Structures, Rev 1, December 1998.

13. Kondo, J, Ultimate Strength of Longitudinally Stiffened Plate Panels Subjected to Combined Axial and Lateral Loading, PhD Thesis, Lehigh University, 1965.

14. Ostapenko, A. and Lee, T. T., Test on Longitudinal Stiffened Plate Panels Subjected to Lateral and Axial Loading, *Fritz Engineering Laboratory Report No. 248.4*, 1960.

15. Tvergaad and Needleman, A., Buckling of Eccentrically Stiffened Elastic-Plastic Panels on Two Simple Supports or Multiply Supported. *International Journal of Solids and Structures*, Vol. 11, pp. 647-663, 1975.

16. Soreide, T. H.; Moan, T. and Nordsve, N. T., On the Behaviour and Design of Stiffened Plates in Ultimate Limit State, *Journal of Ship Research*, Vol. 22, Issue 4, pp. 238-244, 1978.

17. Louca, L.A. and Harding, J. E., Torsional Buckling of Outstands in Longitudinally Stiffened Panels, *Thin-Walled Structures*, Vol. 24, Issue 3, pp. 211-229, 1996.

18. Bai, Y; Xu, X. D. and Cui, W. C., Ultimate Strength Analysis of Ship Hulls Based on Plastic Node Method, *Chuan Bo Li Xue/Journal of Ship Mechanics*, Volume 2, Issue 4, pp. 54-62, 1998.

19. Belkune, R. W. and Ramesh, C. K., Forced Response of Stiffened Plates, *ASME Pap*, pp. 26-30, 1977.

20. Chai, C. W. and Zheng, Y. H., Stability Analysis of Stiffened Plate Using the Compatible Elements, *Acta Mechanica Sinica*, Issue2, pp. 139-148, 1980.

21. Komatsu, S; Nara, S and Kitada, T, Elasto-Plastic Analysis of Orthogonally Stiffened Plates With Initial Imperfections Under Uniaxial Compression, *Computers and Structures*, Vol. 11, Issue 5, pp. 429-437, 1980.

22. O'Leary, J. R. and Harari, I., Finite Element Analysis of Stiffened Plates, *Computers and Structures*, Vol.21, Issue 5, pp. 973-985, 1985.

23. Guo, M. and Harik, I. E., Stability of Eccentrically Stiffened Plates, *Thin-Walled Structures*, Vol.14, Issue 1, pp. 1-20, 1992.

24. Hrabok, M. M. and Hrudey, T. M., Structural Modelling of Stiffened Plates for Analysis and Design, *International Conference on Computational Structures Technology-Proceedings*, pp. 43-48, 1994.

25. Sabir, B. and Djoudi, M. S., Elastic Buckling of Stiffened Plates By the Finite Element Method, *Structural Dynamics and Vibration*, PD-Vol.70, pp. 191-198, 1995.

26. Belkune, R. W. and Ramesh, C. K., Forced Response of Stiffened Plates, *ASME Pap*, pp. 26-30, 1977.

27. Bhattacharyya, S. K. and Vendhan, C. P., Similitude Analysis of Bending of Stiffened Plates, *International Journal of Structures*, Volume 8, Issue 2, pp. 95-105, 1988.

28. Bhimaraddi, A.; Moss, P. J. and Carr, A. J., Finite Element Analysis of Orthogonally Stiffened Annular Sector Plates, *Journal of Engineering Mechanics*, Volume 115, Issue 9, pp. 2074-2088, 1989.

29. Cichocki, K. and Ruchwa, M., Steel Stiffened Plates Subjected to A Blast Load, *Journal de Physique IV (Proceedings),* Volume 10, Issue 9, pp. 535-540, 2000.

30. Gendy, A. S. and Saleeb, A. F., Consistent Mixed Model for Stability of Stiffened Panels with Cut-outs, *Computers & Structures*, Volume 54, Issue 1, pp.119-130, 1995.

31. Grondin, G. Y., Elwi, A. E. and Cheng, J. J. R., Buckling of Stiffened Steel Plate - A Parametric Study, *Journal of Constructional Steel Research*, Volume 50, Issue 2, pp.151-175, 1999.

32. Jiang, W., Bao, G. and Roberts, J. C., Finite Element Modeling of Stiffened and Unstiffened Orthotropic Plates, *Computers & Structures*, Volume 63, No. 1, pp. 105-117, 1997.

33. Kaeding, P. and Fujikubo, M., New Simplified Model for Collapse Analysis of Stiffened Plates and Its Application to Offshore Structures, *Proceedings of the International Offshore and Polar Engineering Conference*, Volume 4, pp. 398-405, 2001.

34. McEwan, M. I.; Wright, J. R.; Cooper, J.E. and Leung, A. Y. T., A Finite Element/Modal Technique for Nonlinear Plate and Stiffened Panel Response Prediction, *Collection of Technical Papers - AIAA/ASME/ASCE/AHS/ASC Structures, Structural Dynamics and Materials Conference*, Volume 5, pp. 3061-3070, 2001.

35. Mukhopadhyay, M. and Mukherjee, A., Finite Element Buckling Analysis of Stiffened Plates, *Computers and Structures*, Volume 34, Issue 6, pp. 795-803, 1990.

36. Nordsve, N. T. and Moan, T., Numerical Collapse Analysis of Compression Members, *Computers and Structures*, Vol. 12, Issue 4, pp. 521-531, 1979.

37. Orisamolu, I. R and Ma, K. T., Probabilistic Finite Element Methodology for the Reliability Assessment of Stiffened Plates, *Proceedings of the International Offshore and Polar Engineering Conference*, Volume 4, pp. 232-238, 1997.

38. Rossow, M. P. and Ibrahimkhail, A. K., Constraint Method Analysis of Stiffened Plates, *Computers and Structures*, Volume 8, Issue 1, pp. 51-60, 1978.

39. Zhou, G. L. and Zhu, J. X., Postbuckling Behaviour of Stiffened Plate, Stability of Metal Structures, pp. 507-515, 1989.

40. Fujikubo, M. and Kaeding, P., New Simplified Approach to Collapse Analysis of Stiffened Plates, *Marine Structures*, Vol. 15, Issue 3, pp. 251-283, 2002.

41. Sheikh, I. A., Grondin, G. Y. and Elwi, A. E., Stiffened Steel Plates Under Uniaxial Compression, *Journal of Constructional Steel Research*, Vol. 58, Issue 5-8, pp. 1061-1080, 2002.

42. Turvey, G. J. and Salehi, M., Large Deflection Analysis of Eccentrically Stiffened Sector Plates, *Computer and Structures*, Volume 68, Issue1-3, pp.191-205, 1998.

43. Turvey, G. J. and Salehi, M., Elastic Large Deflection Analysis of Stiffened Annular Sector Plates, *International Journal of Mechanical Sciences*, Volume 40, Issue1, pp.51-70, 1998.

44. Yao, T.; Fujikubo, M. and Ohno, Y., Collapse Behaviour of Stiffened Plating under Thrust (1st report), *Journal of the Society of Navel Architects of Japan*, Vol. 178, pp. 451-462, 1995.

45. Hu, S. Z. and Jiang, L., A Finite Element Simulation of the Test Procedure of the Stiffened Panels, *Marine Structures*, Vol. 11, Issue 3, pp. 75-99, 1998.

46. Delcourt, C. and Cheung, Y. K., Finite Strip Analysis of Continuous Folded Plates, *IABSE Proceedings*, pp.14-78, 1978.

47. Kakol, W., Stability Analysis of Stiffened Plates by Finite Strips, *Thin-Walled Structures*, Vol. 10, Issue 4, pp. 277-297, 1990.

48. Guo, Y. L. and Lindner, J. Analysis of Elastic-Plastic Interaction Buckling of Stiffened Panels by Spline Finite Strip Method, *Computers and Structures*, Vol. 46, Issue 3, pp. 429-436, 1993.

49. Wang, X and Rammerstorfer, F. G., Effective Width for Postcritically Loaded Stiffened Plates, *Recent Developments in Computational Mechanics; American Society of Mechanical Engineers, Aerospace Division (Publication) AD*, Volume 26, Issue 4, pp.261-286, 1993.

50. Wang, X. and Rammerstorfer, F. G., Determination of Effective Breadth and Effective Width of Stiffened Plates by Finite Strip Analysis, *Thin-Walled Structures*, Volume 26, Issue 4, pp.261-286, 1996.

51. Chen, C. J.; Gutkowski, R. M. and Puckett, J. A., B-Spline Compound Strip Analysis of Stiffened Plates Under Transverse Loading, *Computers and Structures*, Vol.34, Issue 2, pp.337-347, 1990.

52. Sheikii, A. H. and Mukiiopadhyay, M., Analysis of Stiffened Plate With Arbitrary Platform by the General Spline Finite Strip Method, *Computers and Structures*, Vol. 42, Issue 1, pp.53-61, 1992.

53. Kater, W. and Murray, N. W., Elastic Buckling of Stiffened Steel Plates of High Aspect Ratio Under Uniaxial Compression, *Behaviour of Thin-Walled Structures*, pp. 355-373, 1984.

54. Lillico, M.; Butler, R.; Hunt, G.W.; Watson, A.; Kennedy, D., Post-Buckling of Single and Multi-bay Panels Using Strut, Strip and Fe Methods, *Collection of Technical Papers - AIAA/ASME/ASCE/AHS/ASC Structures, Structural Dynamics and Materials Conference*, Vol. 2, pp. 1078-1087, 2001.

55. Riks, E., Buckling and Post-Buckling Analysis of Stiffened Panels in Wing Box Structures, *International Journal of Solids and Structures*, Volume 37, Issue 46-47, pp.6795-6824, 2000.

56. Yoshida, H; Maegawa, K, Buckling Strength of Orthogonally Stiffened Plates Under Uniaxial Compression, *Journal of Structural Mechanics*, volume 7, Issue 2, pp. 161-191, 1979.

57. Xie, W.-C. Buckling Model Localization in Rib-Stiffened Plates with Randomly Misplaced Stiffeners, *Computers and Structures*, Vol. 67, Issue 1-3, pp. 175-189, 1998.

58. Xie, W.-C. and Ibrahim, A., Buckling Mode Localization in Rib-Stiffened Plates with Misplaced Stiffeners - A Finite Strip Approach, *Chaos, Solitons and Fractals*, Vol. 11, Issue 10, pp. 1543-1558, 2000.

59. Xie, W.-C.; Elishakoff, I., Buckling Mode Localization in Rib-Stiffened Plates With Misplaced Stiffeners - Kantorovich Approach, *Chaos, Solitons and Fractals*, Vol. 11, Issue 10, pp. 1559-1574, 2000.

60. Wittrick, W. H., A Unified Approach to the Initial Buckling of Stiffened Panels in Compression, *Aeronautical Quarterly*, Volume 19, pp. 265-283, 1968.

61. Turvey, G. J. and Wittrick, W. H., The Influence of Orthothopy on the Stability of Some Multi-plate Structures in Compression, *Aeronautical Quarterly*, Vol. 24, pp. 1-8, 1973.

62. Dorman, P. and Dwight, J. B., Tests on Stiffened Compression Panels and Plate Panels, *Steel box girder bridges*, pp. 63-75, 1973.

63. Komatsu, S. Masayuki Ushio and Toshiyuki Kitada, An Experimental Study on the Ultimate Strength of Stiffened Plates, *Transations of JSCE*, Volume 8, pp.102-104, 1976.

64. Komatsu, S.; Kitada, T.; Okada, J. and Ushio, M., Study on the Ultimate Strength of Plates and Stiffened Plates With Initial Imperfections Under Uniaxial Compression, *Transactions of the Japan Society of Civil Engineers*, Volume 10, pp.315-318, 1979.

65. Hu, S. Z.; Chen, Q.; Pegg, N. and Zimmerman, T. J. E., Ultimate Collapse Tests of Stiffened-Plate Ship Structural Units, *Marine Structures*, Volume 10, Issues 8-10, pp. 587-610, 1997.

66. Kitada, T.; Nakai, H. and Furuta, T., Experimental Study on Ultimate Strength of Stiffened Plates Subjected to Longitudinal Tension and Transverse Compression, *Journal of Constructional Steel Research*, Volume 19, Issue 3, pp. 203-212, 1991.

67. Plank, R. J. and Williams, F. W., Critical Buckling of Some Stiffened Panels in Compression, Shear and Bending, *Aeronautical Quarterly*, pp.165-179, 1974.

68. Nishihara, S., Ultimate Longitudinal Strength of Mid-ship Cross Section, *Naval Architecture and Ocean Engineering*, Vol. 22, pp. 200-214, 1984.

69. Bedair, O. K., The Elastic Behaviour of Multi-Stiffened Plates Under Uniform Compression, *Thin-Walled Structures*, Volume 27, Issue 4, pp.311-335, 1997.

70. Bedair, O. K., A Contribution to the Stability of Stiffened Plates under Uniform Compression, *Computers & Structures*, Volume 66, Issue 5, pp. 535-570, 1998.

71. Bedair, O. K., Analysis of Stiffened Plates under Lateral Loading Using Sequential Quadratic Programming (SQP), *Computers & Structures*, Volume 62, Issue 1, pp. 63-80, 1997.

72. Bedair, O. K., Influence of Stiffener Location on the Stability of Stiffened Plates under Compression and In-plane Bending, *International Journal of Mechanical Sciences*, Volume 39, Issue 1, pp. 33-49, 1997.

73. Bedair, O. K. and Troitsky, M. S. A Study of the Fundamental Frequency Characteristics of Eccentrically and Concentrically Simply Supported Stiffened Plates, *International Journal of Mechanical Sciences*, Volume 39, Issue 11, pp. 1259-1272, 1997.

74. Bedair, O. K., Buckling Behaviour of Plates Partially Restrained against Rotation under Stress Gradient, *Structural Engineering and Mechanics*, Volume 4, Issue 4, pp. 383-396, 1997.

75. Bedair, O. K. and Sherbourne, A. Unified Approach to Local Stability of Plate/Stiffener Assemblies, *Journal of Engineering Mechanics*, Volume 121, Issue 2, pp. 214-229, 1995.

76. Ueda, Y. and Yao, T., Ultimate Strength of Compressed Stiffened Plates and Minimum Stiffness Ratio of Their Stiffeners, *Eng. Stru.*, Vol. 5, pp. 97-107, 1983.

77. Ueda, Y.; Rashed, S. M. H. and Paik, J. K., An Incremental Galerkin Method for Plates and Stiffened Plates, *Computers and Structures*, Vol. 27, Issue 1, pp. 147-156, 1987.

78. Ueda, Y., Rashed, S. M. H. and Paik, J. K., Buckling and Ultimate Strength Interaction in Plates and Stiffened Panels under Combined Inplane Biaxial and Shearing Forces, *Marine Structures*, Vol. 8, Issue 1, pp. 1-3. 1995.

79. Ueda, Y.; Nakacho, K. and Moriyama, S., Simple Prediction Methods for Welding Deflection and Residual Stress of Stiffened Panels, *Transactions of JWRI (Japanese Welding Research Institute)*, Vol. 15, Issue 2, pp. 369-376, 1986.

80. Alagusundaramoorthy, P., Sundaravadivelu, R. and Ganapathy, C., Ultimate Strength of Stiffened Panels with Cutouts under Uniaxial Compression, *Marine Structures*, Volume 8, Issue 3, pp. 279-308, 1995.

81. Alagusundaramoorthy, P., Sundaravadivelu, R. and Ganapathy, C., Experimental Study on Collapse Load of Stiffened Panels with Cutouts, *Journal of Constructional Steel Research*, Volume 52, pp. 235-251, 1999.

82. Shanmugam, N. E.; Paramasivam, P. and Lee, S. L., Stiffened Flanges Containing Openings, *Journal of Structural Engineering*, Volume 112, Issue 10, pp. 2234 – 2246, 1986.

83. Kuranisi, M.; Niisawa, J.; Sato, R. and Koiso, A.; Nisimura, T., Stress and Deformations in Stiffened Panels with Rectangular Cut-outs. I. On Case of Uniform Tensile Loads, *Journal of the Research Institute of Science and Technology*, Nihon University, Issue 47, pp. 1-16, 1977.

84. Sato, R.; Koiso, A.; Kuranishi, M. and Niisawa, J., Stresses and Deformations in Stiffened Panels with Rectangular Cut-outs. III. On Case of Eccentric Tensile Loads, *Journal of the Research Institute of Science and Technology*, Nihon University, Issue 50, pp. 15-25, 1979.

85. Lee, E. J. and Klang, E. C., Stress Distribution in An Edge-Stiffened Semi-Infinite Elastic Plate Containing a Circular Hole, *Transactions of the ASME. Journal of Applied Mechanics*, Volume 59, Issue 4, pp. 789-795, 1997.

86. Guo, R. X. and Wang, L., The Elastic Buckling of Ship Grillage with Large Hatch Opening and Unevenly Spaced Transverses, *Stability of Metal Structures*, pp. 541-548, 1989.

87. Paik, J. K.; Thayamballi, A. K. and Lee,W. H., A Numerical Investigation of Tripping, *Marine Structures*, Vol. 11, Issue 4-5, pp. 159-183, 1998.

88. Paik, J. K.; Thayamballi, A. K. and Park, Y. E., Local Buckling of Stiffeners in Ship Plating, *Journal of Ship Research*, Volume 42, Issue 1, pp. 56-67, 1998.

89. Danielson, D. A.; Kihl, D. P.; Hodges, D. H., Tripping of Thin-Walled Plating Stiffeners in Axial Compression, *Thin-Walled Structures*, Vol.10, Issue 2, pp. 121-142, 1995.

90. Danielson, D. A., Analytical Tripping Loads for Stiffened Plates, *International Journal of Solids and Structures*, Vol.32, NO. 8/9, pp.1319-1328, 1995.

91. Fujikubo, M. and Yao, T., Elastic Local Buckling Strength of Stiffened Plate Considering Plate / Stiffener Interaction and Welding Residual Stress, *Marine Structures*, 12 (1999), pp.543-564, 1999.

92. Zhang, S. K.; Yu, Q. and Mu, Y., Semi-analytical Method of Assessing the Residual Longitudinal Strength of Damaged Ship Hull, *Proc. of the int. Offshore and Polar Engineering Conference*, Volume 4, pp. 510-516, 1996.

93. Niwa, Y.; Watanabe, E. and Isami, H., New Approach to Predict the Strength of Compressed Steel Stiffened Plates, *Proceedings of the Japan Society of Civil Engineers*, pp. 35-44, 1985.

94. Wei, D. and Zhang, S. K., Ultimate compressive strength prediction of stiffened panels by counterpropagation neural networks (CPN), *Proceedings of the International Offshore and Polar Engineering Conference*, Volume 4, pp.280-285, 1999.

95. Fok, W. C; Walker, A. C. and Rhodes, J., Buckling of Locally Imperfect Stiffeners in Plates, *ASCE J Eng Mech Div*, Vol. 103, Issue 5, pp. 895-911, 1977.

96. Fok, W. C., Interactive Buckling of Stiffened Plate, *Engineering Journal of Singapore*, Vol. 7, Issue 1, pp. 3-8, 1980.

97. Fan, Q. S., Nonlinear Interaction Between Overall and Local Buckling of Stiffened Panels with Symmetric Cross-sections, *Technische Hogeschool Delft, Afdeling der Werktuigbouwkunde (Report) WTHD,* 1987.

98. Koiter, W. T. and Pignataro, M., General Theory for the Interaction Between Local and Overall Buckling of Stiffened Panels, *Tech Hogesch Delft Afd Werktuigbouwkd (Rep) WTHD,* 1976.

99. Koiter, W. T. and Pignataro, M., An Alternative Approach to the Interaction Between Local and Overall Buckling in Stiffened Panels, *Symposium on Buckling of Structures*, pp. 133-148, 1976.

100. Koiter, W. T. and van der Neut, A., Interaction Between Local and Overall Buckling of Stiffened Compression Panels, *Proceedings - Biennial Cornell Electrical Engineering Conference*, pp.61-85, 1980.

101. Kolakowski, Z., Mode Interaction in Wide Plate With Closed Section Longitudinal Stiffeners Under Compression, *Rozprawy Inzynierskie*, Volume 35, Issue 4, pp. 591-609, 1987.

102. Li, L. Y. and Bettess, P., Buckling of Stiffened Plates and Design of Stiffeners, *International Journal of Pressure Vessels and Piping*, Vol. 74, Issue 3, pp. 177-187, 1997.

103. Tvergaad, V., Imperfection-Sensitivity of a Wide Integrally Stiffened Panel Under Compression, *International Journal of Solids and Structures*, Volume 9, pp. 177-192, 1973.

104. Deng, C, G., Equations of Bifurcation Sets of Three-Parameter Catastrophes and the Application in Imperfection Sensitivity Analysis, *International Journal of Engineering Science,* Vol.32, Issue 11, pp. 1811-1822, 1994.

105. Chan, H. C. and Cai, C. W. and Cheung, Y. K., Static Solution of Stiffened Plates, *Thin-Walled Structures*, Volume 11, Issue 4, pp.291-303, 1991.

106. Chong, J. W., Stiffened Plates With Arbitrarily Oblique Stiffeners, *International Journal of Solids and Structures*, Volume 26, Issue 7, pp.779-799, 1990.

107. Dohrmann, R. J.; Wu, J. N. and Beckett, R. E., A Parametric Approach for the Stress Analysis of Orthogonally Stiffened Rectangular Plates, *Transactions of the ASME. Journal of Pressure Vessel Technology*, Vol. 105, Issue 4, pp. 363-368, 1983.

108. Ellinas, C. P. and Croll, J. G. A., Post-Critical Analysis of Torsionally Buckled Stiffener Plates, *International Journal of Solids and Structures*, Volume 17, Issue 1, pp. 11-27, 1981.

109. Elishakoff, I., Li, Y. W. and Starnes, J. H., Buckling Mode Localization in Elastic Plates due to Misplacement in the Stiffener Location, *Chaos, Solitions, & Fractals*, Volume 5, Issue 8, pp. 1517-1531, 1995.

110. Frieze, P. A. and Drymakis, E., An Examination of Shakeout in Stiffened Plate, *Behaviour of Thin-Walled Structures*, pp. 69-91, 1984.

111. Grayhack, W. T. and Mahar, T. J., Buckling of Rib-Stiffened Plates. An Asymptotic Approach, *SIAM Journal on Applied Mathematics*, Volume 50, Issue 4, pp.1126-1133, 1990.

112. Hoon, K. H. and Rhodes, J., Intermediately Stiffened Plates in Uniaxial Compression, *International Journal of Solids and Structures*, Volume 31, Issue 5, pp.711-734, 1994.

113. Ierusalimsky, K. M. and Fomin, V. P., Buckling of Compression-Loaded Multispan Stiffened Panel upon Failure of Joints Between Panel and Supports, *Thin-Walled Structures,* 2001.

114. Lillico, M.; Butler, R.; Hunt, G. W.; Watson, A.; Kennedy, D. and Williams, F. W, Optimum Design and Testing of A Post-Buckled Stiffened Panel, *Collection of Technical Papers - AIAA/ASME/ASCE/AHS/ASC Structures, Structural Dynamics and Materials Conference,* Vol. 1, Issue 3, pp. 1604-1613, 2000.

115. Machacek, J, Effect of Longitudinal Continuity in Steel Stiffened Compression Plating, *Acta Techinica CSAV*, Volume 34, Issue 1, pp. 99-117, 1989.

116. Mikami, I; Dogaki, M and Yonezawa, H., Inelastic Buckling of Continuous Stiffened Plates Under Compression, *Transactions of the Japan Society of Civil Engineers*, Volume 12, pp. 54-55, 1981.

117. Nakai, H.; Kitada, T. and Wada, Y., Experimental Study on Required Flexural Rigidity of Stiffener in Longitudinally Stiffened Plates Subjected to Lateral

Compression, *Memoirs of the Faculty of Engineering*, Osaka City University, Vol. 27, pp. 271-288, 1986.

118. Okada, H.; Kitaura, K. and Fukumoto, Y., Buckling Strength of Stiffened Plates Containing One Longitudinal or Transverse Girder Under Compression, *Bulletin of University of Osaka Prefecture*, Series A, Volume 20, Issue 2, pp. 287-306, 1971.

119. Rahal, K. N. and Harding, J. E., Transversely Stiffened Girder Webs Subjected to Shear Loading. Part 1. Behaviour, *Proceedings - Institution of Civil Engineers, Part 2: Research and Theory*, Volume 89, pp.47-65, 1990.

120. Rahman, M. K. and Chowdhury, M., Estimation of Ultimate Longitudinal Bending Moment of Ships and Box Girders, *Journal of Ship Research*, Volume 40, Issue 3, pp.244-257, 1996.

121. Roren, E. M. Q. and Hansen, H. R., Buckling Design in Ship Structures*, Nor Veritas Publ*, 1975.

122. Satsangi, S. K. and Mukhopadhyay, M., Review of Static Analysis of Stiffened Plates, *Journal of Structural Engineering (Madras),* Vol. 15, Issue 4, pp. 117-126, 1989.

123. Siddiqi, Z. A. and Kukreti, A. R., Analysis of Eccentrically Stiffened Plates with Mixed Boundary Conditions Using Differential Quadrature Method, *Applied Mathematical Modelling*, Volume 22, Issue 4-5, pp.251-275, 1998.

124. Sridharan, S. and Peng, M. H., Performance of Axially Compressed Stiffened Panels. *International Journal of Solids and Structures*, Volume 25, Issue 8, pp.879-899, 1989.

125. Steen, E., Elastic Buckling and Postbuckling of Eccentrically Stiffened Plates, *International Journal of Solids and Structures*, Vol.25, Issue 7, pp.751-768, 1989.

126. Taczala, M. and Jastrzebski, T., Analysis of Ultimate Capacity of Ship Hulls with Transversally Stiffened Plates, *Archives of Civil Engineering*, Volume 45, Issue 2, pp.357-368, 1998.

127. Williams, N. and Diffield, R. C., Parametric Stability of Rectangular Plates Reinforced With Closely Spaced Stiffeners, *Developments in Mechanics*, Volume 5, pp. 387-405, 1969.

128. Yoshinami, Y. and Ohmura, H., Overall Buckling Strength of Stiffened Plate With Initial Deflection, *Bulletin of the Faculty of Engineering, Hiroshima University*, Volume 36, Issue 1, pp. 61-67, 1987.

129. Yusuff, S., Buckling and Failure of Flat Stiffened Panels, *AIAA Bulletin*, volume 11, Issue 3, pp. 127, 1974.

130. Little, G. H., Stiffened Steel Compression Panels - Theoretical Failure Analysis, *The Structural Engineer*, Vol. 54, pp.489-500, 1976.

131. Yin, D. L and Qian, D. S., The Ultimate Capacity of Stiffened Plates Loaded in Plane, *Stability of Metal Structures*, pp. 516-520, 1989.

132. Katsikadelis, J. T. and Sapountzakis, E. J., A Realistic Estimation of the Effective Breadth of Ribbed Plates, *International Journal of Solids and Structures*, Vol. 39, Issue 4, pp. 897-910, 2002.

133. Toulios, M. and Caridis, P. A., The Effect of Aspect Ratio on the Elastoplastic Response of Stiffened Plates Loaded in Uniaxial Edge Compression, *Computer & Structures*, Vol. 80, Issues 14-15, pp. 1317-1328, 2002.

134. Dexter, R. J. and Pilarski, P. J., Crack Propagation in Welded Stiffened Panels, *Journal of Constructional Steel Research*, Vol. 58, Issue 5-8, pp. 1081–1102, 2002.

135. Pu, Y. C., Das, P. K. and Faulkner, D., Ultimate Compression Strength and Probabilistic Analysis of Stiffened Plates, *Proc. of the Int. Conf. on Offshore Mechanics and Arctic Engineering*, Volume 2, pp.151-157, 1996.

136. Wen, P. H.; Aliabadi, M. H. and Young, A., Stiffened Cracked Plates Analysis by Dual Boundary Element Method, *International Journal of Fracture*, Volume 106, Issue 3, pp.245-258, 2000.

137. Wen, P. H.; Aliabadi, M. H. and Young, A., Boundary element analysis of shear deformable stiffened plates, *Engineering Analysis With Boundary Elements*, Vol. 26, Issue 6. pp. 511-520, 2002.

138. Smith, C. S., Analysis of Grillage Structure by Force Method, *Transaction of RINA*, Volume 106, pp. 183-196, 1964.

139. Smith, C. S., Elastic Analysis of Stiffened Plating under Lateral Loading, *Transaction of RINA*, Volume 108, pp. 113-131, 1966.

140. Smith, C. S., Elastic Buckling and Beam-Column Behaviour of Ship Grillages, *Transaction of RINA*, Volume 110, pp. 127-147, 1968.

141. Smith, C. S., Compressive Strength of Welded Steel Ship Grillages, *Transaction of RINA*, pp. 325-359, 1975.

142. Smith, C. S., Anderson, N., Chapman, J. C., Davidson, P. C. and Dowling, P. J., Strength of Stiffened Plating under Combined Compression and Lateral Pressure. *Transactions of RINA,* pp. 131-147, 1991.

143. Parsanejad, S, Nonlinear Analysis of Orthogonally Stiffened Plates under Combined Loads, *Institution of Engineers, Australia, Civil Engineering Transactions*, pp. 207-215, 1986.

144. Bonello, M. A. and Chryssanthopoulos, M. K., Buckling Analysis of Plated Structures Using System Reliability Concepts, Safety and Reliability; *Proceedings*

of the International Conference on Offshore Mechanics and Arctic Engineering - OMAE, Volume 2, pp. 313-321, 1993.

145. Danielson, D. A.; Cricelli, A. S.; Frenzen, C. L. and Vasudevan, N., Buckling of Stiffened Plates under Axial Compression and Lateral Pressure, *International Journal of Solids and Structures*, Vol.30, Issue 4, pp.545-551, 1993.

146. Shanmugam, N. E. and Arockiasamy, M., Local Buckling of Stiffened Plates in Offshore Structures, *Journal of constructional steel*, Volume 38, Issue 1, pp. 41-59, 1996.

147. Bradford, M. A., Buckling of Longitudinally Stiffened Plates in Bending and Compression, *Canadian Journal of Civil Engineering*, Volume 16, Issue 5, pp. 607-614, 1989.

148. Caridis, P. A. and Frieze, P. A., Flexural-Torsional Elasto-plastic Buckling Analysis of Stiffened Plates Using Dynamic Relaxation. Part 1: Theory, *Thin-Walled Structures,* Volume 6, Issue 6, pp.453-481, 1988.

149. Caridis, P. A. and Frieze, P. A., Flexural-Torsional Elasto-plastic Buckling Analysis of Stiffened Plates Using Dynamic Relaxation. Part 2: Comparison with Test Results and Other Formulations, *Thin-Walled Structures,* Volume 7, Issue 1, pp. 37-72, 1989.

150. Wang, X. Z.; Moan, T. and Jiao, G. Y, Reliability Analysis of Production Ships, *International Journal of Offshore and Polar Engineering*, Volume 4, pp.302-311, 1994.

151. Wang, X. Z.; Jiao, G. Y. and Moan, T., Analysis of Oil Production Ships Considering Load Combination, Ultimate Strength and Structural Reliability, *Transactions - Society of Naval Architects and Marine Engineers*, Volume 104, pp.3-30, 1996.

152. Wang, X. Z. and Moan, T., Ultimate Strength Analysis of Stiffened Panels in Ships Subjected to Biaxial and Lateral Loading, *International Journal of Offshore and Polar Engineering*, Volume 7, Issue 1, pp.22-29, 1997.

153. Hu, Y. R., Chen, B. Z and Sun, J. L., Tripping of Thin-Walled Stiffeners in the Axially Compressed Stiffened Panel with Lateral Pressure, *Thin-Walled Structures*, Volume 37, Issue 1, pp.1-26, 2000.

154. Hughes, O. F., and Ma, M., Elastic Tripping Analysis of Asymmetrical Stiffeners, *Computers & Structures*, Vol. 60, Issue 3, pp.369-389, 1996.

155. Mansour, A. E., Effective Flange Breadth of Stiffened Plats Under Axial Tensile Load or Uniform Bending Moment, *Journal of ship research*, Vol. 14, pp. 8-14, 1970.

156. Mansour, A. E., On the Nonlinear Theory of Orthotropic Plates, *Journal of ship research*, Volume 15, pp. 266-277, 1971.

157. Mansour, A. E., Post- Buckling Behavior of Stiffened Plates With Small Initial Curvature Under Combined Loads, *Int Shipbldg Progr*, Volume 18, Issue 202, pp. 217-240, 1971.

158. Mansour, A. E.; de Oliveira, J. G.; Kinra, R. K., Design of Flat Plate Structures for Offshore Applications, *Proceedings of the International Offshore Mechanics and Arctic Engineering Symposium*, Volume 2, pp. 413-421, 1987.

159. Mansour, A. E., Behavior of Plates under Combined Loads, *Proc Second Int Offshore Polar Eng Conf*, pp. 468-474, 1992.

160. White, G. J.; Ayyub, B. M.; Mansour, A. E. and Wirsching, P. H., Probability-Based Design Requirements for Longitudinally Stiffened Panels in Ship Structures, *Probabilistic Mechanics and Structural and Geotechnical Reliability, Proceedings of the Specialty Conference*, pp. 110-113, 1996.

161. Cui, W. C.; Wang, Y. J. and Pedersen, P. T., Strength of Ship Stiffened Panels under Combined Loading, *Chuan Bo Li Xue / Journal of Ship Mechanics*, Volume 4, Issue 3, pp.59-86, 2000.

162. Cui, W. C., Buckling and Ultimate Strength Analysis of Stiffened Panels, *Chuan Bo Li Xue / Journal of Ship Mechanics*, Volume 2, Issue 3, pp.41-61, 1998.

163. Hart, D. K.; Rutherford, S. E. and Wickham, A. H. S., Structural Reliability Analysis of Stiffened Panels, *Naval Architect*, pp.293-310, 1986.

164. Ma, K. T. and Orisamolu, I. R., Reliability of Stiffened-Plated Panels in Offshore Structures, *Proc. of the Int. Offshore and Polar Engineering Conference*, Volume 4, pp. 423-430, 1996.

165. Moghtaderi-Zadeh, M. and Madsen, H. O., Probabilistic Analysis of Buckling and Collapse of Plates in Marine Structures, *Proceedings of the International Offshore Mechanics and Arctic Engineering Symposium*, Volume 2, pp. 449-454, 1987.

166. Mori, N.; Hara, Y.; Shimizu, N. and Kozono, T., On the Strength of Stiffener Ends Under Static Water Pressure, *Hitachi Zosen Tech Rev*, Volume 39, Issue 4, pp. 26-35, 1978.

167. Nikolaidis, E.; Hughes, O.; Ayyub, B. M. and White, G. J, Reliability Analysis of Stiffened Panels, *Structures Congress XII*, pp. 1466-1471, 1994.

168. Paliwal, D. N. and Ghosh, S. K., Stability of Orthotropic Plates on a Kerr Foundation, *AIAA Journal*, Volume 38, Issue 10, pp.1994-1997, 2000.

169. Tanaka, Masa and Bercin, A. N., Static Bending Analysis of Stiffened Plates Using the Boundary Element Method, *Engineering Analysis with Boundary Elements*, Volume 21, Issue 2, pp.147-154, 1998.

170. Tanaka, M., Matsumoto, T. and Oida, S., A Boundary Element Method Applied to the Elastostatic Bending Problem of Beam-Stiffened Plates, *Engineering Analysis with Boundary Elements*, Volume 24, Issue 10, pp.751-758, 2000.

171. Yehezkely, O. and Rehfield, L. W., A New, Comprehensive Theory for Bending and Buckling of Stiffened Plates, *Israel Journal of Technology*, Volume 20, Issue 6, pp. 233-244, 1982.

172. Zheng, Y. and Das, P. K., Improved Response Surface Method and Its Application to Stiffened Plate Reliability Analysis, *Engineering Structures*, Volume 22, Issue 5, pp. 544-551, 2000.

173. Zhou, X. H. and Wang, S. J., Buckling Strength of Edge-Stiffened Plates under Combined Compression and Bending, *Stability of Metal Structures*, pp. 580-586, 1989.

174. Tan, Y. H., Stiffened Plates Subjected to In-plane and Lateral Loads, Mater of Engineering Thesis, National University of Singapore, 2000.

175. Schade, H. A., Design Curves for Cross-Stiffened Plating Under Uniform Bending Load, *Transactions of Society of Naval Architects and Marine Engineers*, Vol. 49, pp. 154-182, 1941.

176. Schade, H. A., The Effective Breadth of Stiffened Plating Under Bending Loads, *Transactions of Society of Naval Architects and Marine Engineers*, Vol. 59, pp. 403-420, 1951.

177. Schade, H. A., The Effective Breadth Concept in Ship Structural Design, *Transactions of Society of Naval Architects and Marine Engineers*, Vol. 61, pp. 410-430, 1953.

178. Klitchief, J. M. and Yugoslavia, B., On the Stability of Plates Reinforced by Ribs, *Journal of Applied Mechanics*, Volume 16, pp.74-76, 1949.

179. Dwight, J. B. and Moxham, K. E., Welded Steel Plates in Compression, *The Structural Engineer*, Vol. 47, pp. 49-66, 1969.

180. Dwight, J. B. and Little, G. H., Stiffened Steel Compression Flange- A Simpler Approach, *The Structural Engineer*, Vol.54, pp. 501-509, 1976.

181. Murray, N. W., Buckling of Stiffened Panels Loaded Axially and in Bending, *Struct Eng*, Volume 51, Issue 8, pp. 285-301, 1973.

182. Murray, N. W., Analysis and Design of Stiffened Plates for Collapse Load, *The Structural Engineer*, Volume 53, No. 15, p. 153, 1975.

183. Carlsen, C. A., Simplified Collapse Analysis of Stiffened Plates, Norwegian Maritime Research, Vol. 5, No. 4, pp. 20-36, 1977.

184. Carlsen, C. A., Collapse Analysis of Stiffeners Subjected to Compression and Hydrostatic Lateral Load, Det norske Veritas Report No. 78-549, 1978.

185. Carlsen, C. A., Parametric Study of Collapse of Stiffened Plates in Compression, *Struct Eng Part B*, Vol. 58B, Issue 2, pp.33-40, 1980.

186. Allen, D., Discussion of "An approximate method for the design of stiffened steel compression panels" by M. R. Horne and R. Narayanan. *Proc. Inst. Civil Engineers*, 61(2), pp. 453-455, 1976.

187. Faulkner, V; Adamchak, J. C.; Snyder, G. J. and Vetter, M. F., Synthesis of Welded Grillages to Withstand Compression and Normal Loads, *Computers & Structures*, Vol. 3, pp.221-246, 1973.

188. Faulkner, D., A Review of Effective Plating for Use in Analysis of Stiffened Plating in Bending and Compression, Journal of Ship Research, Vol. 19, No. 1, pp. 1-17, 1975.

189. Horne, M. R. and Narayanan, R., Influence of the Type of Welding and the Method of Splicing on the Strength of Stiffened Plates, *Weld Res Int*, Volume 6, Issue 2, pp.31-50, 1976.

190. Horne, M. R. and Narayanan, R., The Strength of Straightened Welded Steel Stiffened Plates, *The Structural Engineer*, Volume 54, Issue 11, pp.437-443, 1976.

191. Horne, M. R.; Montague, P. and Narayanan, R., Influence on Strength of Compression Panels of Stiffener Section, Spacing and Welded Connection, *Proc Inst Civ Eng (Lond)*, Volume 63, Part 2, pp.1-20, 1977.

192. Horne, M. R. and Narayanan, R., Design of Axially Loaded Stiffened Plates, *ASCE Journal of Structural Division*, Volume 103, Issue 11, pp. 2243-2257, 1977.

193. Horne, M. R. and Narayanan, R., Ultimate Capacity of Longitudinally Stiffened Plates Used in Box Girders, *Proc Inst Civ Eng (Lond)*, Volume 61, Part 2, pp.253-280, 1977.

194. Narayanan, R. and Shanmugam, N. E., An Approximate Analysis of Stiffened Flanges, *IABSE Proceedings*, pp. 1- 12, 1979.

195. Shanmugam, N. E.; Paramasivam, P. and Lee, S. L., Strength of Stiffened Steel Panels, *International Journal of Structures*, Volume 6, Issue 4, pp. 169-183, 1986.

196. Soares, C. G. and Gordo, J. M., Behaviour and Design of Stiffened Plates under Predominantly Compressive Loads, *International Shipbuilding Progress*, Volume 30, Issue 341, pp. 13-27, 1983.

197. Soares, C. G. and Gordo, J. M., Design Methods for Stiffened Plates Under Predominantly Uniaxial Compression, *Marine Structures*, Volume 10, Issue 6, pp.465-497, 1997.

198. Jetteur, P., A New Design Method for Stiffened Compression Flanges of Box Girders, *Thin-Walled Structures*, Vol. 1, pp. 189-210, 1983.

199. Taido, Y.; Hayashi, H.; Kitada, T. and Nakai, H., Design Method of Wide Stiffened Plates Subjected to Uniaxial and Biaxial Compression, *Stahlbau*, Volume 54, Issue 5, pp.149-155, 1985.

200. Boote, D. and Mascia, D., On the Effective Breadth of Stiffened Platings, *Ocean Engineering (Pergamon)*, Volume 18, Issue 6, pp. 567-592, 1991.

201. Bonello, M. A.; Chrysaanthopoulos, M. K. and Dowling, P. J., Ultimate Strength Design of Stiffened Plates under Axial Compression and Bending, *Marine Structures*, Volume 6, Issue 5-6, pp. 533-552, 1995.

202. Caridis, P. A., The Behaviour of Plat Plates Forming Part of Orthogonally Stiffened Grillages Loaded under Lateral Pressure. *Design of Marine and Offshore Structures*, pp. 535-555, 1992.

203. Mikami, I. and Niwa, K., Ultimate Compressive Strength of Orthogonally Stiffened Steel Plates, *Journal of Structural Engineering*, Volume 122, Issue 6, pp. 674-682, 1996.

204. Usami, T., Simplified Analysis of the Strength of Stiffened Box Members in Compression and Bending, *Journal of Constructional Steel Research*, Vol. 17, Issue 3, pp. 237-247, 1990.

205. Johansson, B.; Maquoi, R. and Sedlacek, G., New Design Rules for Plated Structures in Eurocode 3. *Journal of Constructional Steel Research*, Vol. 57, pp. 279-311, 2001.

206. Gordo, J. M.; Soares, G. C. and Faulkner, D., Approximate Assessment of the Ultimate Longitudinal Strength of the Hull Girder, *Journal of Ship Research*, Volume 40, Issue 1, pp.60-69, 1996.

207. Anderson, M. S., Inclusion of Local Post Buckling Response in the Design of Stiffened Panel, *Collection of Technical Papers - AIAA/ASME/ASCE/AHS/ASC Structures, Structural Dynamics and Materials Conference,* Volume 1, Issue 3, pp. 1646-1653, 2000.

208. Kitada, T.; Yamaguchi, T.; Matsumura, M.; Okada, J. O., K. and Ochi, N., New Technologies of Steel Bridges in Japan, *Journal of Constructional Steel Research*, Volume 58, Issue 1, pp. 21-70, 2002.

209. Paik, J. K.; Thayamballi, A. K. and Jung, S. C., Ultimate Strength of Ship Hulls Under Combined Vertical Bending, Horizontal Bending, and Shearing Forces, *SNAME Transactions*, Vol. 104, pp31-59, 1996.

210. Paik, J. K. and Thayamballi, A. K., Empirical Formulation for Predicting the Ultimate Compressive Strength of Stiffened Panels, *Proceedings of the International Offshore and Polar Engineering Conference*, Volume 4, pp. 328-338, 1997.

211. Paik, J. K.; Thayamballi, A. K. and Kim, D. H., An Analytical Method for the Ultimate Compressive Strength and Effective Plating of Stiffened Panels, *Journal of Constructional Steel Research*, Volume 49, Issue 1, pp. 45-68, 1999.

212. Paik, J. K.; Thayamballi, A. K. and Kim, B. J., Large Deflection Orthotropic Plate Approach to Develop Ultimate Strength Formulations for Stiffened Panels under Combined Biaxial Compression/Tension and Lateral Pressure, *Thin-Walled Structures*, Volume 39, Issue 3, pp.215-246, 2001.

213. Paik, J. K. and Kim, B. J., Ultimate Strength Formulations for Stiffened Panels under Combined Axial Load, In-plane Bending and Lateral Pressure: A Benchmark Study, *Thin-Walled Structures*, Volume 40, Issue 1, pp. 45-83, 2002.

214. Chou, S. K. G; Chapman, J. C and Davidson, P. C., Design of Bulb Stiffened Flat-Stiffened Plating, *Structural Engineer*, Volume 78, Issue 18, pp.24-36, 2000.

215. Bijlaard, F. S. K., The Design of Transverse and Longitudinal Stiffeners for Stiffened Plate Panels, *Heron*, Volume 27, Issue 4, 1982.

216. Leheta, H. W. and Mansour, A. E., Reliability-Based Method for Optimal Structural Design of Stiffened Panels, *Marine Structures*, Vol. 10, Issue 5, pp. 323-352, 1997.

217. Mansour, A. E.; Wirsching, P. H.; Lucket, M. D.; Plumpton, A. M. and Lin, Y. H., Structural Safety of Ships, *Transactions - Society of Naval Architects and Marine Engineer*, Volume 105, pp. 61-98, 1998.

218. Tvergaad, V., Influence of Post-Buckling Behaviour on Optimum Design of Stiffened Panels, *International Journal of Solids and Structures*, Volume 9, pp. 1519-1534, 1973.

219. Brosowshi, B. and Ghavami, K., Multi-criteria Optimal Design of Stiffened Plates Part 1. Choice of the Formula for Buckling load, *Thin-Walled Structures*, Volume 24, Issue 4, pp.353-369, 1996.

220. Brosowshi, B. and Ghavami, K., Multi-criteria Optimal Design of Stiffened Plates Part II. Mathematical Modelling of the Optimal Design of Longitudinally Stiffened Plates, *Thin-Walled Structures*, Volume 28, Issue 2, pp.179-198, 1997.

221. Hatzidakis, N. and Bernitsas, M. M., Comparative Design of Orthogonally Stiffened Plates for Production and Structural Integrity - Part 2: Shape Optimization, *Journal of Ship Production*, Vol. 10, Issue 3, pp.156-163, 1994.

222. De Oliveira, J. G. and Christopoulos, D. A., A Practical Method for the Minimum Weight Design of Stiffened Plates Under Uniform Lateral Pressure, *Computers and Structures*, Volume 14, Issue 5-6, pp. 409-421, 1981.

223. McGrattan, R. J., Weight and Cost Optimization of Hydrostatically Loaded Stiffened Flat Plates, *Journal of Pressure Vessel Technology*, Volume 107, Issue 1, pp. 68-76, 1985.

224. Rothwell, A., On the Efficiency of Stiffened Panels with Application to Shear Web Design, *Asp of the Anal of Plate Struct*, A, pp.105-125, 1985.

225. Williams, F. W., Stiffened Panels with Varying Stiffener Sizes, *Aeron J*, Volume 77, Issue 751, pp. 350-354, 1973.

226. Peng, M. H. and Sridharan, S., Optimized Design of Stiffened Panels Subject to Interactive Buckling, *Collection of Technical Papers - AIAA/ASME/ASCE/AHS Structures, Structural Dynamics & Materials Conference*, pp.1279-1288, 1990.

227. Farkas, J. and Jarmai, K. J., Optimum Design of Welded Stiffened Plates Loaded by Hydrostatic Normal Pressure, *Structural and Multidisciplinary Optimization*, Volume 20, Issue 4, pp. 311-316, 2000.

228. Toakley, A. R. and Williams, D. G., Optimum Design of Stiffened Panels Subjected to Compression Loading, *Eng Optimization*, Volume 2, Issue 4, pp.239-250, 1977.

229. Ellinas, C. P.; Croll, J. G. A.; Kaoulla, P. and Kattura, P., Tests on Interactive Buckling of Stiffened Plates. *Experimental Mechanics,* Volume 17, Issue 12, PP. 455-462, 1977.

230. Zha, Y. F.; Moan, T. and Hanken, E., Experimental and Numerical Study of Torsional Buckling of Stiffeners in Aluminium Panels, *Proc. of the Int. offshore and Polar Engineering Conference*, Volume 4, pp. 249-255, 2000.

231. Zha, Y. F and Moan, T., Ultimate Strength of Stiffened Aluminium Panels with Predominantly Torsional Failure Mode. *Thin-Walled Structures*, Volume 39, pp. 631-648, 2001.

232. Lavan Kumar, C., Stiffened Plates Subjected to Combined Action of Axial Load and Lateral Pressure. Mater of Science (by research) Thesis, Indian Institute of Technology, Madras, 2001.

233. De George, D.; Michelutti, W. M. and Murray, N. W., Studies of Some Steel Plates Stiffened with Bulb-Flats or with Troughs, *Proceedings - Biennial Cornell Electrical Engineering Conference,* pp.86-99, 1980.

234. Pan, Y. G. and Louca, L. A., Experimental and Numerical Studies on the Response of Stiffened Plates Subjected to Gas Explosions, *Journal of constructional steel*, Volume 52, Issue 2, pp.171-193, 1999.

235. Yamada, Y.; Watanabe, E. and Ito, R., Compressive Strength of Plates With Closed-Sectional Ribs, *Transactions of the Japan Society of Civil Engineers*, Volume 10, pp. 81-83, 1979.

236. Winter, G. Commentary on the 1968 edition of light gauge cold-formed steel design manual. American Iron and Steel Institute, Washington, 1970.

APPENDIX A – DESCRIPTION OF DATABASE

In the past few decades, extensive research works have been carried out either experimentally or analytically on the behaviour of stiffened plate. Efforts of reviewing past works have been made by many researchers over the years. However, most reviews only cover the relevant publications to the topic which researchers concern. Thus there is a need to collect all the papers related to stiffened plate for easy access of data in the future. In the present research, an effort was made to collect past papers related to stiffened plate and summarize in a database. Papers related to vibration of stiffened plate and composite stiffened panel are not included in the database. The papers collected for this database are up to year 2002. Due to limitation of available sources, this database contains 230 papers. List of available papers in database has been incorporated in references.

Internet Explorer was chosen as interface to present the database of stiffened plate. With Internet Explorer as interface, this database can easily upload to Internet and facilitate other researchers to search for relevant information. Also this database can be run in local computer without internet connection if whole database is downloaded. Microsoft FrontPage was used to write HTML code and search engine. Users can always add papers to the database with some knowledge of Microsoft FrontPage. The source code of search engine is contained in file evf.html.

The main page of database is shown in Figure 1. A search function is available for this database. User can search relevant papers by author's name or keyword of title. For example, search author "Shanmugam" will lead to a page which lists all the papers from Prof. Shanmugam. The search result is illustrated in Figure 2. A link to

the list of all papers collected is also available in the main page. All the papers available in the database are arranged according to the year in the list. User can click the title of paper to find the information about the paper. Summaries of proposed design formula by researchers are also linked to main page. The available formulas are summarized into two categories. One is formulas for unaxially loaded stiffened plate. The other one is formulas for axially and laterally loaded stiffened plate.

For those papers with experimental results or proposed design formula, summary of available experimental data and formulas are included in the database. Typical examples are shown in Figure 3. For those analytical papers, only abstract of the paper is given in the database. User can obtain the details of paper from the source of paper which is shown on top of abstract.

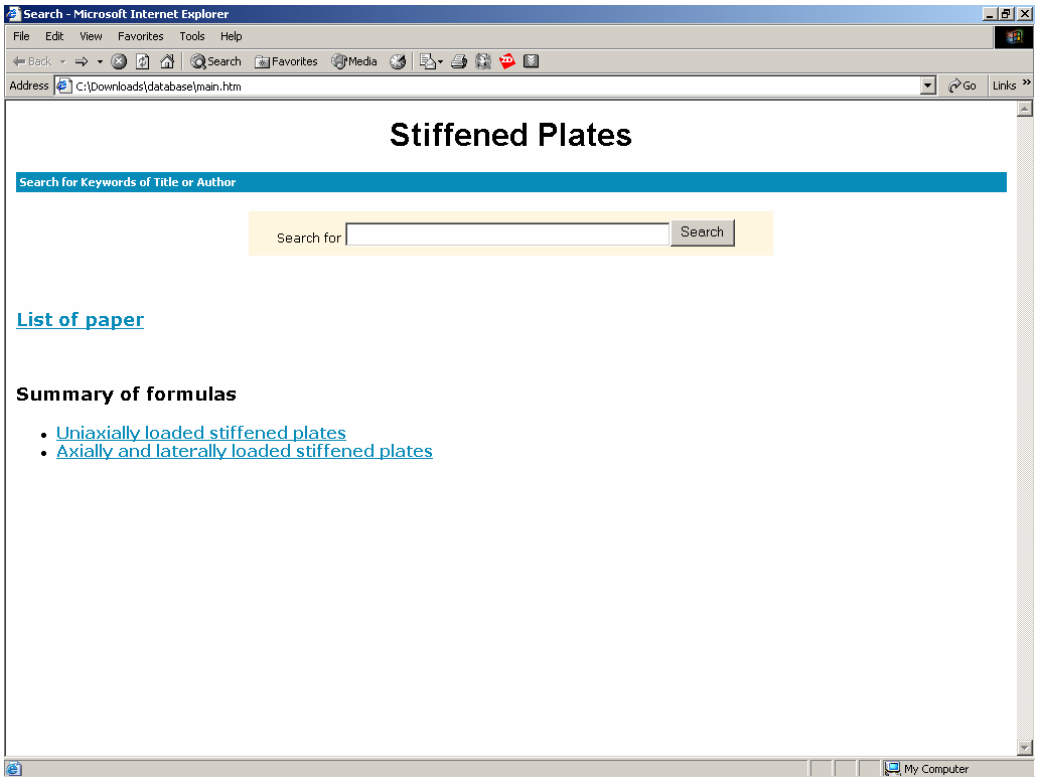

Figure 1. Main Page of Database

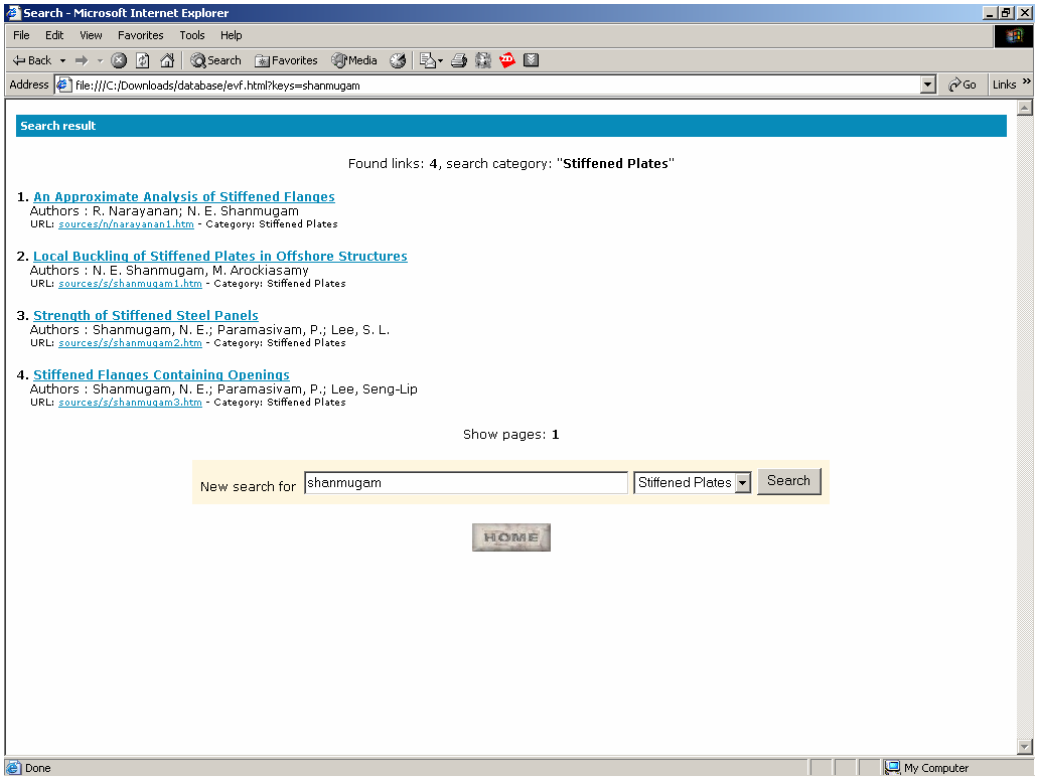

Figure 2. Example of Searching Author's Name in Database

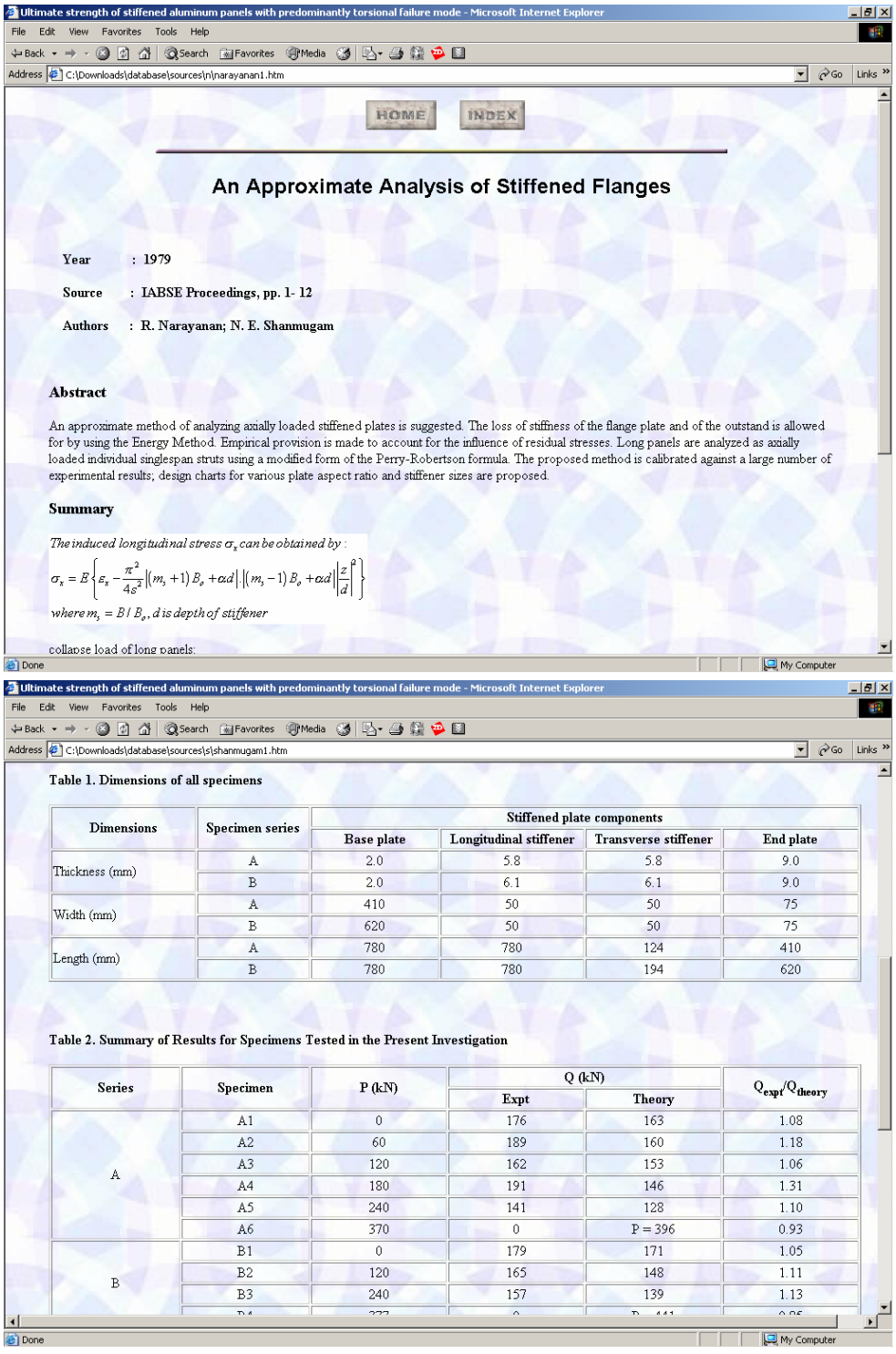

Table 1. Dimensions of all specimens

Dimensions	Specimen series	Stiffened plate components			
		Base plate	Longitudinal stiffener	Transverse stiffener	End plate
Thickness (mm)	A	2.0	5.8	5.8	9.0
	B	2.0	6.1	6.1	9.0
Width (mm)	A	410	50	50	75
	B	620	50	50	75
Length (mm)	A	780	780	124	410
	B	780	780	194	620

Table 2. Summary of Results for Specimens Tested in the Present Investigation

Series	Specimen	P (kN)	Q (kN)		Q_{expt}/Q_{theory}
			Expt	Theory	
A	A1	0	176	163	1.08
	A2	60	189	160	1.18
	A3	120	162	153	1.06
	A4	180	191	146	1.31
	A5	240	141	128	1.10
	A6	370	0	P = 396	0.93
B	B1	0	179	171	1.05
	B2	120	165	148	1.11
	B3	240	157	139	1.13

Figure 3. Typical Summary of Paper in Database

APPENDIX B – MATERIAL STRESS-STRAIN CURVES

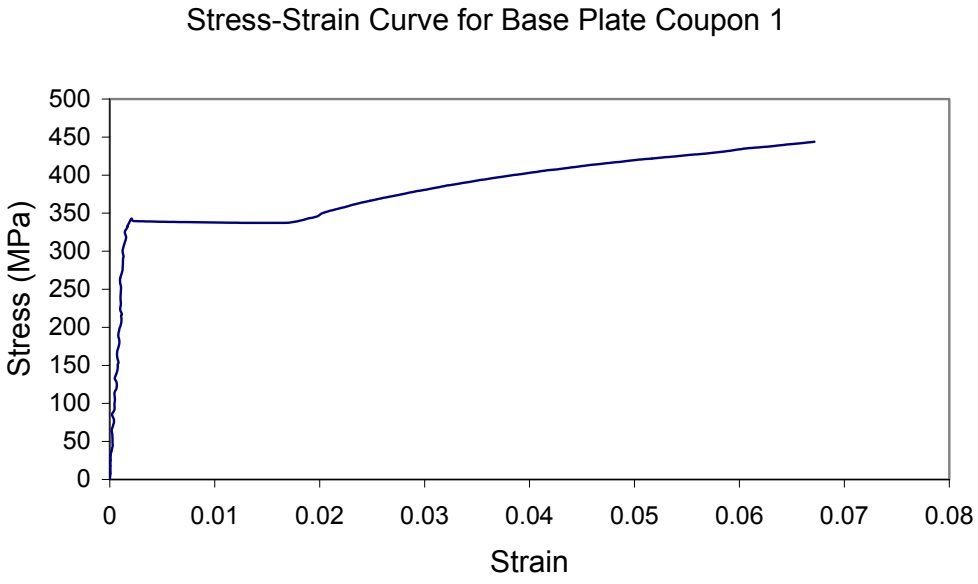

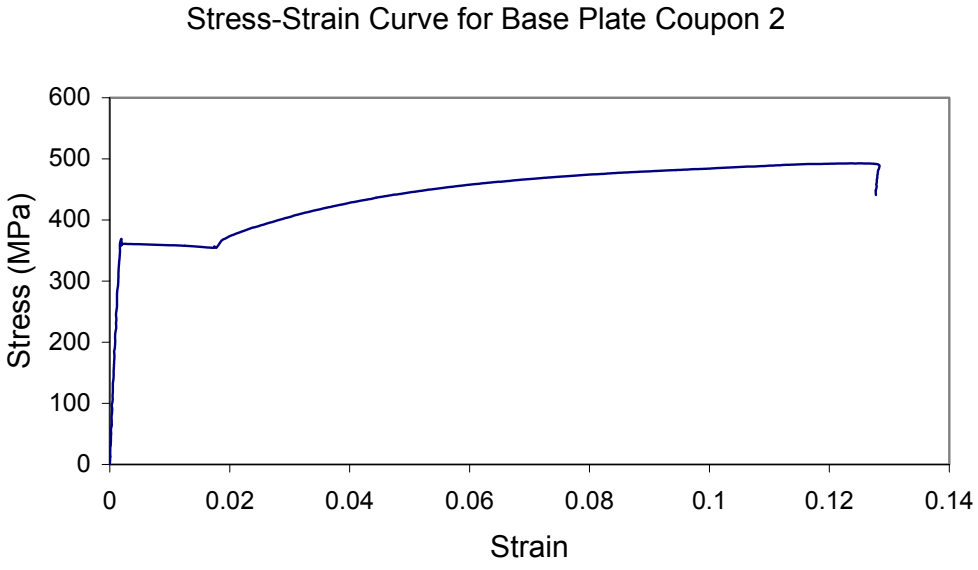

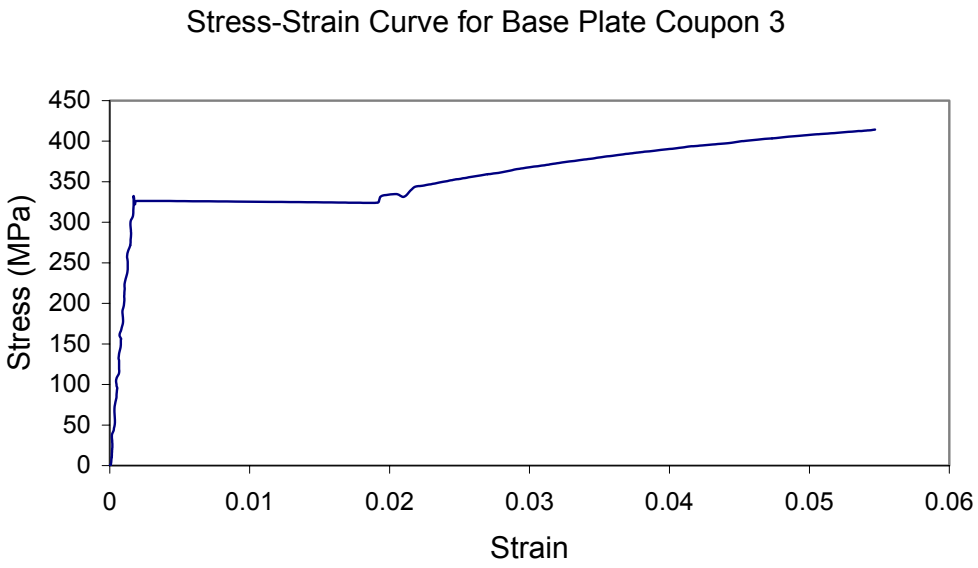
Stress-Strain Curve for Base Plate Coupon 3
Stress (MPa)
450
400
350
300
250
200
150
100
50
0
0
0.01
0.02
0.03
0.04
0.05
0.06
Strain

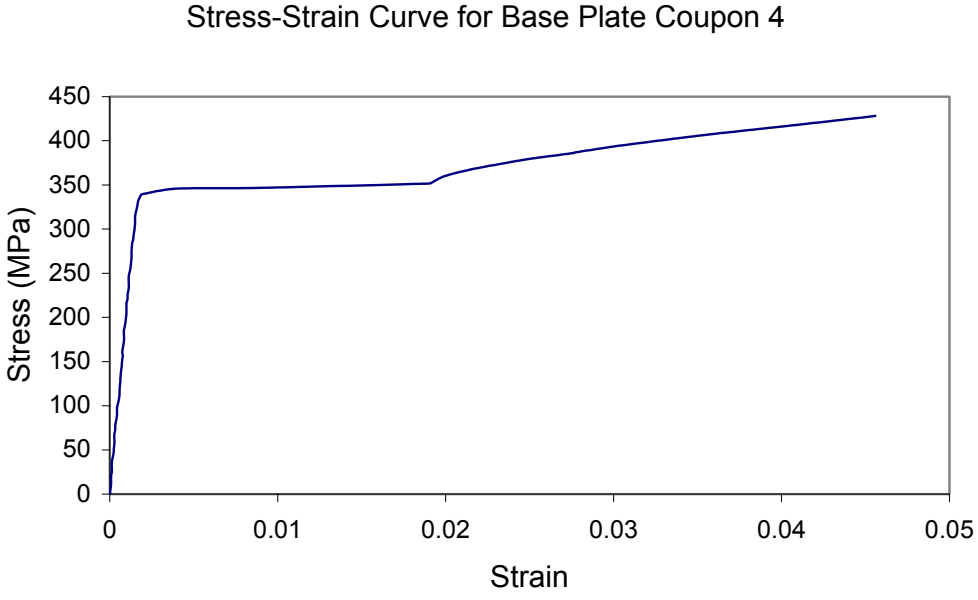
Stress-Strain Curve for Base Plate Coupon 4
Stress (MPa)
450
400
350
300
250
200
150
100
50
0
0
0.01
0.02
0.03
0.04
0.05
Strain

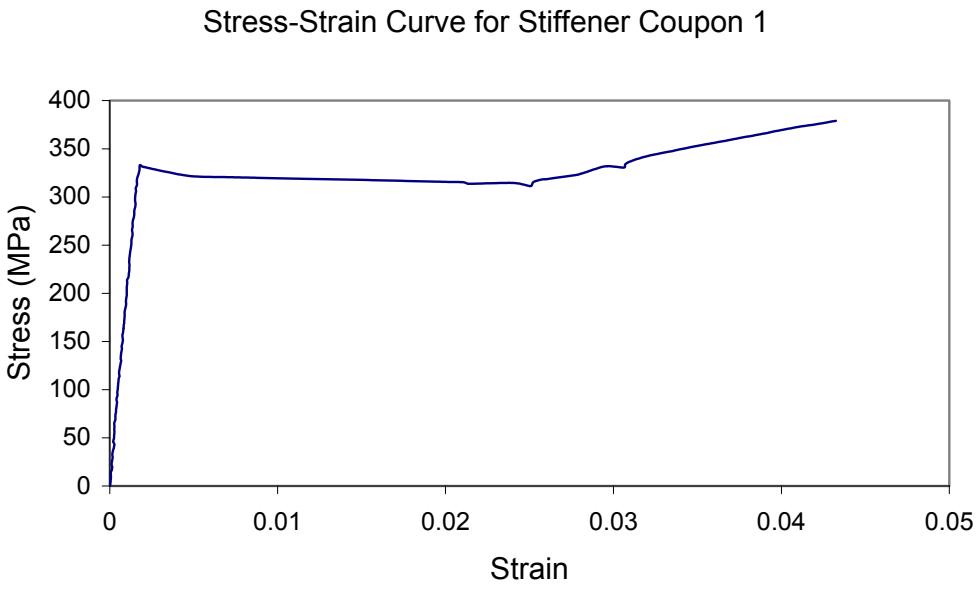
Stress-Strain Curve for Stiffener Coupon 1
Stress (MPa)
400
350
300
250
200
150
100
50
0
0
0.01
0.02
0.03
0.04
0.05
Strain

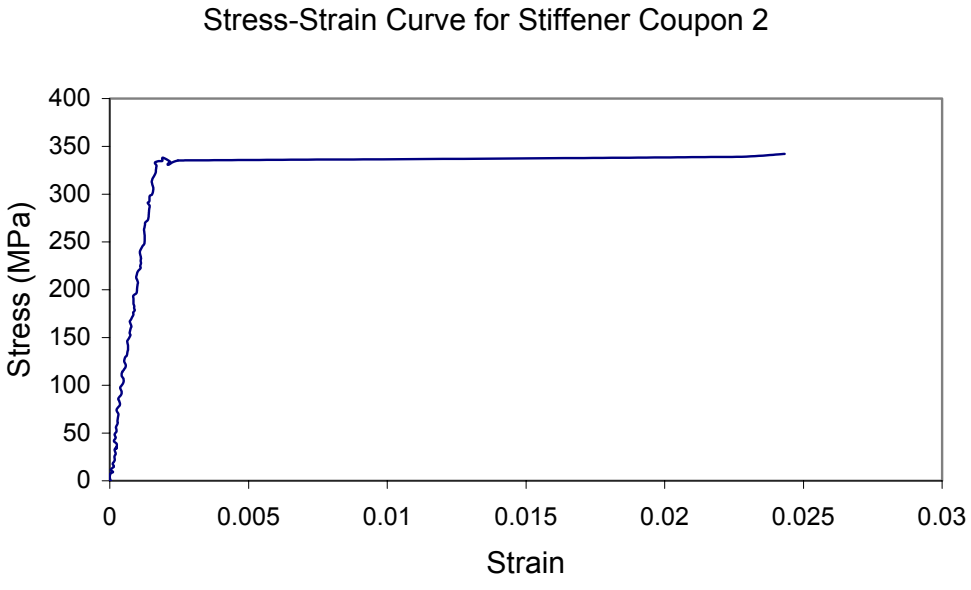
Stress-Strain Curve for Stiffener Coupon 2
Stress (MPa)
400
350
300
250
200
150
100
50
0
0
0.005
0.01
0.015
0.02
0.025
0.03
Strain

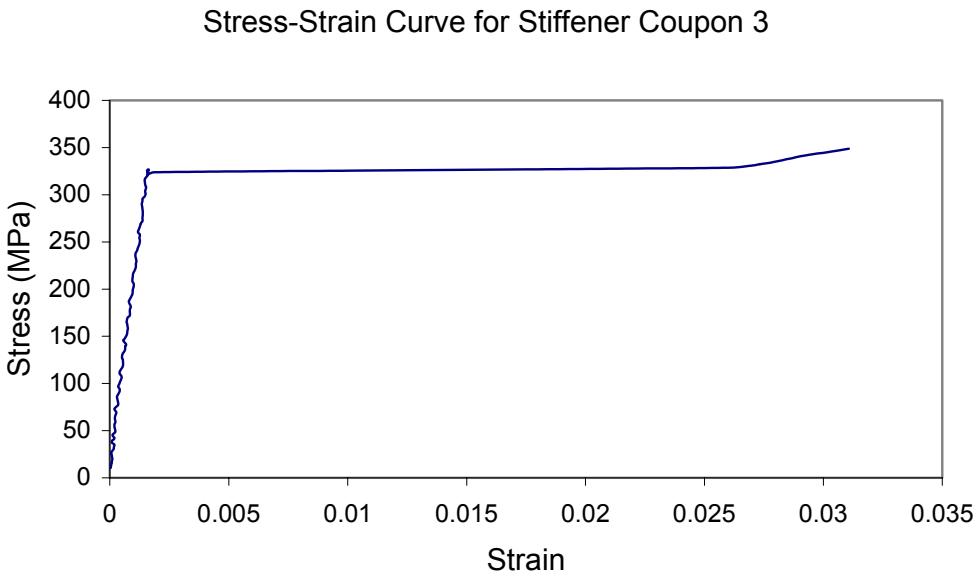
Stress-Strain Curve for Stiffener Coupon 3
Stress (MPa)
400
350
300
250
200
150
100
50
0
0
0.005
0.01
0.015
0.02
0.025
0.03
0.035
Strain

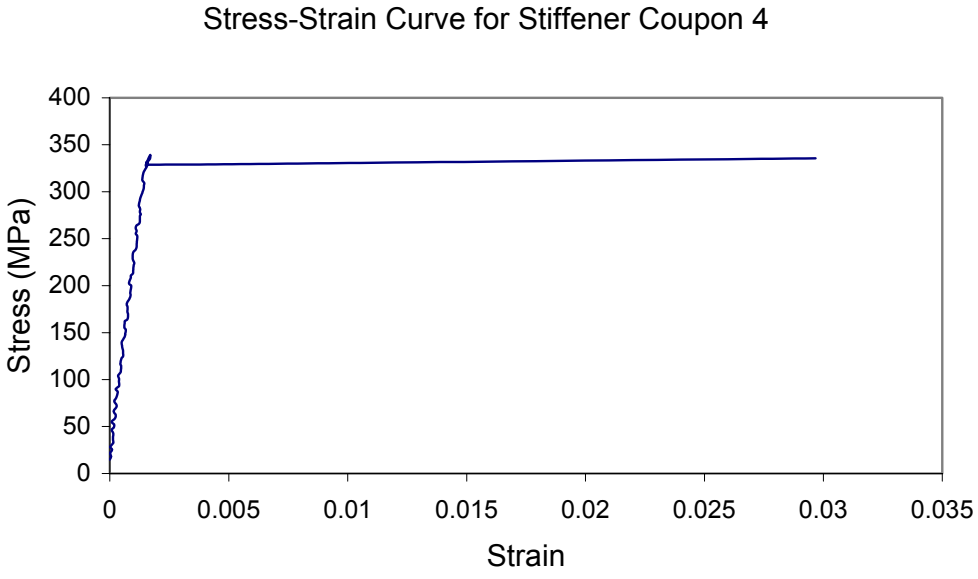
Stress-Strain Curve for Stiffener Coupon 4
Stress (MPa)
400
350
300
250
200
150
100
50
0
0
0.005
0.01
0.015
0.02
0.025
0.03
0.035
Strain

APPENDIX C – TYPICAL ABAQUS INPUT FILE

```
*HEADING
**
**Description of model
**
*Node
      1,        -450.,        -440.,           0.
      2,           0.,        -440.,           0.
```

Node number, X-coord., Y-coord., Z-coord.

```
      .           .           .           .
      .           .           .           .
     9548,           0.,      -233.75,        25.
     9549,           0.,      -233.75,        12.5
*Element, type=S8R5, elset=plate
 1,  123,  124, 1273, 1272, 3192, 3193, 3194, 3195
 2,  124,    1,  125, 1273, 3196, 3197, 3198, 3193
```

Element number, 8 nodes that make the elment

```
 .    .     .     .     .     .     .     .     .
 .    .     .     .     .     .     .     .     .
3045, 1242, 3108, 3111, 1241, 9311, 9318, 9319, 9320
3046, 3108, 3109, 3112, 3111, 9314, 9321, 9322, 9318
**
*Nset, nset=center
      38
*Nset, nset=support
   . . . . .
*Elset, elset=support
     .
     .
**
*Shell Section, elset=plate, material=steel
      2.9,    5
**
** MATERIALS
*Material, name=steel
*Elastic
181000., 0.3
*Plastic
347.,0.
**
*IMPERFECTION,FILE=buckle,STEP=1
eigen mode, scale factor
**
** BOUNDARY CONDITIONS
**
*Boundary
sides, 3, 3
sides, 5, 5
**
*Boundary
support, 1, 1
   .
   .
**----------------------------------------
* ** STEP: Step-1
**
*Step, name=Step-1, nlgeom, inc=200
*Static
```

Node and element setting

Thickness of the section, section point

Material Properties

Retrieve imperfection data

Boundary conditions

Static Analysis under axial load

```
1., 1., 1e-05, 1.
**
*DLOAD, OP=NEW
AXIAL, P,        9.05
**
** OUTPUT REQUESTS
*Restart, write, frequency=1
** FIELD OUTPUT: F-Output-1
**
*Output, field, frequency=2
*Node Output
U,
*Element Output
S,
**
*Output, history
*Node Output, nset=center
U3,
*Node Output, nset=sides
RF3,
*Node Output, nset=ends
RF3,
*El Print, freq=999999
*Node Print, freq=999999
*End Step
** ----------------------------------------
** STEP: Step-2
**
*Step, name=Step-4, nlgeom, inc=200
*Static, riks
1., 1., 1e-05, 1., ,center, 3, 90.
*DLOAD, OP=NEW
AXIAL, P,        9.05
**
*DLOAD, OP=NEW
LATERAL, P,        -0.2
**
** OUTPUT REQUESTS
*Restart, write, frequency=1
**
** FIELD OUTPUT: F-Output-1
**
*Output, field, frequency=2
*Node Output
U,
*Element Output
S,
**
*Output, history
*Node Output, nset=center
U3,
*Node Output, nset=sides
RF3,
*Node Output, nset=ends
RF3,
*El Print, freq=999999
*Node Print, freq=999999
*End Step
```

Specify output required

Non-linear analysis under lateral pressure

Specify output required

APPENDIX D - MEASURED INITIAL IMPERFECTION

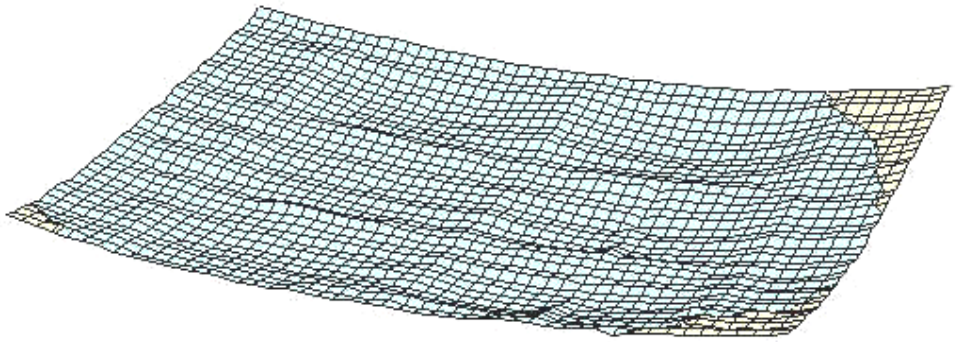

Imperfection of Specimen A1

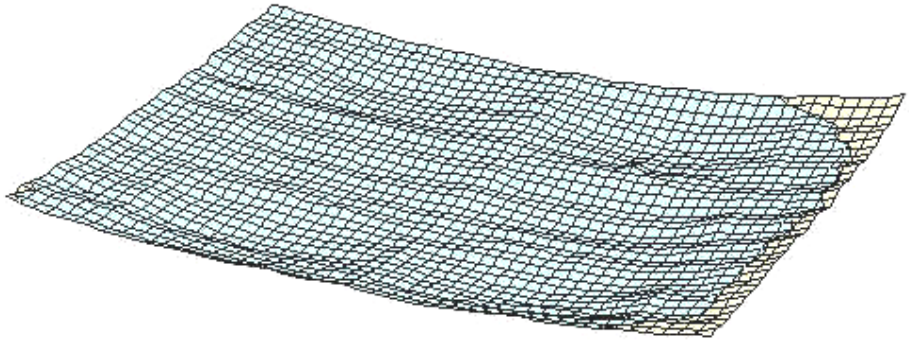

Imperfection of Specimen A2

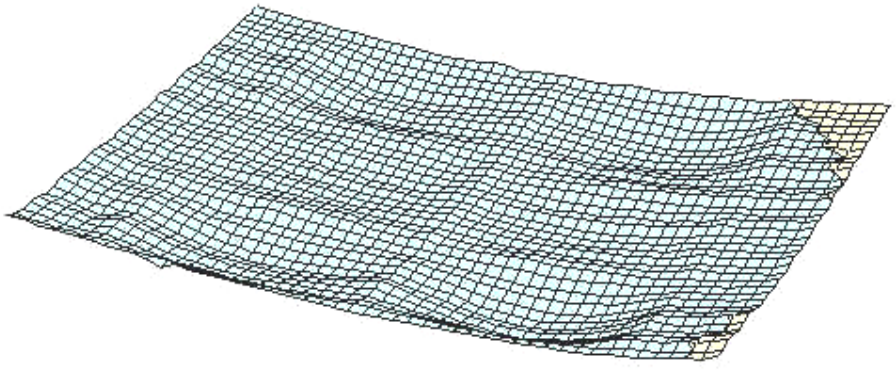

Imperfection of Specimen A3

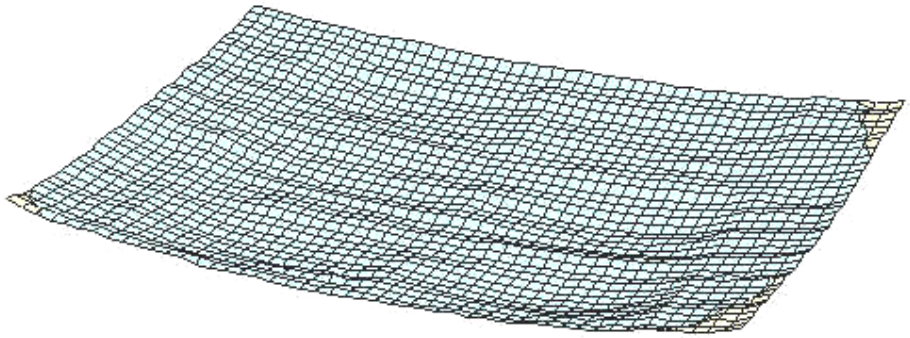

Imperfection of Specimen A4

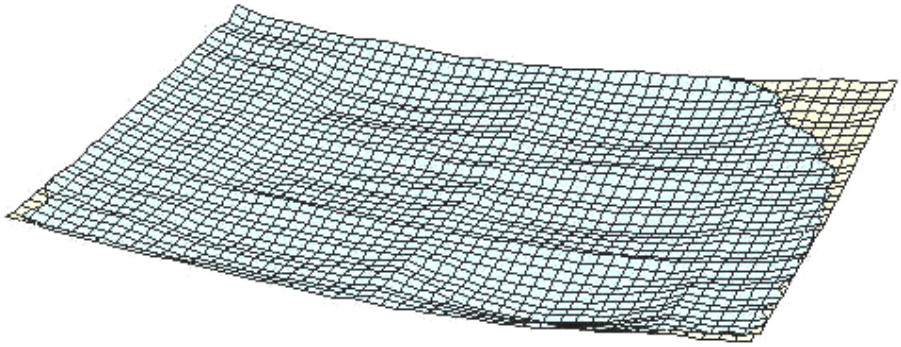

Imperfection of Specimen A5

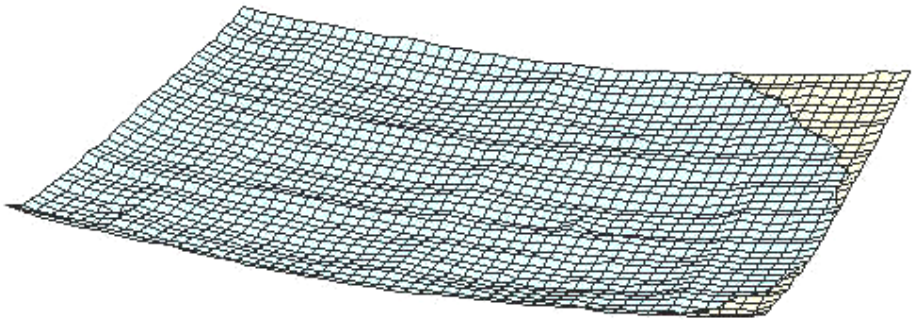

Imperfection of Specimen A6

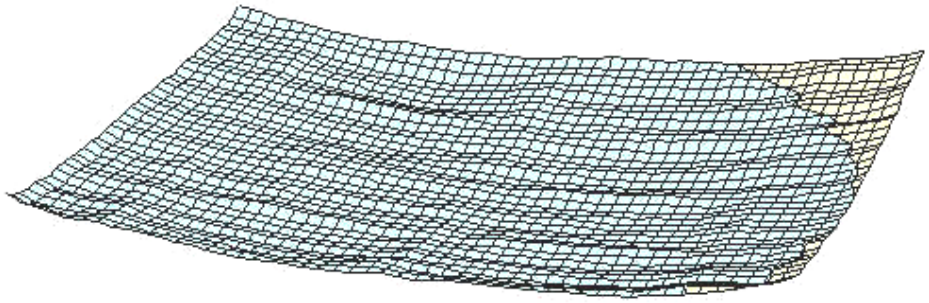

Imperfection of Specimen B1

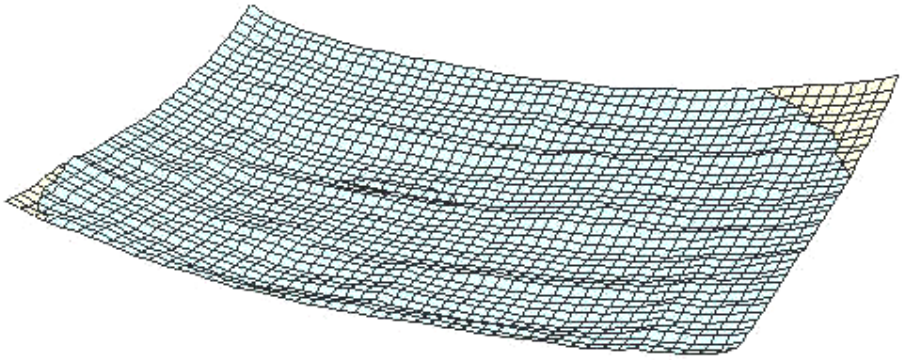

Imperfection of Specimen B2

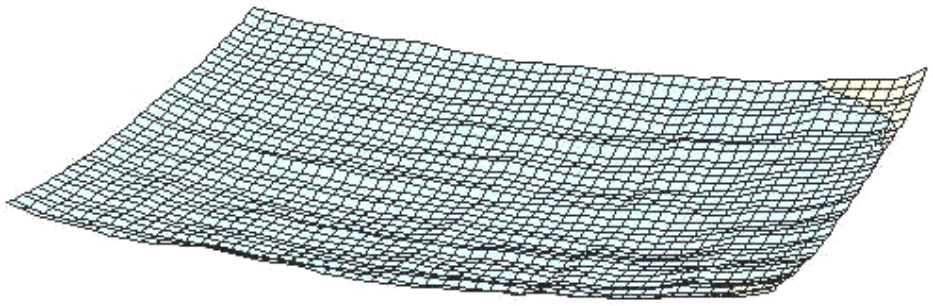

Imperfection of Specimen B3

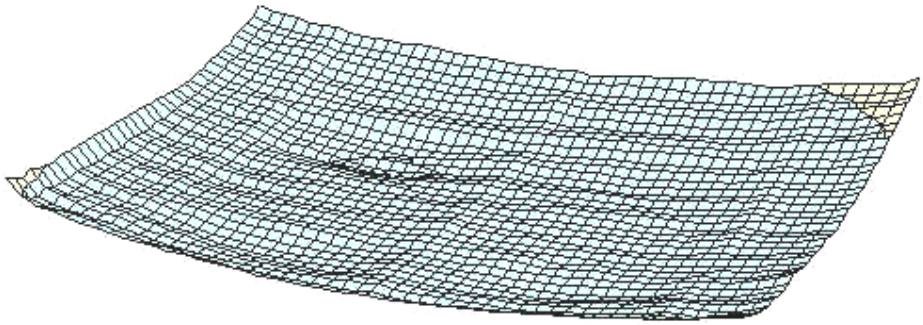

Imperfection of Specimen B4

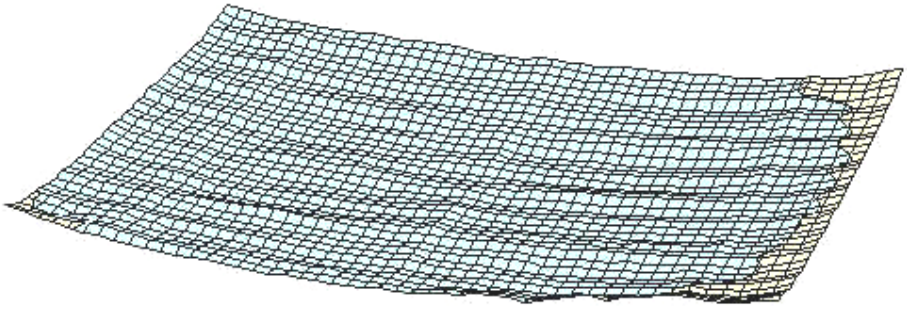

Imperfection of Specimen B5

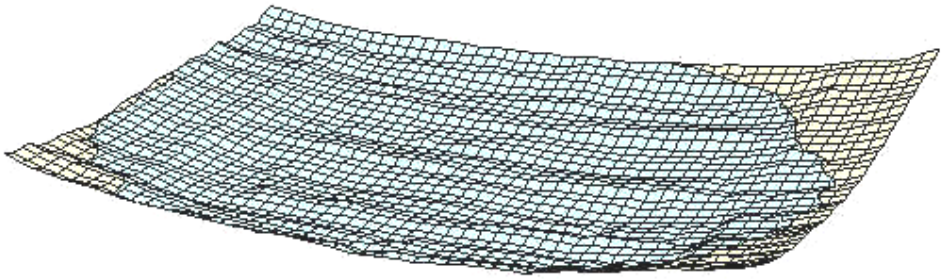

Imperfection of Specimen B6

Table 1. Initial Imperfection for Specimen A3

No. of Points		Long Edge												
		1	**2**	**3**	**4**	**5**	**6**	**7**	**8**	**9**	**10**	**11**	**12**	**13**
Short Edge	**1**	0	0.304	0.67	0.938	1.13	1.404	1.634	1.87	1.872	1.892	2.242	2.56	2.64
	2	0.66	0.908	1.144	1.418	1.33	1.584	1.782	2.224	2.48	2.66	2.714	3.004	3.098
	3	0.558	0.854	1.254	1.51	1.832	1.892	1.836	2.358	2.656	2.984	3.284	3.616	3.84
	4	0.578	0.858	1.172	1.402	1.638	1.75	1.732	2.238	2.648	3.192	3.592	4.042	4.246
	5	0.736	1.108	1.428	1.776	2.088	2.202	2.154	2.69	3.222	3.788	4.184	4.802	5.014
	6	1.012	1.496	1.882	2.242	2.47	2.542	2.522	3.222	3.868	4.49	5.084	5.608	6.018
	7	1.132	1.586	1.872	2.196	2.312	2.412	2.396	3.148	3.77	4.486	5.05	5.566	6.002
	8	0.818	1.246	1.658	1.94	2.196	2.252	2.152	2.92	3.56	4.348	4.858	5.404	5.762
	9	0.9	1.414	1.846	2.184	2.576	2.71	2.53	3.332	4.17	4.936	5.404	5.846	6.276
	10	1.664	2.092	2.43	2.826	3.064	3.134	3.088	3.758	4.394	5.12	5.578	6.008	6.324
	11	1.55	2.086	2.504	2.814	3.02	3.11	2.992	3.552	4.028	4.604	5.054	5.37	5.604
	12	0.96	1.498	1.914	2.29	2.582	2.708	2.654	3.34	3.756	4.222	4.48	4.748	4.874
	13	1.112	1.73	2.176	2.632	2.984	3.25	3.26	3.86	4.244	4.516	4.69	4.894	4.992
	14	1.716	2.142	2.672	3.04	3.282	3.598	3.758	4.196	4.452	4.74	5.018	5.21	5.204
	15	1.612	1.93	2.67	3.14	3.16	3.662	3.71	4.104	4.354	4.62	4.865	5.088	5.177
	16	1.226	1.73	2.18	2.696	3.07	3.33	3.52	3.942	4.116	4.494	4.712	4.966	5.15
	17	1.416	1.922	2.396	2.846	3.188	3.366	3.46	3.942	4.256	4.664	4.966	5.248	5.5
	18	1.552	2.116	2.564	3.04	3.382	3.648	3.554	3.948	4.23	4.712	5.088	5.398	5.8
	19	1.652	2.12	2.514	2.77	3.288	3.46	3.364	4.052	4.426	4.738	5.062	5.314	5.482
	20	1.42	1.842	2.382	2.89	3.25	3.478	3.54	4.026	4.322	4.762	5.094	5.362	5.656
	21	1.394	1.876	2.384	2.87	3.274	3.434	3.564	3.968	4.192	4.576	4.886	5.126	5.402
	22	1.48	2.048	2.464	2.938	3.346	3.622	3.736	4.13	4.578	4.654	4.562	4.78	5.274
	23	1.772	2.25	2.756	3.186	3.486	3.826	3.862	4.17	4.544	4.83	5.134	5.238	5.306
	24	1.59	2.106	2.64	3.132	3.522	3.658	3.72	4.15	4.366	4.598	4.778	4.794	4.848
	25	1.326	1.856	2.36	2.846	3.132	3.394	3.57	4.054	4.278	4.45	4.544	4.454	4.4
	26	1.302	1.818	2.408	2.932	3.266	3.444	3.568	4.05	4.29	4.632	4.852	5.058	4.896
	27	1.382	2.04	2.626	3.154	3.438	3.66	3.748	4.182	4.492	5.004	5.364	5.62	5.708
	28	1.58	1.968	2.45	2.878	3.168	3.334	3.354	3.856	4.298	4.838	5.286	5.59	5.84
	29	1.26	1.784	2.252	2.684	2.926	3.032	3.022	3.612	4.134	4.786	5.29	5.71	6.108
	30	1.182	1.76	2.274	2.712	2.994	3.002	3.002	3.782	4.352	4.97	5.638	6.134	6.588
	31	1.672	2.114	2.63	3.028	2.978	3.28	3.138	3.87	4.538	5.282	5.866	6.364	6.798
	32	1.664	2.056	2.484	2.756	3.242	2.924	2.648	3.286	3.98	4.746	5.314	5.774	6.174
	33	0.984	1.412	1.83	2.15	2.962	2.362	2.098	2.702	3.372	4.12	4.642	5.094	5.474
	34	0.716	1.278	1.738	1.962	2.366	2.41	2.186	2.786	3.398	4.046	4.622	4.938	5.33
	35	1.038	1.25	1.676	2.032	2.348	2.364	2.228	2.712	3.186	3.676	4.082	4.404	4.63
	36	0.55	0.828	1.178	1.42	1.53	1.734	1.598	1.914	2.326	2.728	2.982	3.174	3.392
	37	-0.394	-0.168	0.146	0.47	0.582	0.788	0.848	1.35	1.374	1.682	1.99	3.008	2.1

Continued on next page

Note: 1. Deflection units: mm
2. Deflection towards stiffener side is positive.

Table 1. Initial Imperfection for Specimen A3 (continued)

No. of Points		Long Edge												
		14	**15**	**16**	**17**	**18**	**19**	**20**	**21**	**22**	**23**	**24**	**25**	**26**
Short Edge	**1**	2.774	3.056	3.234	3.256	3.23	3.038	2.794	2.774	3.368	3.244	3.13	2.95	2.99
	2	3.124	3.31	3.478	3.51	3.62	3.58	3.44	3.464	3.584	3.592	3.548	3.238	3.47
	3	3.86	4.086	4.222	4.244	4.212	4.07	3.902	3.874	3.81	3.722	3.608	3.29	3.594
	4	4.466	4.694	4.802	4.888	4.8	4.602	4.478	4.482	4.416	4.11	3.81	3.654	3.936
	5	4.75	5.096	5.318	5.372	5.306	5.208	5.274	5.068	4.888	4.608	4.322	4.036	4.326
	6	6.144	6.35	6.39	6.354	6.238	5.964	5.692	5.46	5.248	4.992	4.726	4.456	4.852
	7	6.168	6.388	6.434	6.376	6.192	5.936	5.679	5.553	5.321	5.088	4.816	4.65	5.059
	8	6.012	6.234	6.324	6.272	6.148	5.928	5.666	5.646	5.394	5.184	4.906	4.844	5.266
	9	6.5	6.722	6.782	6.596	6.542	6.256	6.03	5.924	5.702	5.638	5.45	5.318	5.572
	10	6.47	6.63	6.698	6.7	6.644	6.432	6.222	6.116	5.972	5.784	5.6	5.352	5.674
	11	5.7	5.798	5.926	5.944	5.944	5.806	5.73	5.674	5.64	5.508	5.444	5.208	5.458
	12	4.812	4.934	5.254	5.388	5.476	5.444	5.484	5.714	5.818	5.868	5.926	5.754	5.97
	13	4.702	5.064	5.32	5.462	5.474	5.376	5.716	5.68	6.106	6.21	6.172	5.998	6.202
	14	5.196	5.442	5.652	5.878	6	5.93	6.114	6.38	6.504	6.558	6.368	5.89	6.084
	15	5.241	5.494	5.711	5.915	6.091	6.128	6.371	6.508	6.649	6.653	6.393	5.983	6.202
	16	5.286	5.546	5.77	5.952	6.182	6.326	6.628	6.636	6.794	6.748	6.418	6.076	6.32
	17	5.724	6.086	6.188	6.396	6.604	6.706	6.888	6.944	6.94	6.708	6.29	6.028	6.266
	18	5.968	6.306	6.398	6.578	6.822	6.806	7.022	7.11	7.042	6.746	6.278	6.02	6.192
	19	5.458	5.84	6.078	6.25	6.602	6.672	6.728	6.908	6.93	6.802	6.508	6.07	6.478
	20	5.826	6.104	6.31	6.502	6.76	6.82	6.958	6.892	6.832	6.656	6.38	6.008	6.298
	21	5.588	5.838	6.078	6.34	6.678	6.76	6.734	6.78	6.692	6.58	6.318	6.014	6.29
	22	5.382	5.522	6.09	6.258	6.528	6.552	6.522	6.512	6.498	6.4	6.296	6	6.292
	23	5.388	5.554	5.742	5.874	6.09	6.156	6.31	6.402	6.474	6.468	6.35	6.114	6.408
	24	4.838	4.976	5.202	5.376	5.562	5.546	5.76	5.922	6.06	6.176	6.076	5.812	6.118
	25	4.382	4.582	4.862	4.966	5.158	5.14	5.35	5.814	5.954	6.092	6.076	5.96	6.21
	26	4.496	4.788	5.236	5.48	5.658	5.802	5.922	6.06	6.182	6.314	6.486	6.22	6.414
	27	5.638	5.87	6	6.168	6.328	6.272	6.268	6.352	6.454	6.534	6.506	6.334	6.526
	28	5.914	6.146	6.294	6.384	6.51	6.43	6.338	6.308	6.26	6.182	6.062	5.876	6.098
	29	6.206	6.52	6.596	6.67	6.842	6.75	6.694	6.59	6.432	6.438	6.222	5.75	6.126
	30	6.88	7.222	7.136	7.184	7.284	7.18	7.06	6.866	6.756	6.51	6.232	5.808	6.166
	31	7.032	7.346	7.436	7.454	7.476	7.312	7.158	6.908	6.636	6.286	5.862	5.432	5.88
	32	6.432	6.67	6.822	6.848	6.898	6.746	6.56	6.302	6.06	5.696	5.254	4.762	5.194
	33	5.706	5.962	6.16	6.2	6.352	6.206	6.16	5.884	5.704	5.518	5.206	4.748	5.206
	34	5.564	5.774	5.946	6.04	5.934	5.72	5.606	5.582	5.418	5.258	5.008	4.768	5.126
	35	4.806	5.018	5.206	5.226	5.386	5.272	5.216	5.15	5.07	4.868	4.606	4.242	4.438
	36	3.542	3.698	3.888	3.994	4.056	3.996	4.044	4.05	4.038	3.988	3.876	3.686	3.74
	37	2.306	2.496	2.786	2.912	3.066	3.14	3.284	3.368	3.476	3.584	3.476	3.798	3.756

Continued on next page

Note: 1. Deflection units: mm
2. Deflection towards stiffener side is positive.

Table 1. Initial Imperfection for Specimen A3 (continued)

No. of Points		Long Edge												
		27	28	29	30	31	32	33	34	35	36	37	38	39
Short Edge	1	3.068	2.956	2.81	2.554	2.484	2.456	2.444	2.176	2.032	1.878	1.558	1.438	1.192
	2	3.604	3.658	3.608	3.568	3.618	3.65	3.656	3.52	3.37	3.156	2.888	2.604	2.352
	3	3.782	3.934	3.958	4.066	4.172	4.222	4.302	4.156	4.054	3.938	3.594	3.26	2.856
	4	4.252	4.422	4.332	4.422	4.68	4.82	4.87	5.026	4.89	5.008	4.604	4.108	3.496
	5	4.784	5.03	5.282	5.498	5.704	5.79	5.868	5.814	5.73	5.47	5.1	4.544	4.054
	6	5.246	5.538	5.778	6.1	6.358	6.472	6.556	6.576	6.504	6.234	5.8	5.344	4.74
	7	5.379	5.45	5.72	6.03	6.286	6.426	6.536	6.526	6.45	6.196	5.92	5.406	4.834
	8	5.512	5.7	6.004	6.314	6.64	6.754	6.782	6.75	6.608	6.378	6.09	5.666	5.21
	9	5.87	6.218	6.442	6.382	6.62	6.72	6.906	6.794	6.786	6.45	6.152	5.694	5.014
	10	5.928	6.14	6.236	6.398	6.538	6.55	6.502	6.476	6.346	6.042	5.796	5.408	4.822
	11	5.65	5.718	5.756	5.842	6.306	5.984	5.78	5.704	5.664	5.466	5.332	5.086	4.66
	12	6.152	6.306	6.238	6.116	6.068	6.026	5.91	5.786	5.706	5.548	5.266	4.938	4.622
	13	6.262	6.2	6.038	5.844	5.688	5.622	5.376	5.092	4.966	4.674	4.524	4.286	4.094
	14	6.108	6.048	5.896	5.784	5.58	5.428	5.19	5.044	4.922	4.506	4.286	3.964	3.868
	15	6.317	6.138	6.024	5.98	5.946	5.776	5.708	5.6	5.41	5.24	4.984	4.924	4.644
	16	6.526	6.606	6.6	6.59	6.604	6.498	6.318	6.148	5.968	5.726	5.468	5.304	4.768
	17	6.582	6.832	6.99	7.068	7.108	6.914	6.72	6.638	6.304	5.948	5.796	5.458	5.18
	18	6.53	6.656	6.734	6.68	6.698	6.696	6.548	6.386	6.19	5.852	5.55	5.274	4.87
	19	6.814	7.038	7.142	7.234	7.302	7.236	7.146	7.024	6.86	6.616	6.346	6.022	5.632
	20	6.698	6.954	7.058	7.204	7.24	7.25	7.18	7.094	6.936	6.624	6.324	6.026	5.62
	21	6.544	6.804	6.928	7.084	7.114	7.078	7.276	7.172	6.924	6.582	6.358	5.978	5.684
	22	6.526	6.602	6.784	6.884	6.84	6.78	6.686	6.55	6.47	6.198	6.012	5.72	5.4
	23	6.682	6.866	6.928	6.932	6.886	6.788	6.678	6.62	6.53	6.33	6.128	5.876	5.556
	24	6.336	6.428	6.41	6.386	6.28	6.12	6.066	6.088	5.944	5.886	5.602	5.438	5.246
	25	6.256	6.318	6.216	5.866	5.72	5.802	5.784	5.778	5.884	5.594	5.348	5.206	5.05
	26	6.568	6.594	6.616	6.556	6.518	6.546	6.586	6.526	6.386	6.174	5.978	5.706	5.43
	27	6.714	6.862	6.932	7.106	7.31	7.318	7.416	7.406	7.276	7.088	6.772	6.452	6.036
	28	6.396	6.656	6.868	7.188	7.506	7.63	7.788	7.81	7.704	7.586	7.172	6.764	6.346
	29	6.508	6.906	7.252	7.668	8.044	8.292	8.356	8.466	8.45	8.24	7.858	7.502	6.902
	30	6.72	7.006	7.386	7.998	8.336	8.66	8.846	8.804	8.782	8.498	8.016	7.518	6.818
	31	6.406	6.88	7.314	7.844	8.294	8.548	8.668	8.752	8.592	8.46	7.93	7.288	6.616
	32	5.748	6.19	6.61	7.07	7.53	7.794	8.002	8.102	8.016	7.768	7.35	6.928	6.308
	33	5.784	5.986	6.422	6.854	7.246	7.534	7.724	7.914	7.982	7.454	7.11	6.706	6.014
	34	5.404	5.688	6.02	6.32	6.304	6.566	6.996	7.006	6.818	6.472	6.136	5.7	5.142
	35	4.7	4.874	5.006	5.236	5.348	5.418	5.434	5.482	5.402	5.11	4.774	4.484	3.98
	36	3.886	3.952	3.896	3.962	4.02	4.014	4.002	4.03	3.966	3.72	3.526	3.428	3.218
	37	3.724	3.612	3.48	3.482	3.388	3.39	3.268	3.386	2.988	3.04	2.88	2.846	2.688

Continued on next page

Note: 1. Deflection units: mm
2. Deflection towards stiffener side is positive.

Table 1. Initial Imperfection for Specimen A3 (continued)

No. of Points		Long Edge									
		40	**41**	**42**	**43**	**44**	**45**	**46**	**47**	**48**	**49**
Short Edge	**1**	0.98	0.722	-0.094	-0.48	-0.686	-0.926	-1.302	-1.672	-1.976	-2.31
	2	1.984	1.41	0.712	-0.212	-0.128	-0.382	-0.686	-1.056	-1.434	-1.942
	3	2.336	1.684	0.794	-0.07	-0.128	-0.362	-0.544	-0.878	-1.16	-1.754
	4	2.972	2.122	1.188	0.27	0.24	0.046	-0.406	-0.69	-1.144	-1.572
	5	3.372	2.32	1.224	0.354	0.194	0.04	-0.26	-0.672	-1	-1.7
	6	4	2.968	1.91	0.878	0.726	0.578	0.262	-0.274	-0.694	-1.348
	7	4.18	3.154	1.99	0.978	0.97	0.756	0.052	-0.26	-0.326	-1.012
	8	4.6	3.68	2.576	1.618	1.484	1.216	1.044	0.518	0.004	-0.706
	9	4.302	3.422	2.448	1.402	1.286	1.104	0.686	0.21	-0.254	-0.99
	10	4.184	3.368	2.482	1.396	1.136	0.868	0.6	0.204	-0.212	-0.988
	11	4.248	3.76	3.02	2.218	2.118	1.838	1.52	1.092	0.582	-0.26
	12	4.374	3.842	3.348	2.592	2.434	2.14	1.746	1.242	0.892	-0.008
	13	3.97	3.544	3.014	2.478	2.192	1.894	1.502	0.99	0.584	-0.316
	14	3.354	3.072	2.734	2.216	2.07	1.696	1.472	0.86	0.42	-0.192
	15	4.352	3.966	3.574	2.996	2.854	2.446	2.062	1.648	1.13	0.408
	16	4.496	3.92	3.568	3.07	2.872	2.542	2.062	1.658	1.112	0.332
	17	4.67	4.21	3.478	2.848	2.514	2.162	1.776	1.238	0.83	0.138
	18	4.458	4.008	3.322	2.694	2.638	2.276	1.87	1.442	1.048	0.348
	19	5.246	4.618	3.954	3.202	3.02	2.668	2.29	1.822	1.394	0.69
	20	5.204	4.556	3.838	3.358	3.012	2.636	2.454	2.004	1.488	0.794
	21	5.336	4.66	3.886	3.232	3.056	2.712	2.288	1.776	1.314	0.714
	22	5.046	4.532	3.726	3.214	3.086	2.692	2.276	1.802	1.252	0.556
	23	5.252	4.71	4.142	3.386	3.174	2.852	2.53	2.046	1.506	0.596
	24	4.97	4.55	4.108	3.17	2.978	2.896	2.49	1.962	1.612	0.802
	25	4.838	4.62	4.164	3.726	3.326	2.982	2.398	1.898	1.428	0.706
	26	5.134	4.636	4.114	3.582	3.244	2.798	2.354	1.798	1.304	0.592
	27	5.57	4.844	4.212	3.416	3.068	2.622	2.178	1.65	1.156	0.39
	28	5.774	4.918	4.066	3.252	2.848	2.468	1.866	1.708	0.956	0.314
	29	6.144	5.314	4.264	3.136	2.994	2.564	2.026	1.408	0.882	0.108
	30	6.056	5.07	3.98	2.796	2.524	2.062	1.546	0.97	0.404	-0.354
	31	5.83	4.752	3.554	2.314	2.088	1.456	1.048	0.478	-0.184	-0.942
	32	5.508	4.528	3.582	2.132	2.254	1.816	1.348	0.676	0.088	-0.692
	33	5.362	4.4	3.494	2.38	2.192	1.72	1.214	0.658	0.062	-0.692
	34	4.468	3.734	2.664	1.86	1.604	1.176	0.638	0.058	-0.56	-1.306
	35	3.48	2.716	1.956	1.224	1.282	0.996	0.204	-0.282	-0.834	-1.69
	36	3.018	2.576	2.14	1.552	1.382	1.114	0.718	0.162	-0.402	-1.256
	37	2.626	2.35	1.926	1.552	1.236	0.71	0.444	-0.112	-0.564	-1.462

Note: 1. Deflection units: mm
2. Deflection towards stiffener side is positive.

Table 2. Initial Imperfection for Specimen B3

No. of Points		Long Edge												
		1	2	3	4	5	6	7	8	9	10	11	12	13
Short Edge	1	0	0.472	0.792	1.126	1.414	1.572	1.652	2.294	2.252	2.388	2.402	2.286	2.35
	2	0.434	0.988	1.374	1.566	1.99	2.114	2.356	2.692	2.89	3.094	3.206	3.372	3.466
	3	1.062	1.648	2.106	2.24	2.48	2.54	2.51	2.86	3.076	3.35	3.492	3.72	3.84
	4	1.324	1.922	2.414	2.712	2.804	2.908	2.828	3.272	3.574	3.764	3.982	3.974	4.172
	5	1.89	2.418	2.834	3.086	3.32	3.33	3.132	3.764	3.91	4.442	4.604	4.774	5.008
	6	1.74	2.666	3.128	3.566	3.82	4.022	3.944	4.488	4.78	5.082	5.32	5.508	5.686
	7	2.072	2.688	3.222	3.602	3.874	4.068	4.066	4.528	4.77	5.066	5.286	5.48	5.622
	8	2.342	2.934	3.44	3.832	4.122	4.258	4.416	4.786	4.972	5.224	5.474	5.634	5.774
	9	2.69	3.16	3.668	4.15	4.516	4.592	4.7	5.218	5.394	5.69	5.924	6.192	6.338
	10	2.816	3.472	3.918	4.314	4.642	4.972	5.258	5.562	5.704	5.914	6.14	6.248	6.31
	11	2.866	3.43	3.928	4.206	4.75	5.012	5.098	5.53	5.752	6.03	6.18	6.368	6.476
	12	2.978	3.72	4.234	4.636	5.078	5.376	5.436	5.898	6.162	6.588	6.93	7	7.07
	13	2.962	3.788	4.474	4.89	5.338	5.738	5.782	6.22	6.646	6.928	7.178	7.322	7.454
	14	3.416	4.124	4.718	5.186	5.646	5.932	6.16	6.642	6.902	7.266	7.45	7.66	7.786
	15	3.13	3.814	4.482	4.962	5.384	5.73	5.93	6.386	6.692	7.014	7.19	7.432	7.468
	16	3.17	3.912	4.486	5.056	5.546	5.744	6.116	6.58	6.816	7.164	7.5	7.676	7.714
	17	3.38	4.064	4.766	5.322	5.87	6.152	6.416	6.854	7.238	7.382	7.6	7.75	7.872
	18	3.758	4.436	5.024	5.556	5.89	6.17	6.338	6.832	7.112	7.322	7.518	7.708	7.672
	19	3.468	4.022	4.648	5.034	5.304	5.636	5.974	6.4	6.52	6.67	6.858	7.01	6.932
	20	3.858	4.466	5.06	5.272	5.584	6.11	6.268	6.624	7.046	7.328	7.544	7.84	7.974
	21	3.804	4.43	5.04	5.3	5.742	6.064	6.2	6.77	7.168	7.586	7.856	8.088	8.166
	22	3.832	4.458	5.056	5.45	5.794	6.106	6.262	6.722	7.056	7.408	7.602	7.824	7.964
	23	3.504	4.154	4.694	5.1	5.498	5.766	5.914	6.412	6.756	7.114	7.45	7.664	7.942
	24	3.758	4.354	4.946	5.16	5.626	5.892	6.106	6.728	7.126	7.452	7.784	8.004	8.196
	25	3.762	4.246	4.766	5.288	5.644	5.918	6.048	6.626	6.986	7.37	7.646	7.904	8.034
	26	3.7	4.258	4.814	5.246	5.544	5.716	5.82	6.374	6.714	7.03	7.274	7.426	7.472
	27	3.462	3.842	4.316	4.722	5.058	5.21	5.202	6.012	6.466	6.814	7.01	7.252	7.466
	28	3.356	3.66	4.162	4.71	4.972	5.164	5.374	5.946	6.318	6.542	6.764	6.828	6.714
	29	3.198	3.736	4.224	4.624	4.85	5.024	5.076	5.664	6.024	6.32	6.552	6.746	6.806
	30	3.066	3.656	4.018	4.384	4.762	4.986	4.84	5.34	5.62	5.99	6.088	6.426	6.35
	31	2.734	3.266	3.732	4.264	4.564	4.718	4.822	5.444	5.742	5.956	6.314	6.492	6.544
	32	2.878	3.506	3.946	4.336	4.588	4.774	4.828	5.262	5.402	5.672	5.856	6.022	6.04
	33	2.61	3.178	3.722	4.008	4.388	4.56	4.588	4.87	5.074	5.23	5.364	5.522	5.55
	34	2.446	2.952	3.414	3.762	3.94	4.088	4.254	4.636	4.86	4.972	5.046	4.992	5.196
	35	1.862	2.454	3.26	3.75	4.116	4.294	4.36	4.626	4.81	4.95	4.962	5.054	5.064
	36	1.8	2.538	3.026	3.334	3.56	3.696	3.74	4.068	4.216	4.31	4.308	4.316	4.284
	37	1.202	1.834	2.378	2.766	3.002	3.11	3.418	3.784	3.84	3.924	3.85	3.522	3.38

Continued on next page

Note: 1. Deflection units: mm
2. Deflection towards stiffener side is positive.

Table 2. Initial Imperfection for Specimen B3 (continued)

No. of Points		Long Edge												
		14	15	16	17	18	19	20	21	22	23	24	25	26
Short Edge	1	2.4	2.606	2.848	3.104	3.11	3.154	3.138	3.182	2.952	2.996	2.944	2.674	2.746
	2	3.44	3.7	3.824	3.922	3.938	3.934	3.932	3.888	3.712	3.786	3.528	3.212	3.32
	3	3.728	3.934	4.096	4.168	4.224	4.19	4.202	4.232	4.198	4.042	3.878	3.634	3.92
	4	4.046	4.24	4.508	4.532	4.638	4.726	5.018	4.774	4.938	4.908	4.704	4.472	4.7
	5	5.196	5.39	5.518	5.554	5.592	5.474	5.472	5.35	5.276	5.08	4.832	4.42	4.742
	6	5.718	5.918	6.028	6.094	6.06	6.028	5.796	5.746	5.65	5.548	5.13	4.688	4.946
	7	5.684	5.842	6.018	6.044	6.098	5.95	5.94	5.82	5.914	5.792	5.67	5.5	5.832
	8	5.884	5.922	6.274	6.412	6.494	6.532	6.494	6.436	6.448	6.45	6.298	6.122	6.364
	9	6.372	6.586	6.782	6.796	6.958	6.836	6.656	6.528	6.608	6.64	6.602	6.254	6.468
	10	6.27	6.552	6.736	6.808	6.906	6.756	6.532	6.266	6.55	6.508	6.344	6.36	6.284
	11	6.51	6.566	6.884	6.91	7.018	6.938	7.05	7.048	7.106	7.234	7.384	7.172	7.374
	12	7.352	7.448	7.758	7.85	8.014	7.904	7.854	7.814	7.712	7.792	7.622	7.332	7.562
	13	7.532	7.75	8.064	8.138	8.314	8.118	8.052	8.078	7.966	7.998	7.72	7.434	7.702
	14	7.826	7.896	8.006	8.148	8.212	8.036	8.002	7.784	7.764	7.636	7.422	7.104	7.432
	15	7.49	7.628	7.754	7.894	8.03	8.22	8.256	8.346	8.522	8.514	8.364	8.018	8.306
	16	7.838	8.068	8.27	8.52	8.58	8.61	8.542	8.532	8.47	8.414	8.382	8.202	8.432
	17	7.896	7.972	8.13	8.406	8.468	8.48	8.492	8.574	8.564	8.524	8.488	8.31	8.454
	18	7.546	7.692	7.888	8.032	8.102	8.02	7.964	7.944	8.082	8.178	8.222	8.176	8.278
	19	7.048	7.18	7.558	7.778	8.006	7.89	7.944	8.248	8.524	8.69	8.736	8.86	8.78
	20	8.028	8.258	8.476	8.624	8.742	8.666	8.652	8.63	8.68	8.698	8.672	8.512	8.562
	21	8.244	8.422	8.628	8.762	8.896	8.88	8.79	8.716	8.808	8.72	8.616	8.326	8.528
	22	8.018	8.22	8.42	8.514	8.672	8.624	8.568	8.742	8.718	8.738	8.606	8.314	8.554
	23	8.296	8.708	8.7	9.068	9.212	9.164	9.164	9.114	9.02	8.936	8.762	8.36	8.608
	24	8.292	8.534	8.7	8.828	9.02	8.938	9.002	8.874	8.82	8.664	8.454	7.986	8.208
	25	8.128	8.42	8.598	8.728	8.818	8.838	8.742	8.718	8.64	8.524	8.248	7.928	8.13
	26	7.57	7.708	7.99	8.116	8.444	8.498	8.498	8.532	8.462	8.452	8.196	7.776	7.93
	27	7.408	7.66	7.902	8.112	8.236	8.098	8.102	8.17	8.24	8.206	8.062	7.654	7.868
	28	6.634	6.892	7.092	7.238	7.386	7.258	7.148	7.394	7.544	7.534	7.452	7.356	7.39
	29	6.656	6.926	7.012	7.238	7.26	7.322	7.418	7.428	7.48	7.562	7.432	7.22	7.406
	30	6.454	6.656	6.942	7.114	7.394	7.382	7.356	7.344	7.276	7.254	7.192	6.96	7.108
	31	6.572	6.738	6.904	7.16	7.322	7.25	7.26	7.236	7.204	7.108	6.952	6.652	6.842
	32	6.02	6.176	6.338	6.546	6.746	6.68	6.742	6.628	6.612	6.554	6.448	6.108	6.358
	33	5.478	5.764	5.754	5.972	6.188	6.17	6.254	6.29	6.4	6.468	6.434	6.152	6.086
	34	5.278	5.4	5.6	5.878	6.054	5.95	5.806	5.75	5.692	5.74	5.696	5.484	5.488
	35	5.072	5.23	5.356	5.524	5.638	5.54	5.532	5.464	5.362	5.292	5.168	5.006	4.796
	36	4.142	4.29	4.478	4.59	4.676	4.602	4.56	4.568	4.586	4.678	4.626	4.616	4.59
	37	3.112	3.354	3.516	3.63	3.796	3.91	3.63	4.014	4.254	4.372	4.436	4.392	4.334

Continued on next page

Note: 1. Deflection units: mm
2. Deflection towards stiffener side is positive.

Table 2. Initial Imperfection for Specimen B3 (continued)

No. of Points		Long Edge												
		27	28	29	30	31	32	33	34	35	36	37	38	39
Short Edge	1	2.768	2.678	2.546	2.456	2.318	2.146	2.138	1.884	1.448	1.358	1.268	1.18	0.936
	2	3.316	3.12	3.002	2.77	2.702	2.704	2.692	2.612	1.982	2.066	1.842	1.952	1.542
	3	4.07	4.19	4.294	4.298	4.35	4.212	4.064	3.956	3.226	3.168	2.846	2.866	2.402
	4	4.836	4.904	4.898	4.886	4.804	4.764	4.714	4.55	3.74	3.652	3.31	3.278	2.84
	5	4.93	5.046	5.09	5.104	5.07	5.056	4.9	4.644	3.84	3.728	3.414	3.366	2.972
	6	5.084	5.186	5.2	5.258	5.318	5.382	5.532	5.392	4.722	4.692	4.236	4.264	3.772
	7	6.062	6.308	6.316	6.398	6.37	6.264	6.224	6.046	5.31	5.212	4.994	4.88	4.458
	8	6.618	6.768	6.686	6.628	6.484	6.338	6.152	5.94	5.212	5.204	4.922	4.898	4.508
	9	6.526	6.54	6.492	6.448	6.242	6.018	5.81	5.658	4.818	4.792	4.562	4.48	4.194
	10	6.216	6.364	6.178	6.098	6.226	6.248	6.166	5.918	5.216	5.07	4.724	4.702	4.408
	11	7.438	7.502	7.438	7.43	7.344	7.098	6.822	6.602	5.996	5.89	5.626	5.6	5.214
	12	7.714	7.778	7.824	7.782	7.648	7.354	7.132	6.884	6.082	6.062	5.832	5.794	5.472
	13	7.776	7.92	7.69	7.646	7.692	7.418	7.254	7.134	6.272	6.156	5.902	5.908	5.608
	14	7.62	7.862	7.864	8.04	7.876	7.892	7.744	7.534	6.812	6.606	6.334	6.224	5.846
	15	8.418	8.548	8.506	8.506	8.47	8.32	8.13	7.948	7.226	7.12	6.888	6.754	6.354
	16	8.442	8.53	8.434	8.56	8.476	8.28	8.072	7.832	7.032	6.772	6.646	6.466	6.15
	17	8.34	8.518	8.144	8.044	8.128	7.824	7.714	7.58	6.964	6.816	6.612	6.602	6.348
	18	8.422	8.484	8.286	8.19	8.192	7.92	7.612	7.464	6.83	6.628	6.584	6.582	6.356
	19	8.664	8.562	8.306	8.07	7.804	7.73	7.504	7.328	6.858	6.72	6.37	6.416	6.138
	20	8.5	8.598	8.48	8.334	8.172	8.03	7.79	7.744	7.45	7.18	6.99	6.898	6.59
	21	8.558	8.688	8.518	8.45	8.45	8.276	8.204	8.208	7.644	7.522	7.408	7.286	6.956
	22	8.606	8.706	8.502	8.452	8.406	8.31	8.184	8.154	7.574	7.47	7.346	7.218	6.848
	23	8.688	8.746	8.626	8.548	8.49	8.31	8.244	8.198	7.622	7.566	7.404	7.252	6.848
	24	8.242	8.304	8.126	8.212	8.092	8.044	8.008	8.192	7.684	7.654	7.56	7.252	7.05
	25	8.25	8.374	8.374	8.34	8.31	8.248	8.13	8.098	7.568	7.41	7.324	7.192	6.84
	26	8.022	8.166	8.042	7.976	7.928	7.834	7.702	7.692	7.118	6.97	6.93	6.778	6.488
	27	7.812	7.762	7.578	7.478	7.388	7.248	7.088	6.972	6.418	6.22	6.174	6.112	5.86
	28	7.174	7.162	6.888	6.746	6.606	6.684	6.734	6.63	6.088	5.91	5.856	5.742	5.548
	29	7.548	7.562	7.388	7.306	7.216	7.05	6.87	6.756	6.122	5.856	5.776	5.666	5.296
	30	7.216	7.22	6.994	6.906	6.826	6.676	6.514	6.454	5.858	5.646	5.588	5.422	5.084
	31	6.874	6.876	6.63	6.528	6.414	6.264	6.12	6.198	5.634	5.406	5.42	5.28	5.016
	32	6.476	6.458	6.44	6.52	6.414	6.278	6.13	6.182	5.632	5.404	5.41	5.222	4.888
	33	6.304	6.226	6.044	6.014	5.986	5.892	5.822	5.748	5.008	4.798	4.786	4.472	4.154
	34	5.398	5.326	5.198	5.11	5.024	4.846	4.66	4.528	4.022	3.732	3.75	3.446	3.158
	35	4.672	4.59	4.426	4.068	4.066	3.954	3.936	4	3.436	3.4	3.3	3.09	2.906
	36	4.872	4.754	4.372	4.338	4.258	4.038	3.81	3.83	3.074	2.898	2.93	2.644	2.412
	37	4.304	4.126	3.7	3.534	3.368	3.164	2.792	2.818	2.154	1.846	1.884	1.662	1.354

Continued on next page

Note: 1. Deflection units: mm
2. Deflection towards stiffener side is positive.

Table 2. Initial Imperfection for Specimen B3 (continued)

No. of Points		Long Edge									
		40	**41**	**42**	**43**	**44**	**45**	**46**	**47**	**48**	**49**
Short Edge	**1**	0.516	0.128	-0.212	-0.782	-1.144	-1.45	-1.902	-2.146	-2.926	-4.446
	2	1.226	0.918	0.442	-0.168	-0.438	-0.782	-1.184	-1.39	-1.948	-3.432
	3	2.056	1.6	1.12	0.4	0.188	-0.028	-0.192	-0.544	-1.128	-2.254
	4	2.416	1.932	1.296	0.472	0.374	0.216	-0.068	-0.454	-0.956	-2.252
	5	2.472	1.896	1.346	0.61	0.532	0.478	0.34	0.06	-0.564	-1.192
	6	3.432	2.86	2.188	1.344	1.344	1.234	1.054	0.684	0.12	-0.644
	7	4.02	3.512	2.908	2.276	2.118	1.936	1.624	1.156	0.494	-0.2
	8	4.048	3.6	2.948	2.378	2.132	1.724	1.472	0.906	0.216	-0.686
	9	3.694	3.498	2.96	2.436	2.226	2.03	1.602	0.982	0.4	-0.568
	10	4.046	3.726	3.316	2.932	2.62	2.188	1.656	1.028	0.358	-0.542
	11	4.8	4.458	3.934	3.3	2.944	2.592	2.042	1.486	0.792	-0.146
	12	4.964	4.454	3.814	3.268	2.836	2.458	1.98	1.424	0.734	-0.162
	13	5.228	4.768	4.158	3.506	3.07	2.758	2.292	1.664	0.974	-0.044
	14	5.478	4.992	4.372	3.522	3.268	2.806	2.29	1.694	0.948	-0.028
	15	5.88	5.298	4.542	3.904	3.476	3.074	2.452	1.856	1.166	0.236
	16	5.794	5.378	4.548	3.976	3.788	3.374	2.914	2.18	1.496	0.306
	17	5.984	5.606	5.052	4.484	4.102	3.698	3.176	2.51	1.68	0.612
	18	5.978	5.61	5.1	4.502	4.244	3.878	3.32	2.58	1.814	0.686
	19	5.98	5.564	4.982	4.506	4.07	3.622	3.154	2.452	1.504	0.568
	20	6.18	5.796	5.476	5.012	4.588	4.272	3.704	2.962	2.09	0.934
	21	6.518	5.952	5.356	4.738	4.336	3.882	3.352	2.612	1.804	0.654
	22	6.446	5.874	5.224	4.492	4.11	3.68	3.176	2.446	1.636	0.568
	23	6.446	5.814	5.228	4.312	3.92	3.518	3.106	2.492	1.588	0.638
	24	6.524	6.05	5.358	4.658	4.34	3.896	3.406	2.746	2.018	1.018
	25	6.36	5.744	5.038	4.422	4.07	3.62	3.078	2.39	1.658	0.742
	26	6.01	5.404	4.76	4.236	4	3.44	2.878	2.27	1.494	0.704
	27	5.452	5.096	4.566	4.136	3.778	3.416	2.918	2.286	1.624	0.8
	28	5.228	4.84	4.402	4.022	3.474	2.98	2.548	1.902	1.342	0.512
	29	4.952	4.474	3.922	3.302	2.996	2.572	2.13	1.542	0.904	0
	30	4.642	4.094	3.538	2.768	2.642	2.18	1.684	1.272	0.538	-0.204
	31	4.636	4.15	3.496	2.816	2.718	2.33	1.956	1.374	0.676	-0.28
	32	4.5	3.982	3.284	2.53	2.364	1.986	1.62	0.998	0.308	-0.616
	33	3.742	3.158	2.512	1.822	1.554	1.226	0.848	0.248	-0.456	-1.348
	34	2.758	2.288	1.758	0.976	0.864	0.48	0.11	-0.4	-1.042	-1.844
	35	2.658	2.23	1.744	1.134	0.76	0.362	0.014	-0.506	-1.16	-2.136
	36	2.15	1.784	1.406	0.826	0.43	0.044	-0.38	-0.78	-1.546	-2.448
	37	1.162	0.882	0.376	-0.16	-0.62	-0.99	-1.508	-2.162	-2.824	-3.566

Note: 1. Deflection units: mm
2. Deflection towards stiffener side is positive.